Volume 42 Supplement 1 2026

Available online at www.sciencedirect.com

ScienceDirect

This journal is part of **Science Direct's** free alerting service which sends tables of contents and favourite topics for Elsevier books and journals. You can register by clicking "Alerts" at **www.sciencedirect.com**

ELSEVIER

Indexing Services
Dental Materials is indexed by *Index Medicus*, *BIOSIS*, *Current Contents*, SciSearch, Research Alert, UnCover, Reference Update, UMI, Silver Platter, *Excerpta Medica*, CAB International and CINAHL. The journal is available in microfilm from UMI.

0109-5641(2026)42:S1;1-8

Printed by Henry Ling Ltd., The Dorset Press, Dorchester, UK

42 | S1
dental materials
Volume 42 . Number S1 . 2026 . Pages S1–S62
ELSEVIER

ELSEVIER

Volume 42 Supplement 1 2026 ISSN 0109-5641

dental materials

Journal for Oral and Craniofacial Biomaterials Sciences

www.demajournal.com

Abstracts of the Academy of Dental Materials, Annual Meeting, Panama, 2025

Available online at www.sciencedirect.com

ScienceDirect

Official Publication of the Academy of Dental Materials

academy of dental materials
corporate members

3M

GC

SDI

DMG

Dentsply Sirona

COLTENE

dental materials
Journal for Oral and Craniofacial Biomaterials Sciences

dental materials

doi:10.1016/S0109-5641(26)00255-1

Volume 42 Supplement 1 2026
ISSN 0109-5641

dental materials

Official Publication of the
Academy of Dental Materials
www.academydentalmaterials.org

Contents

Indexing Services

Dental Materials is indexed by *Index Medicus*, *BIOSIS*, *Current Contents*, SciSearch, Research Alert, UnCover, Reference Update, UMI, Silver Platter, *Excerpta Medica*, CAB International and CINAHL. The journal is available in microfilm from UMI.

Amsterdam • Boston • London • New York • Oxford • Paris • Philadelphia • San Diego • St. Louis

S20 **Three-Dimensional Roughness in Prosthetic Bases: PMMA, Polyamides, and 3D-printing**
D Martinez-Torres, A Buitrago-Osuna, M Sarmiento-Delgado

Friday, October 3rd
'Clinical properties'

S21 **Modeling structural relaxation in veneering dental porcelains via FEM**
S Butler

S22 ***In situ* evaluation of EGCG-chitosan dentifrices on dentin loss**
L Franco, K Pintado-Palomino, R Scatolin, L Gusmão, A Tedesco, M Owasawara, R Garcia, T Scaramucci, S Corona

S22 **Ex-vivo study of pulpal inflammation under blue and red lights**
D Oliveira, M Rocha, S Reinhard, S Wallet

S22 **Reducing Biofilms in the Oral Microbiome**
D Nair, M Schurr, H Escobedo, C Puranik, D Danforth, J Stansbury

S23 **AI-Driven Design Boosts Fatigue Resistance in Narrow Dental Implants**
R dos Santos, A Della Bona, J Griggs, U Lenz

S23 **Development of a fully automatic staining apparatus for accelerated aging**
AC Ionescu, D Berri

S24 **Polycystin-1 Activator-loaded Injectable Hydrogel for Periodontal Regeneration**
I De Souza Araujo, R Perkins, G Huang, Z Xiao, W Zhang

S24 **New etching protocols, prism orientation, resin composition: enamel-bonding effects**
M Canadas, T Stape, F Panzeri, ATezvergil-Mutluay

S25 **Beyond Milling: in-vitro Evaluation of 3D Printed Long-Term Dental Restoratives**
F Schmidt, J Yassine, E Prause, F Beuer

S25 **Physicochemical properties of adhesives associated with S-PRG and 0.1% hydroxyapatite**
G Zabeu, M Costa, F Zordan, C Rodrigues, M Giacomini, L Wang

S26 **In-vitro characterization and clinical survival of bulk-fill-composites: A systematic review**
F von Knobloch, J Selbertinger, F Pfefferkorn, A Schedle

S26 **Experimental adhesive loaded with fluoride-containing bioactive particles and biomimetic analogue**
N Carvalho, P Ferreira, F Gomes, S Abreu, T Oliveira, A Loguercio, Jose Bauer

S26 **Effects of Calcium Polyphosphate Bleaching Gels on Eroded Enamel**
C Barbosa, M Guanipa-Ortiz, J Andrade, W Vieira-Junior, K Rischka, F Aguiar, D Lima

S27 **Multifactorial Analysis of Universal Composite Shade Matching**
A AlShabib, T Aloraini, A Alwazzan, F Alhelal, M Alselmi, H Algamaiah

S27 **Impact of Silver Nanoparticles on Alginate: Microbiological and Mechanical Analysis**
A Costa, A Facury, E Franco, G Borges, J Neves, L de Figueiredo, L Correr-Sobrinho

S28 **Influence of different fluoride varnishes on dentin tubule occlusion**
M Barros, J Figueiredo, AB Borges, CRG Torres

S28 **Recycled Zirconia: Influence of Low-Temperature Degradation on Wear Resistance**
L Alves, E Benalcazar-Jalkh, T Campos, E Bergamo, E Oliveira, S Tebscherani, C dos Santos, Y Zhang, E Bonfante

S29 **Influence of Printing Temperature on Accuracy and Strength of Crowns**
A Correr, U Monteiro, G Baccaro, A Rios, L Correr-Sobrinho

S29 **Evaluation of cusp coverage approaches for structurally compromised teeth**
L Bernal, G Ojeda, M Ernst

S29 **Development and characterization of a photoresponsive silver vanadate dental resin**
J Tardelli, ML Leite, A Costa, M Schiavon, A Reis, R Carvalho, A Manso

S30 **Low-peroxide bleaching gel with BioS Nb_2O_5 activated by violet LED**
G Santos, I Matos, M Souza, E Zanotto, V Leitune, V Cavalli

S30 **Spray-Dried Tea-Tree and Eucalyptus Essential-Oil Microcapsules for Antimicrobial Dental Applications**
FP Rodrigues, L de Paula, S Brignone, S Palma, M Marczewski, S Raghu, M Killian

S31 **Niobium Calcium Phosphate in Experimental Resin Endodontic Sealer Properties**
R Tomasi, E Gaviolli, V Leitune

S31 **Light attenuation through varying lithium disilicate thicknesses and opacities**
N Zubair, M Dawoudzai, E Omoto, M Queiroz, J da Silva, A Maluly-Proni, T Fagundes, PH Dos Santos

S31 **Raman-AI models predict color and fatigue strength of zirconia crowns**
MG Rocha, IJ Daulton, A Delgado, E Kee, D Oliveira, J-F Roulet, P Zoidis, P Pereira

S32 **Multi-acrylamide-based adhesives preserve dentin bond strength after radiotherapy**
L Correr-Sobrinho, A Colombino, A Correr, F Tsuzuki, A Costa, C Pfeifer

S32 **In vitro evaluation of single application of two-bottle bleaching gels**
M Teixeira, L Condolo, L Barbosa, K da Cruz, A Reis, A Loguercio, T Matos, M Favoreto

Aims and Scope

The principal aim of *Dental Materials* is to promote rapid communication of scientific information between academia, industry, and the dental practitioner. Original manuscripts on clinical and laboratory research of basic and applied character which focus on the properties or performance of dental materials or the reaction of host tissues to materials are given priority for publication. Other acceptable topics include: application technology in clinical dentistry and dental laboratory technology. Comprehensive reviews written by experts on the topic and editorial commentaries on pertinent subjects will be considered. Only manuscripts that adhere to the highest scientific standards will be accepted.
The Academy's objectives are: (1) to provide a forum for the exchange of information on all aspects of dental materials; (2) to enhance communication between industry, researchers and practising dentists; and (3) to promote dental materials through its activities.
Annual meetings and scientific sessions are held in conjunction with other dental organizations. The Academy sponsors symposia and scientific programs in international meetings; recognizes scholarship at all levels from students to senior scholars; and elects Fellows in the Academy. For a full and complete Guide for Authors, please go to http://www.elsevier.com/locate/dema

USA mailing notice: *Dental Materials* (ISSN 0109-5641) is published monthly by Elsevier Ltd. (The Boulevard, Langford Lane, Kidlington, Oxford Airfreight and mailing in the USA by agent named World Container INC 150-15, 183rd St, Jamaica, NY 11413, USA. Periodicals Postage Paid at Brooklyn, NY 11256.
POSTMASTER: Send address changes to Dental Materials, Air Business Ltd, c/o World Container INC 150-15, 183rd St, Jamaica, NY 11413, USA.

Publication information: *Dental Materials* (ISSN 0109-5641). For 2026, volume 42 is scheduled for publication. Subscription prices are available on request from the Publisher or from the Elsevier Customer Service Department nearest you or from this journal's website (http://www.intl.elsevierhealth.com/journals/dema). Further information is available on this journal and other Elsevier products through Elsevier's website: (http://www.elsevier. com). Subscriptions are accepted on a prepaid basis only and are entered on a calendar year basis. Issues are sent by standard mail (surface within Europe, air delivery outside Europe). Priority rates are available upon request. Claims for missing issues should be made within six months of the date of dispatch.

Advertising Information: Advertising orders and enquiries can be sent to: **USA, Canada** and **South America:** Elsevier Inc., 360 Park Avenue South, New York, NY 10010-1710, USA: phone: (+1) (212) 633 3974. **Europe and ROW:** Sarah Ellis, Advertising Sales Executive, Elsevier Ltd, 32 Jamestown Road, London NW1 7BY, UK. Phone: +44 (0) 207 424 4538; fax: +44 (0) 207 424 4433; e-mail: s.ellis@elsevier.com

Orders, claims, and journal inquiries: Please visit our Support Hub page https://service.elsevier.com for assistance.

Author inquiries: You can track your submitted article at http://www.elsevier.com/track-submission. You can track your accepted article at http://www.elsevier.com/trackarticle. You are also welcome to contact Customer Support via http://support.elsevier.com

Funding body agreements and policies
Elsevier has established agreements and developed policies to allow authors whose articles appear in journals published by Elsevier, to comply with potential manuscript archiving requirements as specified as conditions of their grant awards. To learn more about existing agreements and policies please visit http://www.elsevier.com/fundingbodies

For a full and complete Guide for Authors, please go to: http://www.elsevier.com/locate/dental

♾ The paper used in this publication meets the requirements of ANSI/NISO Z39.48-1992 (Permanence of Paper)
The item fee code for this publication is 0109-66412/ $36.00

Printed by Henry Ling, The Dorset Press, Dorchester, UK.

Publishing Office: Elsevier Inc., 1600 John F. Kennedy Boulevard, Suite 1600, Philadelphia, PA 1910, United States.

Dental Materials 42 (2026) S1–S61

Available online at www.sciencedirect.com

Dental Materials

journal homepage: www.elsevier.com/locate/dental

ADM Abstracts, Panama, 2025

Marshall's Finalists

M1

Recycling Multilayer Zirconia Functionally Enhanced by Antimicrobial Zr-doped Glass Gradation

EB Benalcazar-Jalkh *[1], TMB Campos [1], LM Alves [1], SM Tebscherani [2], GP Thim [3], C dos Santos [4], ETP Bergamo [1,5], L Witek [5,6], PG Coelho [7,8], EA Bonfante [1]

[1] *Bauru School of Dentistry, University of São Paulo, Brazil*
[2] *Department of Production Engineering, Federal University of Technology, Parana, Brazil*
[3] *Sao Jose dos Campos, Brazil*
[4] *Rio de Janeiro State University, Brazil*
[5] *New York University College of Dentistry, USA*
[6] *NYU Tandon School of Engineering, New York University, USA*
[7] *Department of Surgery, University of Miami Miller School of Medicine, USA*
[8] *Department of Biochemistry and Molecular Biology, University of Miami Miller School of Medicine, USA*

Purpose / Aim: This study presents a method to develop recycled multilayer zirconia from CAD/CAM waste with different yttria content, and evaluates the mechanical, microstructural, and biological properties of the resulting ceramics after the application of soda-lime glass (SL), either pure (40% SiO_2, 20% Na_2O, 20% CaO, 10% Al_2O_3, and 10% B_2O_3) or doped with ZrO_2 and Y_2O_3 oxides (SL + Zr).

Materials & Methods: The recycled powder was obtained by mixing 5Y-PSZ and 3Y-TZP zirconia waste in a 1:1 ratio to obtain an intermediate 4Y-PSZ composition. This material was pressed with a pristine 5Y-PSZ top-layer to create multilayer (Recycled-4Y/5Y) disk-shaped specimens (ISO:6872). After sintering (1550° C), three groups were formed: i) Control; ii) SL-glass; and iii) Graded with SL + Zr glass. Microstructure was analyzed by scanning electron microscopy (SEM) and energy-dispersive X-ray spectroscopy (EDS), and crystalline phases were identified by X-ray diffraction (XRD). Biaxial flexural strength was assessed using the piston-on-three-ball test, with data analyzed through Weibull statistics and fractographic evaluation. Biological performance was evaluated through fibroblast (L929) viability assays and Escherichia coli adhesion tests, with data analyzed through two-way ANOVA and post-hoc Tukey tests.

Results: SEM and EDS revealed the presence of zirconia precipitates in SL glass and the formation of zirconia nanotubes in the SL + Zr glass. XRD analysis showed a predominant cubic phase in the 5Y-PSZ surface and a mixed cubic–tetragonal phase in the recycled 4Y-PSZ. These findings confirm that the recycling process effectively produced an intermediate composition typical of 4Y-PSZ. The characteristic strength of the recycled 4Y/5Y system [597 (553–643) MPa] was comparable to the pure SL glass group [610 (581–639) MPa] while higher strength was observed for the SL + Zr glass group [741 (701–781) MPa]. Fractographic analysis indicated crack deflection in the SL + Zr group, contributing to increased flexural strength. No significant differences were observed in Weibull modulus among groups (5.6 – 8.0). Biological assays confirmed no cytotoxicity in any group. Both glasses, SL and SL + Zr, led to a one-log reduction in E. coli colony-forming units, equivalent to a tenfold decrease compared to the glazed control.

Conclusions: The recycling process successfully produced sustainable multilayer zirconia. The incorporation of ZrO_2 and Y_2O_3 into soda-lime glass enhanced both the mechanical strength and antimicrobial activity while maintaining biocompatibility, which supports its potential use in restorative dental applications.

https://doi.org/10.1016/j.dental.2026.03.005

M2

Surface and Cytocompatibility Changes of 3D-printed Aligners Following Salivary Exposure

E-H Choi *[1], U Mangal [1], J-H Ryu [1], J-H Kim [1], G Hwang [2], H Kim [3], S-H Choi [1]

[1] *Yonsei University College of Dentistry, Seoul, Republic of Korea*
[2] *School of Dental Medicine, Center for Innovation & Precision Dentistry, University of Pennsylvania, USA*
[3] *College of Agriculture and Life Sciences, Seoul National University, Seoul, Republic of Korea*

Purpose / Aim: This study aimed to evaluate effects of salivary exposure on 3D-printed clear aligners, focusing on surface properties, cytotoxicity to normal cells, and pro-inflammatory responses in pre-sensitized cells.

Materials & Methods: Eleven aligners were collected from five adult patients after 10 days of use (Clinically Used Group). Two additional groups were established: Saliva-Unexposed Group (immediately after post-processing) and Artificial Saliva-Exposed Group (immersed in artificial saliva). All aligners underwent extraction for one day (Day-1 extraction) and an additional six days (Day-7 extraction). After seven days of extraction, surface properties, including hardness (Shore D) and topography (SEM imaging), were analyzed. Cytotoxicity to normal L929 cells was evaluated using MTT assays. Pro-inflammatory responses in LPS-induced pre-sensitized L929 cells were assessed by qPCR, measuring IL-6, TNF-α, and NOS2 expression levels.

Results: Shore D hardness did not differ among groups. SEM imaging revealed increased surface irregularities after salivary exposure. All groups (Table 1) exhibited no cytotoxicity (>70% viability) in both Day-1 and Day-7 extractions, with the Clinically Used Group showing significantly higher cell viability than the Saliva-Unexposed Group in both extractions ($P < 0.001$). However, when LPS-induced pre-sensitized cells were treated with Day-7 extraction, only the Clinically Used Group showed a significant increase in both IL-6 and TNF-α expression compared to LPS-only-treated cells ($P < 0.001$).

Conclusions: Saliva-exposed 3D-printed aligners exhibited increased surface irregularities and lower cytotoxicity compared to unexposed aligners. However, clinically used 3D-printed aligners may exacerbate pro-inflammatory responses in pre-sensitized cells. Depending on the initial state of the cells, cytological responses to 3D-printed aligners may vary.

Table 1. Cell viability of different aging conditions

Group	Cell viability (%)	
	Day 1 extraction	Day 7 extraction
Negative control	100.0 ± 1.12 ^{A}	100.0 ± 1.12^{A}
Positive control	5.76 ± 0.99 ^{B}	5.97 ± 1.03 ^{B}
No aging	74.16± 0.76 ^{C}	92.47 ± 1.90 ^{C}
Controlled aging	79.19 ± 2.15 ^{D}	100.41 ± 0.59 ^{A}
Natural aging	83.18 ± 1.08 ^{E}	100.08 ± 2.69 ^{A}

$^{A, B, C, D, E}$ The same capital letters in the vertical columns indicate no difference between groups ($P > 0.05$).

https://doi.org/10.1016/j.dental.2026.03.006

M3

Glass-Infiltrated Recycled-Zirconia Bonding to Titanium: Etching and QAM-Based Cement Performance

H Strazzi-Sahyon *[1], F Lucena [2], T Campos [1], M Piza [1], É Omoto [3], M Logan [2], S Lewis [2], PH Dos-Santos [3], AP Fugolin [2], J Ferracane [2], C Pfeifer [2], E Bonfante [1]

[1] *University of São Paulo - USP, Bauru School of Dentistry, Brazil*
[2] *Oregon Health & Science University, OHSU, USA*
[3] *University of Toronto, Canada*

Purpose / Aim: Zirconia implant-supported restorations (ZISRs) present clinical challenges that may compromise longevity, particularly due to debonding at the zirconia–titanium interface and biofilm accumulation. This study aimed to evaluate the surface and mechanical properties of glass-infiltrated recycled zirconia (GIRZ) subjected to different surface treatments and its adhesion to titanium using antimicrobial dual-cure resin cements (DCRCs) before and after biological-hydrodynamic aging (BHA).

Materials & Methods: Recycled zirconia (R-3Y-TZP) powder (<1μm), derived from 3Y-TZP milling waste (Ceramill Zi; Amann-Girrbach), was uniaxially pressed and sintered at 1550°C for 2h. Specimens were divided into five groups: (1) untreated R-3Y-TZP (control); (2) Cojet-blasted R-3Y-TZP; (3) glass-infiltrated R-3Y-TZP (R-3Y-TZP + G); (4) Cojet-blasted R-3Y-TZP + G; and (5) 40% hydrofluoric acid (HFA)-etched R-3Y-TZP + G. Two DCRCs were formulated with/without quaternary ammonium methacrylate (QAM) using BisGMA:UDMA:TEGDMA (5:3:2 mass-ratio). Three study phases were conducted: (I) evaluation of surface properties and antimicrobial activity of ceramics and cements; (II) assessment of biaxial flexural strength and shear bond strength (SBS) using non-antimicrobial cement; and (III) SBS of the optimal ceramic treatment (obtained in the phase-II) was evaluated with both DCRC formulations before and after BHA (5 days in a bioreactor: 2.3 bar/1.5Hz/120min and 1.0 bar/1.0Hz/30min; and 3 days in incubation in a 1:1 co-culture of Porphyromonas gingivalis and Prevotella intermedia). Data were analyzed with ANOVA and Tukey's post-hoc tests ($\alpha = 0.05$). Weibull statistic was employed to determine characteristic strength and Weibull modulus. Scanning electron microscopy was used for fractographic and SBS failure mode analyses.

Results: (I) Cojet-blasted R-3Y-TZP + G exhibited increased roughness (Sa, Sz, Ra, Rz) ($p < 0.05$), as evidenced by confocal, atomic force, and scanning electron micrographs. HFA-etched R-3Y-TZP + G had higher wettability and surface free energy ($p < 0.001$). QAM-DCRC reduced optical density, biomass, and colony forming units ($p < 0.001$), though exhibited higher viscosity and water sorption ($p < 0.001$); and no differences in solubility and degree of conversion compared to the non-antimicrobial cement ($p = 0.399$). (II) HFA-etched R-3Y-TZP + G exhibited greater SBS than control ($p = 0.040$), with no differences in characteristic strength. (III) Titanium bonded with QAM-based cement to HFA-etched R-3Y-TZP + G showed no differences before and after BHA ($p = 0.957$), whereas non-antimicrobial cement exhibited higher SBS after aging ($p < 0.001$). Mixed failure modes predominated in the SBS results of both study phases. Fractographic analysis indicated fracture initiation at tensile-side flaws with propagation toward the compression side.

Conclusions: 40%-HFA etching is effective for GIRZ, enhancing surface and adhesion features without compromising mechanical integrity. QAM-based cement is a promising biofilm-controlling luting agent for ZISRs.

https://doi.org/10.1016/j.dental.2026.03.007

Paffenbarger Finalists

P1

Continuous Stiffness Measurement Over Traditional Nanoindentation of Dental Resin-Based Composites

E Parra *[1,2], S Sauceda [1], M Wendler [2]

[1] *Faculty of Engineering, Universidad de Concepción, Chile*
[2] *Faculty of Dentistry, Universidad de Concepción, Chile*

Purpose / Aim: Nanoindentation is a valuable technique for evaluating the mechanical behavior of dental resin-based composites (RBCs), which exhibit a nanostructured, heterogeneous architecture and viscoelastic-plastic behavior. These characteristics complicate their characterization due to the variability induced by their microstructure. The continuous stiffness measurement (CSM) method is presented as a promising alternative for polymer-based materials, although its use remains limited due to a lack of standardization. This study aimed to compare the CSM method with the traditional quasi-static indentation technique in dental RBCs, assessing its effectiveness in capturing the mechanical behavior profile and properties.

Materials & Methods: Resin discs (1 mm × 6 mm) were fabricated from three commercial RBCs: Filtek z350 XT (3M), Tetric N Ceram (Ivoclar Vivadent), and Neo Spectra ST (Dentsply Sirona), in both sculptable (high-filler) and flowable (low-filler) versions. Three samples were prepared for each resin type, allowing each test to be replicated twice. All specimens were stored in distilled water at 37 ± 1 °C for 24 hours prior to testing. Nanoindentation tests were conducted using a Bruker Hysitron Ti Premier device equipped with a Berkovich diamond tip with a 100 nm radius. For quasi-static testing, 10 indentations were performed per material under load-controlled (1,000–10,000 μN) and displacement-controlled (650 nm) testing. For CSM, 5 indentations per sample were performed with a maximum load of 8,000 μN at 200 Hz. Nanohardness (H) and elastic modulus (E) were evaluated. In CSM, additional viscoelastic parameters—storage, loss, and complex moduli—were recorded.

Results: In quasi-static mode, both groups showed that higher loads produced more stable H and E values, with lower variability observed between 500-800 nm of displacement. In CSM mode, progressive stabilization of values was observed as a function of time and depth, becoming more evident after 35 seconds in both groups. No statistically significant differences were found among brands within each group; however, significant differences in H and E were observed between high- and low-filler-content groups in both methods. CSM provides additional insight into the viscoelastic behavior of the materials.

Conclusions: The strong agreement between CSM results and those obtained through quasi-static indentation supports the use of CSM as a reliable alternative method for characterizing dental RBCs. By enabling the acquisition of continuous data on material behavior as a function of depth within a single indentation, CSM offers reduced testing time and a more comprehensive analysis of viscoelastic properties through the determination of storage, loss, and complex moduli.

https://doi.org/10.1016/j.dental.2026.03.008

P2

Dense Translucent Zirconia via Extrusion-based 3D-printing: From Paste to Applicability

J Silva *[1], MF Alves [2], I Dias [3], AC Silva [1], TM Campos [4], M Laranjo [3], RM Marinho [1], SM Olhero [2]

[1] *Sao Paulo State University (UNESP), Sao Jose dos Campos, Brazil*
[2] *University of Aveiro, Portugal*
[3] *University of Coimbra, Portugal*
[4] *Federal University of Pelotas, Brazil*

Purpose / Aim: To produce highly densified samples of zirconia powder partially stabilized with 5mol% of yttrium oxide (5Y-PSZ), by an additive manufacturing technology (Direct Ink Writing – DIW) with mechanical properties, translucency and cytotoxicity response following the requirements for dental applications.

Materials & Methods: Colloidal processing approach was employed to develop the paste, using 5Y-PSZ zirconia powder (PX-430 - TOSOH Corp., Japan), combined with two different dispersants (Dolapix Ce64 or Duramax D-3005), thickener (carboxymethyl cellulose - CMC) and a flocculant agent (polyethyleneimine solution - PEI). Rheological behavior was assessed through the Kinexus Pro+ rheometer (Netzsch, UK). The optimized paste was composed of 47vol% solid load, Duramax D-3005, CMC and PEI in specific concentrations. DIW equipment (EBDR-A32, 3D Inks, LLC, USA) was used to print cylindrical samples (20mm x 2mm) by varying filament overlaps in xy and zz directions: Z5Y-DIW-20 (20% overlaps), Z5Y-DIW-25 (25% overlaps) and Z5Y-DIW-30 (30% overlaps). The ceramic-paste extrusion was made with a printing speed of 10mm/s through a nozzle of 0.410mm. Following the printing process, the green bodies gradually dried for 24 hours. The control group (Z5Y-P) was uniaxially pressed. All groups were sintered (1550˚C-2h) and characterized in terms of Relative Density (%), Scanning Electron Microscopy (SEM), X-ray Diffraction (XRD), translucency (TP00), biaxial flexural strength (MPa), Vickers Hardness (GPa), KIC ($MPa.m^{1/2}$) and cytotoxicity test (MTT assay-fibroblast). The results were analyzed by one-way ANOVA and Tukey's test ($\alpha = 0.05$).

Results: The relative density ranged from 98.7% to 99.6%, with the highest values observed in the Z5Y-DIW-30 (99.31%) and Z5Y-P (99.59%) groups. The groups did not present significant differences in the translucency parameter. For the flexural strength the groups showed values of: Z5Y-DIW-20 (328.9 ± 37 MPa A), Z5Y-DIW-25 (350.9 ± 73 MPa A), Z5Y-DIW-30 (432.6 ± 37 MPa B), Z5Y-P (561.2 ± 54 MPa C). The SEM and XRD did not present any differences when comparing the pressed and printed groups. The Vickers hardness showed similar values for the Z5Y-DIW-30 (13.82GPa) and Z5Y-P (13.9GPa) groups. For the KIC the Z5Y-DIW-30 (3.6 $MPa.m^{1/2}$) and Z5Y-P (3.9 $MPa.m^{1/2}$) showed significant statistical differences. The printed and pressed groups did not induce cytotoxic effects on fibroblast cells ($P = 0.465$).

Conclusions: The mechanical and optical properties revealed that when properly formulated and processed, the 5Y-PSZ paste can produce highly dense structures and good mechanical reliability in compliance with ISO 6872, representing a viable alternative to conventional subtractive manufacturing in dental applications, especially for the fabrication of dental crowns.

Image upload

https://doi.org/10.1016/j.dental.2026.03.009

P3

Color match of one-shade composite post-bleaching: a randomized clinical trial

LMM Barbosa *[1], MW Favoreto [2], M de Oliveira Mendes [2], TP Matos [2], D Jiménez-Díez [1,3], KR da Cruz [2], L Ceballos [3], AD Loguercio [1], A Reis [1]

[1] *State University of Ponta Grossa, Ponta Grossa, Brazil*
[2] *Tuiuti University of Paraná, Curitiba, Brazil*
[3] *Rey Juan Carlos University, Madrid, Spain*

Purpose / Aim: This double-blind and split-mouth randomized clinical trial evaluated the color matching performance of a one-shade resin composite compared to a multi-shade resin composite in the restoration of non-carious cervical lesions (NCCLs) following in-office bleaching.

Materials & Methods: Eighty-four NCCLs were restored using two resin composites (n = 42): Vittra APS (multi-shade, FGM) and Vittra Unique (one-shade, FGM). After prophylaxis, the teeth were isolated with a rubber dam, and the universal adhesive system Ambar Universal APS (FGM) was applied in the selective enamel etching mode using 37% phosphoric acid (Condac, FGM). Restorations were placed incrementally in both groups. Patients underwent in-office bleaching with 35% hydrogen peroxide gel (Automixx Plus 35%, FGM) in two 50-minute sessions, at a one-week interval. The Whiteness Index for Dentistry (WID) was used to assess the color progression in the different regions of the tooth (the cervical third corresponding to the restoration area, and the middle third to the adjacent tooth structure). Color differences (ΔEab and ΔE00) between the cervical and middle thirds were measured using a digital spectrophotometer at four time points: before bleaching, after the first session, after the second session, and one month later from baseline. Data were analyzed using a two-way repeated measures ANOVA followed by Tukey's post hoc test ($\alpha = 0.05$).

Results: In the middle third, both groups exhibited statistically significant higher WID values after first bleaching session ($p < 0.05$), showing similar progression over time. In the cervical third, a significant increase in WID value was observed only for the one-shade composite after first and second bleaching session ($p < 0.05$). After two weeks of bleaching, higher color difference (ΔEab and ΔE00) between the cervical and middle thirds were observed compared to baseline in the multi-shade composite group ($p < 0.05$). In contrast, the one-shade composite did not show statistically significant variation across the time periods ($p > 0.05$).

Conclusions: The one-shade composite demonstrated increased whiteness in the cervical third and maintained uniform color matching with the surrounding tooth structure throughout the evaluation period, whereas the multi-shade composite showed greater color differences between thirds after bleaching.

https://doi.org/10.1016/j.dental.2026.03.010

P4

eDentin: a Bioengineered Membrane for Dental Pulp Capping

MA Fraga *[1,2], D Cunha [3], S Vignolo [2], A Taheri [2], A Athirasala [2], CM França [2], M Souza [2], AB Correr [1], L Bertassoni [2]

[1] *Unicamp, Piracicaba, Brazil*
[2] *OHSU, Portland, USA*
[3] *UFC, Fortaleza, Brazil*

Purpose / Aim: The dental pulp's primary defense against cavities is the secretion of reparative dentin, a process that is slow and difficult to control. To tackle these limitations, we developed an enhanced biomaterial, named eDentin (short for Engineered Dentin), intended for use as a dentin membrane in dental pulp capping.

Materials & Methods: eDentin was engineered using acid-solubilized collagen Type-I, which was then processed into a dense fibrillar collagen scaffold and mineralized for 3 days. The resulting biomimetic membranes were characterized and evaluated for their mineral contents using scanning electron microscopy (SEM), Fourier-transform infrared spectroscopy (FT-IR), and Alizarin Red staining. Additionally, eDentin was loaded with dentin matrix molecules (DMMs) followed by a 7-day BCA Protein Assay. To evaluate eDentin in vivo, we implanted eDentin into eighteen Wistar rats' maxillary first molars. Teeth were divided into 3 groups (n = 6): (i) Biodentine (clinical gold standard), (ii) eDentin, and (iii) negative control. After 30 days, animals were euthanized, and teeth were processed for histological analysis of pulp reaction and tertiary dentin formation.

Results: SEM demonstrated that eDentin was comprised of randomly arranged intrafibrillar mineralized fibers showing evidence of a hybrid layer akin to that observed with native dentin. FT-IR confirmed the mineralization, with a mineral:matrix ratio and crystallinity index significantly higher than controls. The inclusion of DMMs enhanced mineral matrix formation as detected via Alizarin Red stain, while in vivo results showed increased tertiary dentin formation with eDentin.

Conclusions: eDentin shows promise as an alternative for creating a dentin-material interface that closely mimics natural dentin composition.

https://doi.org/10.1016/j.dental.2026.03.011

P5

Experimental Post-polymerization and Mn-TiO_2 nanoparticles Effects on 3D Printed Resins

P Magão *[1,2], G Cardoso [1], G Moura [1], A Furuse [2], F Rizzante [1]

[1] *James B. Edwards College of Dental Medicine, Medical University of South Carolina, USA*
[2] *Faculdade de Odontologia de Bauru, Universidade de São Paulo, Bauru, Brazil*

Purpose / Aim: Additive manufacturing is transforming dentistry, yet optimal post-polymerization protocols remain uncertain. This study investigates the effects of manganese-doped titanium dioxide (TiO_2) nanoparticles and experimental post-polymerization protocols utilizing a customized post-polymerization chamber and a broadband LED curing device on key properties of 3D-printed dental resins. It aims to evaluate how incorporating manganese-doped titanium dioxide (TiO_2) nanoparticles and different post-polymerization methods influence the physical and mechanical properties of resin composites intended for additive manufacturing.

Materials & Methods: Two commercially available resins—Crown and Bridge B1 (DENTCA) and OnX B1 (SprintRay)—were modified by adding 0.5% by mass of manganese-doped TiO_2 nanoparticles (<100 nm, Sigma-Aldrich) and compared to non-modified controls. Specimens were printed using the Pro95—SprintRay printer (n = 10) and subjected to three distinct post-polymerization protocols: a commercially available chamber (ProCure, SprintRay), a broadband LED curing device (Grand Valo, Ultradent Products) operating at 1000 mW/cm² for 120 s, and an experimental customized chamber employing both UV and visible light. The evaluated properties included flexural strength and Knoop microhardness. Statistical analyses were conducted using factorial ANOVA and Tukey's multiple comparison test at a significance level of 5%.

Results: Significant differences in flexural strength were identified based on resin type ($p < 0.01$), nanoparticle modification ($p < 0.01$), and post-polymerization methods ($p < 0.01$). The flexural strength results (Table 1) exhibited the following trend: OnX > Crown and Bridge; without nanoparticles > with nanoparticles; and Custom 60 min > ProCure 1 > Valo 120 s. Regarding Knoop microhardness, significant differences were observed based on resin type, nanoparticle modification, and post-polymerization method ($p < 0.01$). Microhardness values demonstrated a general trend: OnX > Crown and Bridge, and Custom 60 minutes > ProCure 1 > Valo 120 s, with slight improvements noted in certain nanoparticle-modified groups depending on resin type and curing method.

Conclusions: In conclusion, while the addition of manganese-doped TiO_2 nanoparticles slightly increased Knoop microhardness under certain conditions, it generally reduced flexural strength across tested groups. The customized 60-min post-polymerization method consistently provided superior results compared to other methods, suggesting potential for optimizing curing protocols in dental additive manufacturing processes.

Image upload

Table 1. Mean and standard deviation values for Flexural strength and Knoop microhardness

Resin	Modification	Post-polymerization	Flexural strength (Mpa)	Knoop microhardness (KHN)
Crown and Bridge	None	Custom 60 minutes	111,33 (7,37)de	19,02 (2,14)ab
		ProCure 1	93,88 (5,54)c	21,60 (3,98)b
		Valo 120 seconds	125,91 (13,76)ef	16,16 (2,37)a
Crown and Bridge	0,5 wt % of Mn-doped TiO_2 nanoparticles	Custom 60 minutes	73,03 (4,97)ab	23,01 (2,79)bc
		ProCure 1	87,68 (6,23)bc	22,98 (2,40)bc
		Valo 120 seconds	70,73 (15,91)a	20,41 (2,47)ab
OnX	None	Custom 60 minutes	179,17 (10,39)f	33,83 (4,49)f
		ProCure 1	166,12 (11,90)f	26,53 (2,72)cd
		Valo 120 seconds	129,31 (8,34)f	26,78 (2,63)cde
OnX	0,5 wt % of Mn-doped TiO_2 nanoparticles	Custom 60 minutes	101,27 (13,50)cd	29,21 (3,66)de
		ProCure 1	103,71 (10,60)cd	31,09 (1,93)ef
		Valo 120 seconds	102,27 (17,48)cd	28,59 (3,26)de

Different letters indicate statistically significant differences in the same column.

https://doi.org/10.1016/j.dental.2026.03.012

Thursday, October 2nd

'Physico-mechanical properties'

1
Novel Pretreatment's Effect on Microtensile Bond Strength of Universal Adhesive

A Alshehri *

Prince Sattam Bin Abdulaziz university, Alkharj, Saudi Arabia

Purpose / Aim: This study aims to investigate the impact of a novel pretreatment on the mTBS of a of an innovative universal adhesive to conventional and CAD/CAM resin composites

Materials & Methods: A total of eighty recently extracted human molars (n = 80) were chosen, placed in transparent acrylic blocks to expose the crowns entirely. Nano-filled resin composite and CAD/CAM resin blocks were selected. Based on the dentin pretreatment, type of resin composite and adhesion strategy, teeth were randomly allocated into eight equal groups (n = 10), Figure 1. Group 1 (No dentin pre-treatment + Etch-and-rinse + Nano-filled composite); Group 2 (CuSO4 + K2HPO4 + Etch-and-rinse + Nano-filled composite); Group 3 (No dentin pre-treatment + Self-etch + Nano-filled composite); Group 4 (CuSO4 + K2HPO4 + Self-etch + Nano-filled composite); Group 5 (No dentin pre-treatment + Etch-and-rinse + CAD/CAM resin blocks); Group 6 (CuSO4 + K2HPO4 + Etch-and-rinse + CAD/CAM resin blocks); Group 7 (CuSO4 + K2HPO4 + Self-etch + CAD/CAM resin blocks); Group 8 (CuSO4 + K2HPO4 + Self-etch + CAD/CAM resin blocks). The microtensile bond strength (μTBS) and fracture mode were determined

Results: Significant differences were detected between no dentin pre-treatment and CuSO4 + K2HPO4 pre-treatment for both nano-filled and CAD/CAM resin blocks (P < 0.001). Moreover, for nanofilled composites and CAD/CAM resin blocks, there was no discernible difference between the etch-and-rinse and self-etch groups for both groups lacking dentin pre-treatment (0.653) and with CuSO4 + K2HPO4 pre-treatment (P = 0.620).

Conclusions: Dentin μTBS was enhanced by a copper-based treatment when used with nanofilled and CAD/CAM resin blocks

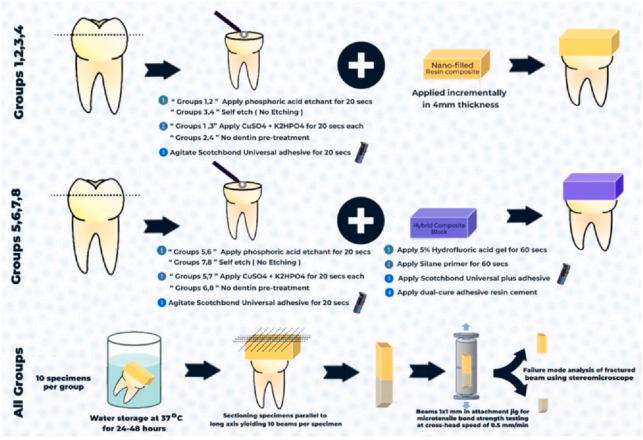

Figure 1.

https://doi.org/10.1016/j.dental.2026.03.013

2
Bond strengths: Self-adhesive flowable vs. flowable with universal adhesive

Mark Agre *[1], Tim Dunbar[2], Shira Zary[3]

[1] *Solventum, Rosemount, USA*
[2] *Solventum, Woodbury, USA*
[3] *Solventum, Tel Aviv, Israel*

Purpose / Aim: This study compares the adhesive bond strength of Kerr SimpliShade™ Self-Adhesive Flow on dentin and cut enamel vs a new simplified shade flowable composite (Solventum™ Filtek™ Easy Match Flowable Restorative), in combination with 3M™ Scotchbond™ Universal Plus adhesive, using various adhesive approaches.

Materials & Methods: Bond strength was tested using the Shear Bond Strength Notched Edge Method, on both cut enamel and dentin. Crowns of bovine incisors were cut from their roots and the pulp removed. These crowns were potted in methacrylate, then ground with 120-grit, followed by 320-grit sandpaper to reveal the proper substrate. Phosphoric Acid Etchant (if necessary), adhesive (if necessary), and flowable were all placed and cured according to their Instructions For Use. Flowable buttons (2.38mm diameter) were formed using a plastic mold. 5 groups of 10 samples each were evaluated.

Results: The results demonstrated varying levels of adhesive bond strength across different materials and methods (see Table 1). For Cut Enamel, ANOVA analysis indicated a significant difference in bond strength among the three groups (p = 0.000). Post-hoc analysis using Tukey's HSD test revealed all groups were statistically different, and that the Total Etch approach with Scotchbond Universal Plus and Filtek Easy Match Flowable Restorative had the highest bond strength relative to the two other methods. For Dentin, a two-sample t-test was performed to compare the Self-Etch approach with Scotchbond Universal Plus and Filtek Easy Match Flowable Restorative against SimpliShade Self-Adhesive Flow. The t-test results showed a significant difference in bond strength between the two methods (p = 0.000), with the Self-Etch approach demonstrating higher bond strength.

Conclusions: Adhesive bond strength varies significantly depending on the substrate, material and adhesive approach used. The Total-Etch approach with Scotchbond Universal Plus and Filtek Easy Match Flowable Restorative provided the highest bond strength on cut enamel, while the Self Etch approach with the same materials showed the highest bond strength on dentin. SimpliShade Self-Adhesive Flow exhibited lower bond strengths on both cut enamel

and dentin compared to the other methods tested. These findings suggest that the choice of adhesive approach and material is crucial for optimizing bond strength in dental restorations.

Table 1: Adhesive values (MPa) for each group, with standard deviation (SD).

Substrate	Restorative	Adhesive	Average (MPa)	SD (±)
Cut Enamel	Solventum™ Filtek™ Easy Match Flowable Restorative (FEMF)	3M™ Scotchbond™ Universal Plus, Total etch (SBU+TE)	37.65[A]	3.79
	Solventum™ Filtek™ Easy Match Flowable Restorative (FEMF)	3M™ Scotchbond™ Universal Plus, Self etch (SBU+SE)	27.36[B]	4.33
	Kerr SimpliShade™ Self-Adhesive Flowable (SSSAF)	-	17.76[C]	3.77
Dentin	Solventum™ Filtek™ Easy Match Flowable Restorative (FEMF)	3M™ Scotchbond™ Universal Plus, Self etch (SBU+SE)	29.07[I]	5.87
	Kerr SimpliShade™ Self-Adhesive Flow (SSSAF)	-	10.74[II]	7.89

Table Footer: Superscripted letters indicate statistical differences in the Cut Enamel ANOVA analysis. Superscripted Roman numerals indicate statistical differences in the Dentin 2-sample t-test analysis.

https://doi.org/10.1016/j.dental.2026.03.014

3

Polymerization kinetics of universal resin cement with delayed- and touch-cure

M Sinhoreti *[1], A Detogni [1], A Correr [1], D Oliveira [2], M Rocha [2], J-F Roulet [2]

[1] *Piracicaba Dental School, University of Campinas, Piracicaba, Brazil*
[2] *College of Dentistry, University of Florida, Gainesville, USA*

Purpose / Aim: To investigate the effect of the touch-cure mechanism of a universal adhesive (Scotchbond Universal Plus, Solventum) and different light-cure delay periods on the polymerization kinetics of a universal resin cement (RelyX Universal, Solventum).

Materials & Methods: The URC (RelyX Universal, Solventum) was used with or without SBUp (Scotchbond Universal Plus, Solventum) adhesive to analyze the effect of the touch-cure mechanism. The polymerization kinetics were measured continuously in real-time for 1,800 s using a Fourier-transform infrared spectroscopy (FTIR) with an attenuated total reflectance (ATR) accessory. The specimens were evaluated in dark-cure and at light cure delay times of 0, 1, 3, 5, 10, 15, and 20 min of photoactivation. The degree of conversion (DC) and the maximum rate of polymerization (Rpmax) were calculated for all test conditions ($n = 3$). The data were analyzed by two-way ANOVA and Tukey's post-hoc ($p < 0.05$).

Results: The resin cement showed a significant increase in the DC after photoactivation ($p = 0.00001$) in both adhesive conditions. The resin cement combined with the adhesive showed a significant increase ($p = 0.00001$) in the DC for the 10-, 15-, and 20-min delay periods and the control. No significant difference in DC was observed among the light cure delay periods. Combined with the adhesive, the resin cement showed DC mean values significantly higher for the 10-, 15-, and 20-min delay periods, when compared with 0, 1, 3, and 5 min. The dark-cured resin cement (control) showed the lowest DC mean values in both adhesive conditions. In comparing the adhesive conditions, the DC mean values of the resin cement combined with the adhesive at 10-, 15-, 20-min delay periods and the control were significantly higher than those obtained at 0-, 1-, 3-, and 5-min delay periods. A significant reduction in the Rpmax was observed for the resin cement at dark cure and 20-min delay period (cement without adhesive) and at dark cure and 15- and 20-min delay periods (cement with adhesive). The adhesive significantly reduced the Rpmax at 10- and 15-min delay periods.

Conclusions: The 10-, 15-, and 20-min photoactivation delay periods improved the DC of the resin cement in both adhesive conditions. The adhesive improved the DC of the resin cement at 10-, 15-, 20-min delay periods and at dark cure (control). The delayed photoactivation significantly reduced the Rpmax in both adhesive conditions; the adhesive significantly reduced the Rpmax at 10- and 15-min delay periods.

https://doi.org/10.1016/j.dental.2026.03.015

4

Tribological analysis of debris released from glass fiber-reinforced composite implant

A Väisänen *, N Moritz, P Vallittu

University of Turku, Turku, Finland

Purpose / Aim: The aim of this study was to evaluate the release of debris from semi-anatomic GFRC plates in cyclic loading conditions. In vitro test-setup was designed to simulate masticatory cycle in a mandible with right sided segmental defect that has been reconstructed by using GFRC plate. The size, chemical composition and mass of released debris was characterized by using laser mass spectrometry and scanning electron microscopy.

Materials & Methods: GFRC of bidirectional S3-glass fiber weaves with dimethacrylate resin matrix were used to fabricate semi-anatomic reconstruction plates. Two types of GFRC plates were used. Group A had simple molded screw holes while group B had added 0,25mm resin layer surrounding the screw holes. The plate design followed the contour of the resected part of the bone, and the medial surface was concave allowing for placement of a microvascular bone flap in the next stages of the research. Plates were fixed with bicortical titanium screws to a 3D-printed plastic model of the mandible with a large segmental defect in the region DD 45-47. The mandible-plate system was cyclically loaded (10000 cycles) from incisal location with load of 100 N by using universal testing machine (ZwickRoell). Material abrasion and release of debris was studied by collecting the released debris particles. To extract released debris implant plates were placed into ultrasonic cleaner. Thereafter, debris material was filtered through filter paper. The mass of debris samples was recorded, and SEM/EDS samples were prepared for elemental and morphologic characterization of debris.

Results: All implant types survived mechanical loading without visible damage by fracture or buckling. The results showed that improved plate design in group B significantly decreased the amount of wear debris formation. The composition of wear debris showed parts of resin matrix and glass fiber particles. In group A titanium particles were detected among the wear debris. However, in group B titanium particles were not present in the wear debris.

Conclusions: All implant types survived mechanical loading without visible damage. The results showed that improved plate design significantly decreased the amount of wear debris formation and eliminated titanium debris formation altogether.

https://doi.org/10.1016/j.dental.2026.03.016

5
Post retentive ability of a bulk fill flowable resin composite

MC Erhardt *, A Bavaresco, L Gonçalves

UFRGS, Porto Alegre, Brazil

Purpose / Aim: This in vitro study aimed to evaluate the use of a bulk-fill flowable resin composite as either a luting agent or a filling material for glass fiber post (GFP) cementation, comparing its performance with conventional and self-adhesive dual-cure resin cements under different adhesive protocols.

Materials & Methods: A total of 120 roots from extracted single-rooted bovine teeth were endodontically treated and randomly assigned to six groups (n = 20), according to the adhesive strategy used: G1 (Single Bond 2 Adper 3M + RelyX ARC + GFP); G2 (Single Bond 2 Adper 3M + Filtek Bulkfill Flow + GFP); G3 (Single Bond 2 Adper 3M + Filtek Bulkfill Flow); G4 (U200 + GFP); G5 (Scotchbond 3M Universal + Filtek Bulkfill Flow + GFP); G6 (Scotchbond 3M Universal + Filtek Bulkfill Flow). After cementation, the roots were sectioned perpendicularly into 1 mm-thick slices and subjected to a push-out bond strength test using a universal testing machine (0.5 mm/min). Data were analyzed using one-way ANOVA and Tukey's post hoc test ($\alpha = 0.05$).

Results: Statistically significant differences in bond strength were found between G2 and G5 ($p < 0.01$), with both groups showing the highest values. Significant differences were also observed among root regions (cervical, middle, apical) in groups G2 and G6 ($p < 0.001$).

Conclusions: The tested bulk fill flowable resin composite may represent a viable alternative for luting glass fiber posts, regardless of the adhesive strategy used (total-etch or self-etch).

https://doi.org/10.1016/j.dental.2026.03.017

6
Development of Sustainable Abrasive Compounds for Dental Polishing

S Seif *, R Carvalho

University of British Columbia, Vancouver, Canada

Purpose / Aim: This study aimed to develop dental polishing pastes using renewable materials and to compare their performance with commercial abrasives on zirconia, lithium disilicate, and resin composite. Surface roughness and topography were evaluated using a profilometer and scanning electron microscopy (SEM).

Materials & Methods: Experimental pastes were formulated with chitin (5.8%), cellulose nanocrystals (CNC, 14%), pistachio shell powder (24.5%), and sea sand (38.1%), using a mixture of glycerol, distilled water, and methyl cellulose as a vehicle to achieve the desired viscosity. Viscosities were adjusted to match those of commercial references: Lucida Paste (DiaShine, Canada), Clay Paste, and Diamond Paste (PHS, Brazil). Viscosity ranged from 450 to 1,200 Pa·s. Particle sizes were standardized at 3–15 µm. The abrasive weight percentage in control pastes were Lucida (30%), Clay (39.48%), and Diamond (10%), with experimental pastes falling within this range. A total of 27 groups (n = 5 discs/group) were tested: three commercial, four experimental, one Alox (negative control), and one felt-only. Substrates included discs (10 mm × 2 mm) of zirconia, lithium disilicate, and resin composite, pre-roughened with 320-grit SiC paper. Polishing was performed using a Buehler Ecomet 300 for 2 minutes at 200 rpm with 10 lbs of pressure. A total of 0.5 mL of paste was applied at both 0 and 1 minute. Surface roughness (Ra and Rz) was recorded at five points per disc before and after polishing. SEM analysis was conducted at 500× to 10,000× magnification.

Results: Chitin paste produced the greatest Ra reduction (Fig. 1) on composite resin (ΔRa = -0.55 µm; $p < 0.001$), and similar to Diamond paste (ΔRa = -0.51 µm). Pistachio paste performed best on lithium disilicate (ΔRa = -0.49 µm; $p = 0.002$). Lucida Paste showed excellent results on composite (ΔRa = -0.28 µm) and Clay Paste was similarly effective (ΔRa = -0.21 µm) but performed poorly on zirconia and lithium disilicate. Sand paste yielded good results on lithium disilicate (ΔRa = -0.30 µm). CNC paste showed consistently poor performance (ΔRa < -0.07 µm) Felt-only polishing had minimal effect (ΔRa = 0.03–0.08 µm), while Alox paste increased roughness (ΔRa = < 0.25 µm). Differences in Ra and Rz were statistically significant (ANOVA, $p < 0.05$), with Tukey's test confirming pairwise differences. SEM results corroborated the profilometry findings.

Conclusions: Chitin, pistachio, and sand pastes demonstrated promising polishing outcomes, often similar to commercial references. These natural compounds represent sustainable alternatives for dental polishing applications.

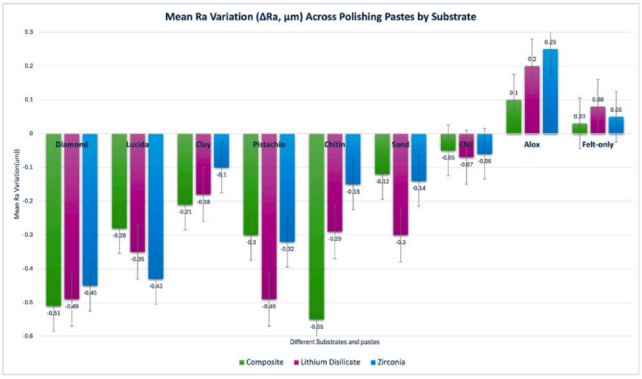

Figure 1

https://doi.org/10.1016/j.dental.2026.03.018

7
Effect of Bioactive Adhesives and Composites on Adjacent Dentin Microhardness

LC Monteiro *[1], M Falcon [2], N Orsino [2], R Lins [3], WF Vieira Jr[2], FH Aguiar [2]

[1] *University of Louisville School of Dentistry, Louisville, USA*
[2] *Piracicaba Dental School at University of Campinas, Piracicaba, Brazil*
[3] *Federal University of Alagoas, Maceió, Brazil*

Purpose / Aim: The objective of this study was to investigate the demineralization-preventive and remineralizing effects of adhesive systems and resin composites containing S-PRG filler particles on dentin adjacent to restorations, using cross-sectional microhardness testing after subjecting the samples to thermal, mechanical, and erosive/abrasive aging protocols.

Materials & Methods: Bovine teeth were prepared to expose dentin on the buccal surface. Restorations (4 × 4 × 2 mm) were then performed using combinations of self-etch adhesives (Beauti-Bond and bioactive FL-Bond II, Shofu) and resin composites: conventional [CR] (Filtek Z250 XT, 3M), and S-PRG filler-containing composites (Beautifil II [BII], Beautifil II LS [BII-LS], and Beautifil Bulk Restorative [BBulk], Shofu) (n = 10). The Knoop microhardness (MHV) was determined at distances of 100, 200 and 300 µm and at depths of 100, 200, 300, 400 and 500 µm. The analyses were

performed 24 hours after the restorative procedure (immediate) and after cycling (thermal, mechanical and erosive/abrasive - aged). The data were evaluated using four-way ANOVA, and Bonferroni post-hoc test ($\alpha = 0.05$).

Results: The four-way interaction was not significant ($p = 0.932$); however, a significant three-way interaction was observed among resin composite, adhesive system, and time point ($p < 0.001$). The depth factor was not relevant in any evaluation combination nor as an isolated factor ($p > 0.8$). Although all combinations showed a decrease in microhardness after cycling (Table 1), the combinations of BeautiBond adhesive with BBulk and BII-LS composites, as well as FL-Bond II with the conventional resin composite (RC), exhibited a more favorable performance compared to the other combinations. For the BII composite, inferior results were observed regardless of the adhesive used.

Conclusions: The protective and remineralizing potential on dentin promoted by the bioactive adhesives and resin composites tested in this study may depend on the specific combination of materials used during application.

Mean ± SD of Microhardness (MHV) for Resin Composites and Adhesives Across All Depths (*) at Immediate and Aged Time Points.

RESIN COMPOSITE	ADHESIVE SYSTEM	IMMEDIATE	AGED
RC	BeautiBond	71.1 (8.9) aA	30.2 (20.4) dB
RC	FL-Bond II	67.9 (8.3) abA	46.0 (7.2) bB
BII	BeautiBond	66.5 (8.0) abA	23.9 (17.1) dB
BII	FL-Bond II	66.8 (12.0) abA	21.2 (4.0) dB
BII-LS	BeautiBond	67.3 (3.0) abA	42.4 (7.6) bcB
BII-LS	FL-Bond II	74.1 (7.6) aA	38.4 (13.4) bcB
BBULK	BeautiBond	69.6 (4.0) aA	51.4 (4.5) aB
BBULK	FL-Bond II	72.9 (5.5) aA	44.7 (6.2) bB

Means followed by different letters indicate statistically significant differences: lowercase letters (a–d) compare resin × adhesive × time groups; uppercase letters (A, B) compare time (T0 vs T1) within each group.
(*) Data represent the average depths from 100 to 500 µm, since this factor showed no significant effect either alone or in interaction with the other factors (four-way ANOVA; Bonferroni post-test, $p < 0.05$).

Table 1

https://doi.org/10.1016/j.dental.2026.03.019

8

Color Appearance of CAD/CAM Materials under CIE-Illuminants and Backgrounds

LF Rondón *[1], BA Mascaro [1], M Tejada [2], M del Mar Pérez [2], RG Fonseca [1], JM Reis [1]

[1] *São Paulo State University (UNESP), Araraquara, Brazil*
[2] *University of Granada, Granada, Spain*

Purpose / Aim: To evaluate the influence of standard CIE illuminants and different colored backgrounds on the color appearance of CAD/CAM ceramics and a resin-based composite, using the D65 standard illuminant as a reference.

Materials & Methods: Specimens (Ø7.5 × 1.0 ± 0.05 mm) of CAD/CAM hybrid VITA Enamic (VE) and feldspathic VITABLOCS Mark II (VM) (VITA Zahnfabrik) ceramics and resin-based composite Grandio Blocs (GB) (VOCO) of shade A2, high translucency, were obtained ($n = 3$) by milling the blocks into cylinders and sectioning them using a cutting machine. Silicon carbide papers (600, 1200, 1500, and 2000 grit) were used for polishing. Colored backgrounds (Ø18 × 1.0 ± 0.1 mm) of IPS Natural Die Material (Ivoclar Vivadent) in five shades (ND1, ND3, ND5, ND7, and ND9) were fabricated to simulate different substrates ($n = 1$ per shade). The spectral reflectance of the samples over the backgrounds was measured using a spectroradiometer (SpectraScan PR670, Photo Research) placed 40 cm away from the sample surface with a 45º/0º illuminating/measuring geometry with CIE 2° standard observer under CIE illuminants (D65, A, F2, and F6) and LED sources (B1, B2, B3, B4, BH1, RGB, V1, and V2). CIEDE2000 color differences (ΔE00) were calculated for each illuminant in comparison to the D65 standard, and perceptibility (PT) and acceptability thresholds (AT) were used for pairwise comparisons. Due to the varying illumination conditions, the CIE 2016 Colour Appearance Model for Colour Management Systems (CIECAM16) chromatic transformation was implemented in MATLAB software (MathWorks) to convert the corresponding color coordinates of a sample under each tested illuminant to CIECAM16 space.

Results: The restorative materials exhibited similar ΔE00 values. Differences above the AT were observed under illuminants A, F2, F6, B1, B2, BH1, RGB, and V1, regardless of the background. Illuminants B3, B4, and B5 produced values below the AT across all backgrounds for both GB and VB, with GB even presenting values below the PT on ND1 and ND9 backgrounds. In contrast, VE showed values above or close to the AT under the same illuminants on the ND5 background. Illuminant V2 produced values close to the AT, independent of the background, for all the materials.

Conclusions: The color appearance of CAD/CAM ceramics and a resin-based composite varied depending on the illuminants and colored backgrounds, relative to the D65 standard illuminant.

https://doi.org/10.1016/j.dental.2026.03.020

9

Effect of Light Exposure on a Novel Dual-Cure Self-Adhesive Cement

C Maucoski [1], P Farrar [2], L Prentice *[2], R Price [1]

[1] *Dalhousie University, Halifax, Canada*
[2] *SDI Limited, Bayswater, Australia*

Purpose / Aim: This study investigates the effect of light exposure on the immediate degree of conversion (DC) and Vickers hardness (VH) at multiple time points (10 min, 1h, and 24h) of a novel dual-cure self-adhesive cement (Set Maxx, SDI Limited) used in conjunction with its recommended primer (Stela Primer, SDI Limited).

Materials & Methods: Stela primer and Set Maxx were tested after light curing (LC) for 20s with Valo X (Ultradent), or self-curing only (SC). The primer was applied on the temperature-controlled Attenuated Total Reflectance sensor set at 32°C under manufacturer's instructions. A 1-mm thick aluminium ring (6-mm internal diameter) was set on top of the ATR, and the cement was dispensed into it. The DC was analysed using a Vertex 70 FT-IR spectrometer. The immediate DC at 420s was measured. After the DC measurements had been completed, the same discs were removed from ATR and bottom VH was measured at 10 min, 1h and 24h. The specimens were kept in dry, dark conditions for 24h at 37°C between analysis. A total of 5 repetitions were made per group ($n = 5$). DC and VH results were compared with ANOVA and Tukey's post hoc test ($\alpha = 0.05$).

Results: The immediate %DC when no light was used was 64.0% ± 1.6 without light and 66.3% ± 3.2 when exposed to light, with no significant difference between groups ($p = 0.203$). Overall, VH values increased significantly over time ($p < 0.001$), with the highest values recorded at 24 hours (52.7 ± 1.0 without light and 53.3 ± 1.2 with light) and the lowest at 10 minutes (26.4 ± 1.1 without light and 30.6 ± 2.6 with light). When comparing groups at the same time point, no significant differences in VH were observed (Figure 1).

Conclusions: Light curing did not significantly increase Set Maxx's immediate DC and VH when used with its corresponding primer. Thus, Set Maxx is a viable cement for clinical situations with limited light access.

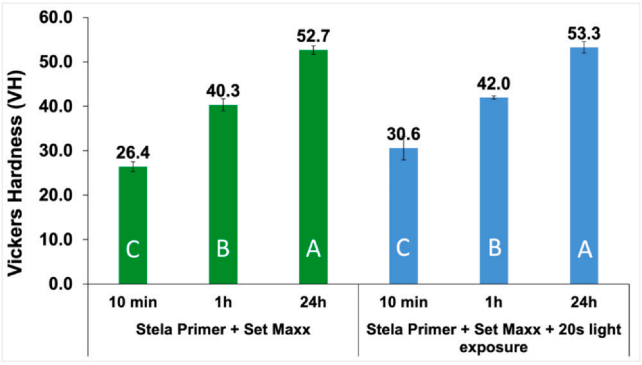

Figure 1

https://doi.org/10.1016/j.dental.2026.03.021

10

3D-Printed PMMA Modified with Niobium Pentoxide: Strength and Roughness

EC Bridi *[1], E Nemi [1], T Navega [1], M Dal Picolo [1], JP Rangel-Coelho [1], RT Basting [1], J Martins [1], V Ortega [1], V Leitune [2], V Cavalli [3]

[1] *Faculdade São Leopoldo Mandic, Campinas, Brazil*
[2] *Universidade Federal do Rio Grande do Sul, Porto Alegre, Brazil*
[3] *Universidade Estadual de Campinas, Piracicaba, Brazil*

Purpose / Aim: The aim of this study was to investigate the effect of incorporating niobium pentoxide (Nb_2O_5) into a 3D-printed poly(methyl methacrylate) (PMMA)-based resin, focusing on its influence on flexural strength and surface roughness.

Materials & Methods: Three different concentrations of Nb_2O_5 were tested (0.5%, 1%, and 2.5% by weight) and compared to a control group (CTR) with no additive. Specimens were fabricated using a Phrozen Sonic Mini 8K 3D printer and standardized CAD design parameters. For the flexural strength test (n = 10), rectangular bars (25 × 2 × 2 mm) were printed following ISO 10477. For roughness analysis (n = 10), disc-shaped specimens (5 mm diameter × 2 mm thickness) were used. All printed samples were washed in isopropyl alcohol for 5 minutes using the Anycubic Wash and Cure system and post-cured under 405 nm UV light (60 W, 15 minutes). Flexural strength was measured using a three-point bending test at 0.5 mm/min in a universal testing machine (Emic). Surface roughness (Ra, μm) was determined by profilometry (Surftest SJ-210, Mitutoyo), based on the average of three readings per specimen. Normality (Shapiro-Wilk) and homogeneity of variance (Bartlett) were confirmed, allowing parametric analysis (one-way ANOVA, α = 0.05) followed by Tukey's post hoc test.

Results: The CTR group presented the highest flexural strength (124.4 ± 7.37 MPa), significantly higher than all experimental groups. Groups with 0.5% (NB05) and 1% (NB1) Nb_2O_5 showed statistically similar strength values (113.3 ± 4.14 MPa and 113.9 ± 3.68 MPa), both higher than the group with 2.5% (NB25) (98.73 ± 2.56 MPa). Regarding surface roughness, CTR exhibited the highest value (0.6110 ± 0.0747 μm), followed by NB05 (0.4440 ± 0.1284 μm). NB1 and NB25 presented the lowest roughness (0.2500 ± 0.0451 μm and 0.2170 ± 0.1376 μm), with no statistical difference between them.

Conclusions: In conclusion, Nb_2O_5 incorporation in 3D-printed PMMA resin significantly reduced surface roughness, particularly at concentrations of 1% and 2.5%. However, this modification also led to a decrease in flexural strength, more notably at 2.5%. The 1% Nb_2O_5 concentration appears to offer a promising balance between mechanical integrity and improved surface characteristics, making it a potential candidate for future formulation studies.

https://doi.org/10.1016/j.dental.2026.03.022

11

Irradiance effect on sorption and conversion of resin cement

L dos Santos Souza *, E Rebelo, T Caneppele, CRG Torres, E Bresciani

São Paulo State University, São José dos Campos, Brazil

Purpose / Aim: This study evaluated the physicochemical properties of a light-cured cement (Bifix Veneer LC Translucent – VOCO, Germany), focusing on water sorption, solubility, and degree of conversion when lightcured using two curing units with different irradiance levels.

Materials & Methods: Discs measuring 15 mm in diameter and 1 mm in thickness (n = 10 per group) were light-cured for 40s on each side using RADII-CAL (860 mW/cm^2) and RADII XPERT (1110 mW/cm). For the degree of conversion analysis, additional specimens measuring 3 mm in diameter were prepared to match the dimensions of the attenuated total reflectance (ATR) crystal used in Fourier-transform infrared (FTIR) spectroscopy. Spectral readings were taken before polymerization and 24h after, based on the ratio between absorption peaks corresponding to aliphatic and aromatic carbon bonds. For the sorption and solubility tests, larger specimens were dried in a desiccator until reaching a constant mass (M1), subjected to 5,000 thermocycles between 5 °C and 55 °C in distilled water, then weighed again (M2), and returned to the desiccator until a second constant mass was achieved (M3). The values were calculated in micrograms per cubic millimeter (μg/mm^3). Data were analyzed using one-way ANOVA followed by Tukey's post hoc test (α = 0.05).

Results: A statistically significant difference in water sorption was found between groups (p = 0.037), with higher absorption observed in specimens cured with the lower-irradiance Radii-cal. In contrast, no statistically significant differences were found in solubility (p = 0.405) or degree of conversion (p = 0.645) between the two curing protocols. The increased sorption in the RADII-CAL group may be attributed to a less densely cross-linked polymer network, which facilitates water diffusion. Nonetheless, the consistently high degree of conversion observed in both groups suggests efficient chemical activation of the cement regardless of light intensity. Clinically, these findings indicate that the tested cement demonstrates reliable chemical performance across different light-curing units, although higher irradiance may enhance resistance to hydrolytic degradation.

Conclusions: In conclusion, while both curing devices yielded adequate conversion and low solubility, the RADII XPERT unit, due to its higher irradiance, provided superior resistance to water sorption and is therefore the preferred option for maximizing the clinical longevity of the cement.

https://doi.org/10.1016/j.dental.2026.03.023

12
Microhardness and translucency of resin cement using different light-curing unit

E Rebelo *, L dos Santos Souza, T Caneppele, CRG Torres, E Bresciani

São Paulo State University, São José dos Campos, Brazil

Purpose / Aim: This study investigated the Knoop microhardness and translucency of light-cured cement (Bifix Veneer LC Translucent – VOCO, Germany) subjected to different light-curing unit.

Materials & Methods: Discs measuring 15 mm in diameter and 1 mm in thickness (n = 10 per group) were light-cured for 40 seconds on each side using two curing units: the RADII-CAL (860 mW/cm^2) and RADII XPERT (1110 mW/cm^2). Microhardness was assessed using nine Knoop indentations distributed across the entire surface of each specimen to obtain mean and standard deviation values. Translucency was measured using a CM-2600 spectrophotometer by calculating the ΔE_{00} between black and white backgrounds. All specimens underwent artificial aging through 5,000 thermal cycles in distilled water alternating between 5 °C and 55 °C. Both microhardness and translucency were measured before and after thermocycling. The values were analyzed using repeated-measures one-way ANOVA followed by Tukey's post hoc test ($\alpha = 0.05$).

Results: A statistically significant difference in microhardness was observed between curing units ($p = 0.005$), with higher values in specimens cured with Radii XPERT. Thermocycling significantly reduced microhardness in both groups ($p < 0.001$), while translucency remained stable regardless of curing unit ($p = 0.210$) or aging process ($p = 0.223$). Clinically, these results suggest that higher irradiance promotes greater polymer cross-linking, enhancing mechanical resistance, which is crucial for maintaining long-term cement integrity under thermal and moisture stress. The observed decline in hardness after aging reflects the material's exposure to simulated oral conditions, yet the unchanged translucency underscores the optical stability of the experimental cement.

Conclusions: In conclusion, both curing protocols preserved the esthetic properties of the material, but Radii XPERT yielded superior microhardness, indicating it is the preferred option to optimize the clinical performance of the cement. The combination of mechanical durability and stable translucency supports the potential of this material for restorative procedures that demand strength and long-lasting esthetics, reinforcing its viability for commercial application in synergy with high-performance light-curing devices.

https://doi.org/10.1016/j.dental.2026.03.024

13
Effect of Temperature and Platform Size on 3D-Printed Restoration Accuracy

U Monteiro *[1], A Rios [1], M Rocha [2], L Correr-Sobrinho [1], A Correr [1]

[1] *FOP/UNICAMP, Piracicaba, Brazil*
[2] *College of Dentistry/UF, Gainesville, USA*

Purpose / Aim: This study evaluated the influence of printing temperature and build platform size on the surface accuracy and volume of resin composite crowns fabricated via 3D printing.

Materials & Methods: Full crowns were digitally designed (DentalCAD 3.2) and printed using resin composite (Vitality, SmartDent, 58 wt% glass filled) at three temperatures (25 °C, 37 °C, and 50 °C) and on two platform sizes (original and reduced). A custom reduced-area printing platform was designed and fabricated for the Photon Mono 2 LCD printer (Anycubic). The platform dimensions were reduced from 143 × 89 mm to 47 × 12 mm, with an inverted trapezoidal geometry (20 mm height) to improve resin drainage. Ten crowns were printed per group (n = 10), resulting in a total of 60 specimens. Each specimen was scanned using an intraoral scanner, and the STL files were exported. Surface deviation from the original reference STL was assessed in the marginal, intaglio, and occlusal regions (Zeiss Inspect). Volumetric data were also obtained. Data were analyzed using two-way ANOVA followed by Tukey's post-hoc test ($\alpha = 0.05$).

Results: Platform size significantly affected intaglio deviation ($p < 0.0001$), with lower values observed for the reduced platform (Table 1). In contrast, marginal and occlusal deviations showed no significant differences with temperature, platform size, or their interaction ($p > 0.05$). For overall surface accuracy, both temperature ($p = 0.0040$) and platform ($p < 0.0001$) had significant effects. The highest overall surface deviation occurred at 25 °C (16.10 ± 0.65 µm), while 37 °C (13.10 ± 0.64 µm) and 50 °C (13.56 ± 0.64 µm) did not differ significantly. The original platform showed greater deviation (16.00 ± 0.53 µm) compared to the reduced one (12.51 ± 0.51 µm). Both temperature and platform size had significant effects on crown volume ($p < 0.0001$), while their interaction was not significant ($p > 0.05$). Crowns printed at 50 °C presented the highest volume (359.56 ± 2.07 mm^3), differing from those printed at 25 °C (349.16 ± 2.07 mm^3) and 37 °C (352.38 ± 2.07 mm^3), which did not differ from each other. Similarly, crowns fabricated on the original platform had significantly higher volume (358.36 ± 2.07 mm^3) than those made on the reduced platform (348.38 ± 1.95 mm^3).

Conclusions: Temperature and platform size significantly influenced surface deviation and volume of printed crowns. Printing at elevated temperatures (37°C and 50°C) and on a reduced-area platform resulted in crowns with superior dimensional fidelity. Adjusting these parameters may improve the accuracy and predictability of additive manufacturing in dental applications.

Table 1. Mean values and standard deviation of surface deviation and volume followed by the statistical grouping according to temperature and platform size.

Factor	Overall (µm)	Oclusal (µm)	Intaglio (µm)	Marginal (µm)	Volume (mm^3)
Temperature (°C)					
25	16.10 ± 0.65 A	12.32 ± 1.48 A	16.17 ± 1.94 A	18.69 ± 1.89 A	349.16 ± 2.07 B
37	13.10 ± 0.63 B	11.53 ± 1.40 A	11.33 ± 1.94 A	16.45 ± 1.84 A	352.38 ± 2.07 B
50	13.55 ± 0.63 B	11.51 ± 1.40 A	14.74 ± 1.94 A	14.42 ± 1.84 A	359.56 ± 2.07 A
Platform					
Original	16.00 ± 0.53 A	12.68 ± 1.20 A	19.12 ± 1.62 A	15.45 ± 1.54 A	358.36 ± 2.07 A
Reduced	12.51 ± 0.51 B	10.89 ± 1.13 A	9.04 ± 1.49 B	17.59 ± 1.49 A	348.38 ± 1.95 B

https://doi.org/10.1016/j.dental.2026.03.025

14
Dimensional distortion of dental models produced by different 3D printers

F Porras-Arancibia, F Murillo-Gómez, G Mojica-Córdoba, J Soto-Montero *

Universidad de Costa Rica, San José, Costa Rica

Purpose / Aim: To compare the accuracy of dental study models produced using four 3D printers commonly employed in dentistry.

Materials & Methods: An ideal acrylic dental model was scanned with the Ineos X5 scanner by Dentsply Sirona to obtain a master model. This model was modified in Blender4Dental to incorporate reference points. Five models (n = 5) were printed on four dental-use 3D printers (Anycubic Photon Mono 4K, M3 Plus, Asiga Max UV, and Phrozen Sonic Mighty 4K), all using a 100-micron layer setting. The printed models were subsequently digitized again using the Ineos X5 scanner and compared with the master STL

model in CloudCompare to measure deviations along the X, Y, and Z axes. Data were analyzed using Minitab 18 through ANOVA or, for non-parametric variables, Mood's median test.

Results: The study revealed variations in outcomes, grouping printers according to consistency and accuracy. The lower-cost printers (Anycubic and Phrozen Mighty 4K) did not show statistically significant differences from the Asiga Max UV in nominal X and Z values, although the latter demonstrated superior accuracy in the Y dimension. Analysis of absolute values in the Z dimension indicated significant differences between the Anycubic Photon Mono 4K and Phrozen Mighty 4K. Printing technology itself was not found to be a determinant of greater accuracy.

Conclusions: This study demonstrates that the current range of 3D printers can achieve clinically acceptable levels of accuracy for dental study models. It also shows that there are no statistically significant differences in the X and Z dimensions between lower-cost and higher-end printers.

https://doi.org/10.1016/j.dental.2026.03.026

15

Properties of resin-based materials exposed to dynamic erosive challenge

C Neto [1], GM De Souza *[2], A Furuse [1]

[1] *University of Sao Paulo Bauru School of Dentistry, Bauru, Brazil*
[2] *University at Buffalo School of Dental Medicine, Buffalo, USA*

Purpose / Aim: The present study aims to evaluate the mechanical and surface properties of direct and indirect restorative resin composites exposed to a dynamic erosive challenge combining fluid flow and toothbrushing.

Materials & Methods: One hundred and twenty resin composite disk specimens (ø 14 mm X 1.2 mm) were prepared and divided into 10 groups: Nanohybrid resin 1 - Empress Direct (NH1)-with erosive challenge (e), NH1-control (c), Nanohybrid resin 2 - Harmonize (NH2)-e, NH2-c, Nanoceramic resin block 1 - Camouflage Now (NC1)-e, NC1-c, Nanoceramic resin block 2 - Shofu Block (NC2)-e, NC2-c, Polymer-infiltrated ceramic network - Vita Enamic (PICN)-e, PICN-c. Specimens with erosive challenge were submitted to 5% hydrochloric acid (HCl, pH =1.2) flow for 96 h, and, subsequently, brushed for 14,600 cycles. Surface topography was analyzed through scanning electron microscope (SEM). Biaxial flexural strength (BFS – 0.5mm/min), surface hardness (Vickers) and roughness (non-contact profilometer) were also analyzed. The data obtained was subjected to normality and homogeneity tests, followed by the ANOVA and Tukey tests and results were evaluated at a significance level of 5%.

Results: SEM images revealed surface degradation for all materials submitted to erosive challenge, except for PICN-e. Two-way ANOVA results indicated that only material had a significant effect on BFS ($p < 0.001$): highest values were presented by NC1 and NC2. The interaction material*aging significantly affected roughness and surface hardness; all materials presented significantly higher roughness after the erosive challenge. Microhardness was reduced for all materials submitted to HCl and toothbrushing, except PICN-e.

Conclusions: The erosive challenge with HCl acid flow simulation has affected the surface of most resin-based materials tested, without compromising their flexural strength. Nanoceramic resin blocks presented the greatest mechanical performance, while Polymer-infiltrated ceramic network blocks exhibited the best surface properties.

https://doi.org/10.1016/j.dental.2026.03.027

16

Color and roughness change of a stained monochromatic resin composite

R Tango *, F Lessa, R Eguti, G Yamada, M Barcellos, B Ciciliati

Institute of Science and Technology, Sao Jose dos Campos, Brazil

Purpose / Aim: To evaluate the change in color and superficial roughness of a monochromatic resin composite upon immersion in staining solutions and to accelerated artificial aging under UV light.

Materials & Methods: Sixty-four specimens (8mm in diameter x 2mm in height), 32 of each material (Vittra APS Unique - monochromatic and Vittra APS – micro-hybrid), were light-cured, polished, and submitted to color and roughness measurements using a benchtop spectrophotometer (CIE D65 standard illuminant, d/8°, 2° 1931 standard observer, specular component included, UV component included) and a contact surface profilometer, respectively. The specimens were then divided according to treatment (n = 8): deionized water, coffee, red wine, and UV aging. Changes in color (ΔEab and ΔE00) and roughness (Ra - mm) were measured at baseline and after two different time intervals: 2.5 days (T1) and 5 days (T2). Data of ΔEab, ΔE00, and Ra values were tabulated and were submitted to ANOVA and Tukey test, both with a = 0,05. The color differences of $\Delta E00 \leq 0.8$ and ≤ 1.8 were used to interpret the results according to 50/50% perceptibility and acceptability thresholds.

Results: Vittra APS Unique showed greater color change (ΔEab and ΔE00) compared to Vittra APS ($p < 0.001$). The roughness of the specimens decreased at T1 and increased at T2 ($p < 0.001$).

Conclusions: The color stability and roughness of monochromatic resins were influenced by exposure time to different staining solutions. Vittra APS resin showed the most satisfactory performance in relation to the parameters analyzed.

https://doi.org/10.1016/j.dental.2026.03.028

17

Physical Properties Comparison for Bis-GMA Free Light-Cure Composites

Q Ma *[1], B Liu [1], J Sun [2], BI Suh [1]

[1] *BISCO, Inc, Schaumburg, USA*
[2] *ADA Forsyth, Somerville, USA*

Purpose / Aim: With outstanding mechanical properties and wear resistance, bisphenol A-glycidyl methacrylate (Bis-GMA) as a monomer has been widely used in dental composites. Meanwhile, new monomers have been explored as Bis-GMA alternatives to improve clinical performance. Recent studies highlighted a combination of triethylene glycol divinylbenzyl ether (TEG-DVBE, V) and urethane dimethacrylate (UDMA, U) as a promising resin system for developing durable dental resin composites. However, studies evaluating the mechanical performance of TEG-DVBE-based composites versus commercial Bis-GMA-based composites remains rare. In this study, experimental Composites 1-4 were formulated using UDMA and TEG-DVBE (U/V= 3/1 or 1/1) resins and different percentages of filler particles compared with commercially available universal composite (Quantium, BISCO, Inc). Compressive Strength (CS), Flexural Strength (FS), Degree of Conversion (DC), and Volumetric Shrinkage (Sv) were used as screening methods to examine their physical properties comparison.

Materials & Methods: Methods: Specimens for CS test were prepared in 6 mm high by 4 mm diameter cylinders with 40s light curing each side, which were stored in deionized water at 37 ± 1°C

for 23 h ± 15 min. FS was evaluated according to procedure ISO4049. DC of the composites were examined at 30 min post-irradiation by ATR-FTIR (iS50, Nicolet) using the aromatic C=C absorption band as the internal standard. Sv was tested using AcuVol (BISCO, Inc) at 5 min post-irradiation. All specimens were light cured by VALO LED (Ultradent, Inc) at 1000 mW/cm^2. One-Way ANOVA and post hoc Tukey were performed for the statistical analysis.

Materials: Quantium Universal Composite (Incisal, Lot#2400014085; A3.5B, Lot#2400013743; BISCO, Inc), Experimental Composites 1-4 (formulated using the same powder blend as Quantium).

Results: In Table 1

Conclusions: As an alternative to traditional Bis-GMA/TEGDMA based composite, Bis-GMA-free experimental composites containing UDMA and TEG-DVBE demonstrated comparable mechanical performance. Although the degree of vinyl conversion was lower, resin composites based on U/V exhibited higher CS than Quantium. In general, CS, FS, and Sv were enhanced with the addition of more fillers. Additional tests, including staining resistance, hardness, hydrolytic stability, and formulation optimization, will be conducted for further evaluation.

Table 1. Collected CS, FS, DC and S_V of **Composite 1-4** and **Quantium**

Sample	CS (MPa) (n=8)	FS (MPa) (n=5)	DC (%) (n=1)	S_V (%) (n=3)
Composite 1 (U/V: 3/1, filler: 84.9%)	321.1 ± 21.6^{ab}	115.4 ± 11.9^{a}	55.6	3.0 ± 0.1^{a}
Composite 2 (U/V: 3/1, filler: 83.9%)	321.9 ± 34.0^{abc}	93.3 ± 5.9^{c}	55.6	3.0 ± 0.2^{a}
Composite 3 (U/V: 1/1, filler: 84.6%)	338.7 ± 28.2^{a}	103.6 ± 4.5^{b}	52.2	2.9 ± 0.1^{a}
Composite 4 (U/V: 1/1, filler: 83.9%)	309.2 ± 15.9^{bc}	102.9 ± 2.6^{b}	52.2	3.0 ± 0.1^{a}
Quantium (Incisal, Filler: 78-83%)	292.8 ± 27.7^{c}	108.0 ± 13.7^{abc}	64.6	3.0 ± 0.2^{a}
Quantium (A3.5B, Filler: 85-89%)	305.1 ± 32.5^{bc}	119.2 ± 8.4^{a}	62.6	2.3 ± 0.1^{b}

Different superscript letters in each column indicate groups that are significantly different ($p < 0.05$). Groups identified with the same superscript letters in each column are not significantly different ($p > 0.05$).

https://doi.org/10.1016/j.dental.2026.03.029

18

Enhancing Dental Restorations with Extended Longevity: Impact of Tetramethyl-Methacrylate Incorporation

J Batista *[1], MA Fraga [1], V Torso [2], M Yoshida [2], AC Aranha [2], AP Fugolin [3], A Correr [1], M Sinhoreti [1]

[1] *State University of Campinas, Piracicaba, Brazil*
[2] *University of Sao Paulo, Sao Paulo, Brazil*
[3] *Oregon Health & Science University, Portland, USA*

Purpose / Aim: Evaluate physicochemical effects of incorporation of an elastomeric urethane monomer (Exothane-24) as an alternative material for improvement of Non-carious cervical lesions (NCCL) resin-based restorations.

Materials & Methods: Two experimental groups were evaluated: Exothane-24 60 wt% or 65 wt% filler particles (E60 and E65), and two control groups containing UDMA with 60 wt% or 65 wt% (U60 and U65). Organic matrix of Exothane-24 or UDMA (control) 25 wt %, TEGDMA 25 wt%, and BisEMA 50 wt%. Photoinitiation system were 0.5 wt% of camphorquinone and 0.5 wt% of DMEAM. Barium-aluminum-silicate glass (0.7 μm) 80 wt% and nanosilica particles (0.05 μm) 20 wt% as filler particles. Photocuring under 1.200 mW/cm^2 irradiance. Specimens were submitted to 10,000 cycles of simulated toothbrushing for surface wear assessment by 3D optical profilometer. The crosslink density was measured by the variation in Knoop hardness (KHN) before and after incubating the samples (5 x 5 x 2 mm, n = 10) in absolute ethanol for 24 hours. Two-way ANOVA and Tukey's post-hoc test ($p < 0.05$) were performed.

Results: Exothane-24 significantly increased wear resistance (U60 = 6.73 μm and E60 = 5.13 μm, p = 0.013) and the crosslinking density (U60 = 54.22 % and E60 = 76.30 %) (Fig. 1). There was no statistical difference on surface wear for E65 and U65.

Conclusions: Exothane-24 enhanced cross-link density and wear resistance. These outcomes may culminate in the development of a resin composite formulation that offers potential to extend the clinical lifespan of NCCL dental restorations, thereby enhancing overall oral health care.

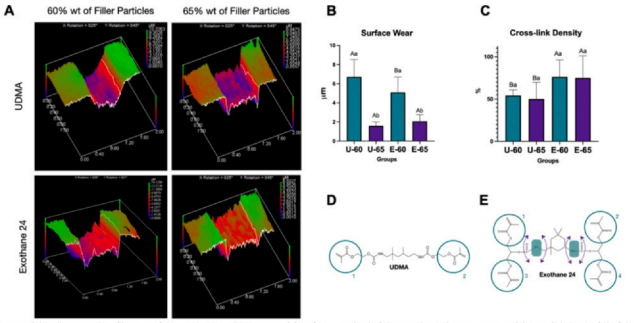

Figure 1. (A) Tridimensional profilometry of U60, U65, E60 and E65 groups. (B) Surface wear (μm) of the tested resin-base composites. (C) Cross-link density (%) of the tested resin-based composites. For (B) and (C) Tukey's post-hoc test: different capital letters indicate a statistically significant difference between the monomers. Different lowercase letters indicate a statistically significant difference between the fillers content. (D) Molecular structure of urethane dimethacrylate (UDMA). (E) Molecular structure of Exothane-24.

https://doi.org/10.1016/j.dental.2026.03.030

19

Zirconia-Based Glass Coatings as a finishing alternative for 5Y-PSZ

AC Silva *[1], J de Freitas Gouveia [1], B Serralheiro [1], K Souza [1], J Junqueira [1], RM Melo [1], T Campos [2]

[1] *UNESP, São José dos Campos, Brazil*
[2] *UFPel, Pelotas, Brazil*

Purpose / Aim: To evaluate the coating of 5Y-PSZ zirconia with experimental zirconia-based glasses as a strategy to provide antimicrobial properties while remaining its aesthetic and mechanical behavior.

Materials & Methods: After sintering, 40 disc-shaped (12 × 1.2 mm) and 20 square-shaped specimens (4 × 4 × 1.6 mm) of 5Y-PSZ zirconia (Zpex Smile) were divided into the following coatings groups: as-sintered (C), commercial glaze (G), experimental glass containing 5 g of zirconia (5 g), and experimental glass containing 10 g of zirconia (10 g). The commercial glaze (Vita Akz 25, VITA Zahnfabrik, Germany) was applied to the samples using a brush and then fired at 900°C for 1 min. Experimental glass powders (5 g and 10 g) were individually mixed with propylene glycol, applied with a brush, and fired following a two-step firing process (1200 °C for 20 min, and 700 °C for 30 min). Biaxial flexural strength (MPa), translucency (TP00), and surface roughness (Ra and Rz) were measured. Antimicrobial activity was assessed by quantifying colony-forming units (CFU/mL) of Escherichia

Results: The biaxial flexural strength showed statistically similar results among groups: C (488.5 ± 61.0 MPa), G (518.1 ± 83.0 MPa), 5 g (494.4 ± 100.0 MPa), and 10 g (440.0 ± 31.0 MPa) ($p > 0.05$). The 5 g group presented translucency values statistically similar to the C and G groups ($p > 0.05$). Additionally, the 5 g group exhibited the lowest roughness values (Ra and Rz) ($p < 0.001$). Both 5 g and 10 g groups demonstrated significant antimicrobial activity against E. coli, showing lower CFU counts compared to C and G ($p < 0.001$).

Conclusions: Experimental zirconia-based glass coatings (5 g and 10 g) applied to 5Y-PSZ zirconia effectively impart antimicrobial activity against E. coli without compromising the material's mechanical strength or optical properties. The 5 g formulation showed favorable outcomes in terms of surface smoothness and aesthetics.

https://doi.org/10.1016/j.dental.2026.03.031

20

Curing Depth of Flowable Bulk-Fill Composites: Short Fiber-Reinforced vs. Conventional

E Säilynoja *[1,2], S Garoushi [2], P Vallittu [3], L Lassila [2]

[1] *Stick Tech Ltd - a GC Europe company, Turku, Finland*
[2] *Turku Clinical Biomaterial Center, University of Turku, Turku, Finland*
[3] *University of Turku, Turku, Finland*

Purpose / Aim: The use of flowable bulk-fill short fiber-reinforced composite (SFC) as a root canal post cement has been proposed by several researchers. However, whether light-curing provides sufficient polymerization in the deeper regions of the root canal space remains uncertain. This study aimed to evaluate the depth of cure of a flowable SFC (everX Flow, GC Corporation) and a conventional bulk-fill composite (SDR flow+, Dentsply-Sirona) by assessing surface microhardness (VH) and degree of conversion (DC %) at various depths within prepared root canals.

Materials & Methods: Root canals of human teeth with single, straight roots were prepared to a depth of 12 mm. The test materials were applied into the canals in bulk and polymerized using a light-curing unit (D-Light Pro, GC Corporation) for 40s (n = 4 teeth per material). Following polymerization, the teeth were sectioned mesiodistally using a ceramic cutting disc operating at 100 rpm under water cooling. The sectioned surfaces were then gently polished using #4000-grit silicon carbide papers. DC% was determined at coronal, middle, and apical depths using FTIR spectroscopy, and surface microhardness was measured using a Vickers indenter.

Results: The everX Flow composite demonstrated higher DC% values, ranging from 75 to 62, and higher VH values compared to the SDR flow+ composite, which showed DC% values ranging from 59 to 53 at various depths ($p < 0.05$). The SDR flow+ exhibited a marked decrease in VH values beyond 4 mm depth inside the root canal, whereas for everX Flow, this decline was observed only beyond 8 mm.

Conclusions: Flowable bulk-fill composite reinforced with microglass fibers demonstrates greater curing depth than conventional bulk-fill composite. These results support the suitability of everX Flow as a post-luting material in endodontically treated teeth.

https://doi.org/10.1016/j.dental.2026.03.032

21

Fabrication of CAD/CAM graded ceramic-reinforced resin post-and-core system

Y Wang *, J Yun

Hospital of Stomatology, Sun Yat-sen University, Guangzhou, China

Purpose / Aim: This study aims to develop a functional resin composite material characterized by a gradient of mechanical properties for computer-aided design and computer-aided manufacturing (CAD/CAM) post-and-core restoration and to investigate its influence on the biomechanical behavior of severely defective teeth.

Materials & Methods: Urethane dimethacrylate (UDMA)-based resins were reinforced with ZrO2 ceramic nanoparticles in the 0–20 wt% concentration range to fabricate CAD/CAM composites. The resulting composites were further designed to construct a post-and-core with graded elastic modulus with finite element analysis. Three groups were created according to the materials and techniques: FPC, traditional prefabricated fiber post plus resin composite core; HPC, CAD/CAM homogeneous post-and-core; GPC, CAD/CAM graded post-and-core. Finite element analysis and in vitro fracture test were performed to compare the biomechanical behavior of the restored teeth.

Results: Experimental resin composites presented an improved elastic modulus from 6.7 GPa to 9.8 GPa as the ZrO2 contents increased from 0 wt% to 10 wt%. Finite element analysis suggested that the GPC model with the coronal–apical layer design of 6-4-3 mm based on the experiential elastic modulus of 9.8-8.5-6.7 GPa demonstrated a more favorable stress distribution than FPC and HPC. In vitro fracture tests revealed that both GPC and HPC groups possessed a higher root repairable failure rate of 33%, compared with the FPC group.

Conclusions: Newly developed CAD/CAM composite with a gradient of mechanical properties may offer a wide range of restorations with reliable clinical long-term survival.

https://doi.org/10.1016/j.dental.2026.03.033

22

Effects of Er:YAG laser on debonding of LiSi veneers

X Li *[1], R Sun [1], X Xu [1], W Bi [2], R Carvalho [3], Z Yan [1], L Sun [1]

[1] *Hefei Clinical School of Stomatology, Anhui Medical University., Hefei, China*
[2] *UPCERA Collaborative Research Center, Liaoning Upcera Co., Ltd., Shenyang, China*
[3] *Division of Biomaterials, Department of Oral Biological & Medical Sciences, Faculty of Dentistry, University of British Columbia, Vancouver, Canada*

Purpose / Aim: To evaluate the effects of Er: YAG laser energy level and veneer thickness on the time required for debonding Lithium disilicate (LiSi) veneers.

Materials & Methods: LiSi veneers of 0.2 mm and 0.5 mm were fabricated and bonded to enamel using a standard protocol. Debonding was performed using an Er: YAG laser (10 Hz) at five energy levels (140, 160, 180, 200, and 220 mJ; n = 6 per group). Debonding time and pulpal temperature changes were recorded for each group. Post-debonding enamel surfaces were examined by scanning electron microscopy (SEM) to assess debonding mode and potential surface damage and adhesive residue. Statistical analysis was conducted using two-way ANOVA with Bonferroni post hoc tests ($\alpha = 0.05$).

Results: All laser application protocols were able to debond the veneers. The temperature changes in the pulpal cavity during laser removal ranged from -0.39°C to +2.71°C. At 180 mJ of Er: YAG laser, the 0.2 mm veneer removal time was 10.9 ± 2.3 s, which was significantly lower than that in the 140 mJ group (71.5 ± 8.4 s) and 160 mJ group (54.3 ± 6.9 s) ($P < 0.05$); at 200 mJ of Er: YAG laser, the 0.5 mm veneer removal time was 9.1 ± 3.1 s, which was significantly lower than that of the 140 mJ group (96.1 ± 6.8 s), 160 mJ group (66.8 ± 10.1 s) and 180 mJ group (21.0 ± 2.8 s) ($P < 0.05$). In addition, the removal time was always longer for thicker veneers under the same energy level. SEM showed that the bond failure mode shifted from adhesive-veneer interface fracture and internal adhesive fracture to enamel-adhesive interface fracture

with increasing laser energy, and enamel exposure was observed in the 220 mJ group.

Conclusions: Both the laser energy level and veneer thickness had a significant effect on the time required to debond LiSi veneers bonded to enamel. In general, thinner veneers and higher energy levels resulted in less time required to debond the veneers.

https://doi.org/10.1016/j.dental.2026.03.034

23

Physicochemical and mechanical properties of a flavonoid-modified universal adhesive

J Oliveira *[1], M Pires [1], H Vilela [2], V Peruchi [1], L Fernandes [1], A Campos [2], IP Soares [1], F Mon [1], R Braga [2], CA de Souza Costa [1], J Hebling [1]

[1] *São Paulo State University, Araraquara, Brazil*
[2] *University of São Paulo, São Paulo, Brazil*

Purpose / Aim: This study evaluated the impact of incorporating quercetin (QU) or proanthocyanidins-rich grape seed extract (GSE) on the physicochemical and mechanical properties of a universal adhesive system.

Materials & Methods: Different concentrations of QU (0.025%, 0.05%, 0.075%, 0.1%, and 0.5%) or GSE (0.25%, 0.5%, 0.75%, 1%, and 5%) (% w/v) were incorporated in the Scotchbond Universal Adhesive, and compared with the non-modified adhesive (control). The degree of conversion and maximum polymerization kinetics (FTIR/ATR, n = 3) guided the selection of the concentrations for further evaluation of water sorption (n = 6), solubility (n = 6), restorative resin color change (ΔE_{00} - total color difference according to the CIEDE2000 method, TP_{00} - translucency parameter, and ΔWID - whiteness index for dentistry; n = 8), ultimate tensile strength, and flavonoid release (n = 10). The data were analyzed using ANOVA and specific post-hoc tests (α = 5%).

Results: No differences were observed in the degree of conversion and polymerization kinetics between the two highest concentrations of QU (0.1% and 0.5%) or GSE (1% and 5%) and the control ($p > 0.05$). Thus, these concentrations were used in the subsequent tests. Water sorption was similar to the control group ($p > 0.05$), but solubility increased by 80.6% with the incorporation of 5% GSE ($p < 0.0001$). The 5% GSE concentration promoted a significantly greater color change of the restorative resin (ΔE_{00} and ΔWID) compared to the control ($p < 0.0001$), exceeding the acceptability threshold. The other concentrations of QU and GSE showed no significant differences in TP_{00} ($p > 0.05$). The incorporation of QU did not affect ultimate tensile strength at any tested concentration, while the addition of 1% and 5% GSE significantly reduced this property compared to the control ($p < 0.0001$). Flavonoid release was detected only for SBU + 5% GSE.

Conclusions: The concentrations of 0.5% QU and 1% GSE were the highest that could be incorporated into the universal adhesive, presenting the least negative impact on its physicochemical and mechanical properties. However, no drug release was detected for these concentrations.

https://doi.org/10.1016/j.dental.2026.03.035

24

Impact of Different Sintering Temperatures and Aging on Second-Generation 3Y-TZP

M Piza *[1], T Campos [2], H Strazzi-Sahyon [1], AC Pereira [1], E de Oliveira Sousa [1], EB Benalcázar-Jalkh [1], LM Alves [1], EA Bonfante [1]

[1] *Bauru School of Dentistry, University of São Paulo, Bauru, Brazil*
[2] *Federal University of Pelotas, Pelotas, Brazil*

Purpose / Aim: To evaluate the effects of sintering temperature and hydrothermal aging on the physical, mechanical, and optical properties of a second-generation 3Y-TZP.

Materials & Methods: A total of 320 specimens were prepared through uniaxial pressing of the ceramic powder (Zpex, Tosoh) at 3 tons for 30s using a cylindrical steel die, resulting in disk-shaped specimens with 1.25 mm thickness and 12.2 mm diameter. All specimens underwent presintering at 600 °C for 1 h and 1000 °C for 1 h. Four sintering temperatures were evaluated: 1450 °C, 1500 °C, 1550 °C, and 1600 °C (2 h, 5 °C/min; n = 80 per group). Aging was performed in a hydrothermal reactor at 134 °C for 20 h under 2.2 bar, with specimens immersed in distilled water (n = 40). For each sintering temperature, 10 specimens were first used for density evaluation (Archimedes' method), then polished for optical measurements (contrast ratio and translucency parameter) before and after aging (repeated measures). Biaxial flexural strength testing was performed on 30 specimens per condition, and Weibull analysis was employed to calculate characteristic strength (MPa) and Weibull modulus (m), both with 95% confidence intervals. Density was analyzed by one-way ANOVA, and optical properties by two-way ANOVA with repeated measures, both with post hoc Tukey test (α = 0.05).

Results: All groups exhibited high relative density (> 98.1%), with no significant differences among sintering temperatures. In the immediate condition, contrast ratio (CR) and translucency parameter (TP) showed no significant differences among temperatures. After aging, CR and TP significantly changed for 1550 °C and 1600 °C, with 1600 °C presenting the highest opacity and lowest translucency. Characteristic strength was similar among temperatures in the immediate condition, although 1500ºC exhibited numerically higher values. No significant changes in characteristic strength were observed after aging in any of the groups. Weibull modulus was comparable among temperatures in both conditions but significantly increased after aging for 1550 °C and 1600 °C.

Conclusions: Sintering at 1450 °C and 1500 °C produced a 3Y-TZP with reliable optical and mechanical properties, maintaining stability after aging.

https://doi.org/10.1016/j.dental.2026.03.036

25

Thermographic evaluation of incremental vs bulk-fill techniques in deep cavities

H Algamaiah *[1], A Alayed [1,2], J Yang [3], D Watts [2], A Alshabib [1]

[1] *Department of Restorative Dental Science, College of Dentistry, King Saud University, Riyadh, Saudi Arabia*
[2] *Biomaterials Science, Dentistry, School of Medical Sciences, University of Manchester, Manchester, UK*
[3] *Applied Oral Sciences and Community Dental Care, Faculty of Dentistry, The University of Hong Kong, Hong Kong, China*

Purpose / Aim: To thermographically evaluate and compare different resin composite placement techniques-incremental versus bulk-fill-on pulpal temperature dynamics in deep cavities with a remaining dentin thickness (RDT) of 1 mm, using high-resolution infrared thermography.

Materials & Methods: Fifteen 1-mm dentin slices derived from human molars were integrated into standardized 3D-printed molds to simulate deep cavities. Three clinically relevant protocols were compared: (1) conventional incremental layering with two 2-mm applications of non-flowable Tetric Powerfill (INC), a flowable-first incremental approach using Tetric Evoflow bulkfill followed by Powerfill (INC-F), and a single 4-mm bulk-fill application of Powerfill (Bulk). All specimens were polymerized using a calibrated Elipar S10 unit (1200 mW/cm^2, 10 s). A thermal imaging system recorded spatiotemporal heat distribution at critical anatomical landmarks: 3 mm and 1 mm above the dentin, dentin surface, and pulp roof. Key parameters included peak temperature rise (ΔT) and time-to-maximum (Tmax).

Results: While polymerization reaction resulted in temperature rise (ΔT) 11.6 to 18.00 °C within the composite. However, with 1 mm remaining dentin thickness, ΔT across dentin (pulpal roof) recorded were 8.5-9.2 °C in first increment and 3.8-4.6 °C with second increment. Bulk-fill restorations produced highest temperature rise in the upper composite segment, however this did not translate linearly to the pulpal roof point ($p > 0.5$). In fact, the thermal burden at the pulp roof was consistently low in all protocols. Tmax values (Table 1) revealed delayed heat arrival at the pulp roof ranging from 10.1-11.6 s to reach maximum temperature. Thermal energy dispersion remains consistent across different placement protocols, however the time to reach maximum temperature (Tmax) is significantly extended on the dentin surface during the second increment of placement.

Conclusions: Resin composite polymerization produced a localized exothermic behavior within each increment, yet increasing the distance from the dentin surface did not significantly reduce pulpal heat transfer with 1 mm of remaining dentin thickness. Placement techniques and material types showed no significant impact on temperature rise. Notably, the first cured increment served as a thermal barrier, delaying heat transmission from subsequent layers. These findings highlight the importance of considering thermal kinetics alongside material selection and layering protocols in restorative procedures.

Mean temperature rises (ΔT, °C) of the three application protocols: incremental (INC), incremental using flowable first increment (INC-F), and bulkfill (Bulk) techniques.

Materials		Positions			
		3 mm above dentin	1mm above dentin	Dentin surface	Pulp roof
INC	Adhesive	8.1 ^{cA} (0.18)	5.8 ^{cB} (0.77)	6.5 ^{bAB} (1.59)	5.7 ^{bcdB} (1.59)
	1st layer	13.3 ^{bAB} (1.06)	14.4 ^{aA} (1.43)	11.7 ^{aB} (0.79)	9.0 ^{aC} (0.92)
	2nd layer	14.3 ^{bA} (1.08)	7.6 ^{bcB} (0.63)	5.5 ^{bC} (0.32)	3.8 ^{dD} (0.32)
INC-F	Adhesive	8.0 ^{cA} (1.25)	5.7 ^{cB} (0.53)	7.2 ^{bAB} (0.77)	7.3 ^{abAB} (0.98)
	1st layer	13.4 ^{bB} (2.41)	16.5 ^{aA} (1.43)	13.1 ^{aB} (0.98)	9.2 ^{aC} (1.55)
	2nd layer	16.9 ^{aA} (0.86)	10.0 ^{bB} (2.79)	6.4 ^{bC} (1.33)	4.6 ^{cdC} (0.85)
Bulk	Adhesive	8.4 ^{cA} (0.34)	6.1 ^{cA} (0.53)	7.2 ^{bA} (1.94)	6.8 ^{abcA} (2.25)
	Bulk	18.0 ^{aA} (0.51)	14.2 ^{aB} (1.41)	11.6 ^{aC} (1.32)	8.5 ^{aD} (0.50)

For each position, the same lower case superscript letters indicate homogeneous subsets among the groups. For each group, the same CAPITAL superscript letters indicate homogeneous subsets among different positions.

Table 1

https://doi.org/10.1016/j.dental.2026.03.037

26

Flexural strength of different layers in 4/5Y TZP zirconia materials

U Lohbauer *, R Belli

University of Erlangen, Erlangen, Germany

Purpose / Aim: Zirconia recently showed an emerging trend towards universal applications. Multilayer materials with either color grading or additional strength-translucency grading were introduced to the market. Along with new developments in powder technology, and hence stronger and still highly translucent precursor granulates, a series of all-in-one multilayer materials entered the market, aiming to serve for universal clinical indications. The aim of this study was to analyze the flexural strength of the different layers of representative 4/5Y-TZP zirconia materials under three-point bending conditions.

Materials & Methods: Oversized specimens of 5mmx4mmx30mm were CAD/CAM milled (Brain Expert, DeguDent) from zirconia discs ($n = 13$ per disc) in three different layers: 5.0mm from the cervical edge, 3.3mm and 1.1mm from the incisal edge. The following 4/5Y-TZP materials were compared (A4 shades): Cercon yo ML ((CE) DeguDent), Katana Zirconia YML ((KA) Kuraray Noritake), Optimill 3D ProZir ((PZ) Aidite), and IPS e.max ZirCAD Prime Esthetic ((PE) Ivoclar). All specimens ($n = 30$ per group) were densely sintered using standard sintering regimes in a Zyrcomat 6000 MS furnace (Vita Zahnfabrik). The specimens were finished (P1200) on a Tegramin-25 polishing device (Struers) to final dimensions of 4x3mm. The specimen flanges were beveled and the tension faces were further polished up to P2400 grit size. The

uniaxial fracture tests were conducted in a universal testing machine (2KN load cell, 20N/s) on a 20mm three-point bending fixture (ISO6872). The fracture strength mean values were calculated and statistically analyzed using Weibull statistics as well as ANOVA, including a post hoc S-N-K analysis (alpha = 0.05). Selected specimens were fractographically inspected for reasons of defect types.

Results: The fracture strength and Weibull data are presented in Table 1.

Conclusions: Table 1 shows highest characteristic strength for the material Cercon yo ML, regardless of the tested layer. Katana Zirconia YML offers high strength in the dentin layer, with significant drop towards the enamel region. The material 3D Pro Zir showed the lowest strength in the dentin layer and stays far behind manufacturer data (> 1100 MPa). IPS e.max ZirCAD Prime Esthetic consisted of a continuous gradient of 4Y- and 5Y-TZP, even in the dentin layer (45% 4Y-TZP) and hence clinical indications are limited to class 4 use (up to 3-unit bridges). ISO 6872:2024 provides a flexural strength threshold of > 800 MPa for the clinical use as class 5 material. Only the material Cercon yo ML fulfilled this criterion in all tested layers and is thus clinically recommended for all-in-one use.

Table 1: Fracture strength data FS (± SD), m, and σ_0, including respective 90% confidence intervals.

	Mean Flexural strength (±SD) [MPa]	Weibull-modulus m	90% Confidence interval	Characteristic strength σ_0 [MPa]	90% Confidence interval [MPa]
CE_1.1	1036.87 ± 157.7 ^{A}	9.4	7.0 – 11.4	1097.04	1058.57 – 1137.35
CE_3.3	1131.43 ± 284.7 ^{A}	5.2	3.9 – 6.3	1236.02	1158.53 – 1319.63
CE_5.0	1142.73 ± 316.9 ^{A}	4.7	3.5 – 5.8	1254.10	1168.37 – 1347.19
KA_1.1	622.50 ± 109.9 $^{C, D}$	7.3	5.5 – 8.9	665.60	635.85 – 697.09
KA_3.3	867.84 ± 147.7 ^{B}	8.5	6.3 – 10.3	921.50	885.82 – 959.02
KA_5.0	1045.97 ± 82.1 ^{A}	16.5	12.3 – 20.1	1080.85	1059.15 – 1103.24
PZ_1.1	623.82 ± 131.6 $^{C, D}$	5.5	4.1 – 6.7	676.05	636.16 – 718.92
PZ_3.3	704.86 ± 99.6 ^{C}	8.4	6.3 – 10.3	747.06	718.07 – 777.57
PZ_5.0	685.71 ± 93.2 ^{C}	9.8	7.3 – 11.9	723.07	698.77 – 748.50
PE_1.1	571.97 ± 91.7 ^{D}	6.5	4.8 – 7.9	611.00	580.22 – 643.78
PE_3.3	802.02 ± 97.7 ^{B}	9.3	6.9 – 11.3	844.71	814.80 – 876.07
PE_5.0	853.62 ± 102.5 ^{B}	10.0	7.4 – 12.2	897.17	867.00 – 928.75

Same superscript letters indicate statistically homogeneous subgroups.

https://doi.org/10.1016/j.dental.2026.03.038

27

Tests for Evaluating the Bond Strength of Adhesives to Dentin

P Moreira *[1], J Soyama [2], V Araujo-Neto [1], M Giannini [1]

[1] *University of Campinas, Piracicaba, Brazil*
[2] *University of Campinas, Campinas, Brazil*

Purpose / Aim: This study aimed to compare mechanical testing methodologies for evaluating the bond strength of two adhesive systems to dentin.

Materials & Methods: Three mechanical tests were evaluated: microtensile bond strength, shear bond strength, and interfacial fracture toughness. Two adhesives were tested, one self-etching (Clearfil SE Bond 2/CSEB, Kuraray) and a universal used in etch-and-rinse mode (Tetric N-Bond Universal/TNBU, Ivoclar). Extracted human molars were used, which had occlusal enamel removed to expose the coronal dentin. For the microtensile test, parallelepiped-shaped specimens with a cross-sectional area of less than 1 mm^2 were used (n = 12). For the shear test, the mold-enclosed technique with a bonded area of 3.14 mm^2 was used (n = 12). The Splint-Chevron-Notched-Beam specimens were used to evaluate the interfacial fracture toughness (n = 12). The specimens from the three methodologies were tested on a universal testing machine (1 mm/min). The data were analyzed by one-way ANOVA ($\alpha = 0.05$).

Results: No statistical difference was found between the adhesives for any of the tests performed. For the microtensile test, the bond strength values ranged from 41.4 (5.2) MPa (TNBU) to 42.1 (4.9) MPa (CSEB). For the shear bond strength test, the values ranged from 13.0 (4.8) MPa (TNBU) to 14.2 (4.8) MPa (CSEB). The fracture toughness test yielded 1.24 (0.15) $MPa{\cdot}m^{1/2}$ for TNBU and 1.28 (0.19) $MPa{\cdot}m^{1/2}$ for CSEB.

Conclusions: The fracture toughness results showed substantially lower data dispersion compared to conventional tensile and shear tests; however, the complexity of specimen preparation may compromise its reproducibility.

Supported by FAPESP (2024/18594-9)

https://doi.org/10.1016/j.dental.2026.03.039

28

Influence of different impression areas on 3D resin-based composites properties

A Germano, F Trevisan, F Collares *

UFRGS, Porto Alegre, Brazil

Purpose / Aim: The aim of this study was to evaluate the influence of different 3D printing regions on the properties of 3D printed resin composites (3D RBCs).

Materials & Methods: The radiant light exposure on the LCD of the Photon Mono M5s Pro printer (AnyCubic) was mapped and converted into irradiance (mW/cm^2) using a UV meter with an 8 mm diameter aperture. The 3D RBCs used (VS, VARSEO SmileCrown, Bego, and BC, Prizma BioCrown, MakertechLabs) were processed according to the manufacturer's instructions. To assess the printing region, specimens were printed in 12 distinct areas of the printer platform and evaluated for degree of conversion (DC, n = 3), using FTIR-ATR spectroscopy (Vertex70, Bruker), analyzing the percentage of aliphatic C = C bonds converted into C-C bonds, and for flexural strength (FS, n = 5), following ISO 4049/2019. Data were analyzed with a 5 % significance level.

Results: Irradiance ranged from 2.94 mW/cm^2 to 3.68 mW/cm^2, representing a 14 % decrease between different regions. The DC did not differ among the different printing regions ($p > 0.05$), with 52.5 ± 9.8 % for VS and 69.6 ± 8.2 % for BC after post-curing. FS reached 131.2 ± 15.3 MPa for VS and 94.9 ± 6.5 MPa for BC after post-curing, with no difference between the printing regions ($p > 0.05$).

Conclusions: In this study, different printing regions did not influence the DC and immediate FS of 3D resin-based composites.

https://doi.org/10.1016/j.dental.2026.03.040

29

Biodegradable and Bioactive 3D-Printed Alg-Gel/AMP Hydrogels for Bone Regeneration

JR de Souza *, IM Soares, C Anselmi, P Sikder, J Hebling, A Borges, E Trichês, M Bottino

Purpose: This study aimed to develop and characterize 3D-printed hydrogel scaffolds composed of sodium alginate and gelatin (Alg-Gel) with the incorporation of amorphous magnesium phosphate (AMP), and to evaluate the biological response of alveolar bone–derived mesenchymal stem cells (aBMSCs) cultured in contact with these materials.

Methods and Materials: Hydrogel inks were prepared using sodium alginate, gelatin, $CaCl_2$, and different concentrations of AMP (0%, 5%, and 10%). The scaffolds were fabricated using an

extrusion-based 3D bioprinter. The printed scaffolds were cross-linked using $CaCl_2$ and $BaCl_2$ solutions and characterized for rheological behavior, printability, morphology (SEM, n = 3), chemical composition (EDS, FTIR; n = 3), mechanical properties (compression, n = 4), and swelling/degradation profiles (n = 4). For in vitro evaluation, scaffolds were seeded with aBMSCs and analyzed for cell viability (alamarBlue, n = 10), matrix mineralization (Alizarin Red S, n = 8), and osteogenic gene expression (RT-qPCR; n = 6). Statistical analysis was performed using ANOVA, and confidence intervals were calculated (α = 5%).

Results: Rheological analysis showed that all alginate-based hydrogel inks exhibited shear-thinning behavior, more pronounced in AMP-containing formulations, indicating AMP's influence on viscosity. Oscillatory strain sweeps revealed a typical transition from elastic to viscous behavior. Filament drop and printability tests demonstrated improved filament uniformity and structural fidelity in AMP-containing inks. Morphological analysis confirmed well-defined shapes and smooth microstructures. FTIR spectra verified AMP incorporation through characteristic phosphate and hydroxyl bands, while EDS confirmed the presence of phosphate and magnesium elements in AMP-containing scaffolds. Mechanical testing showed similar compressive moduli across the scaffolds, although AMP-modified scaffolds presented different stress–strain profiles. Swelling behavior increased over 24 hours, and all samples fully degraded in 35 days. All formulations increased cell viability over time ($p \leq 0.0092$); however, only the 5% formulation showed a significant increase compared to the control after 7 days ($p < 0.0001$). Nevertheless, AMP-containing scaffolds enhanced the gene expression of COL1A1, ALPL, and RUNX2, as well as mineralized matrix deposition under osteogenic stimulation ($p < 0.0001$), compared to the control, particularly in the 10% AMP group.

Conclusion: AMP incorporation into alginate-based hydrogels modulated the rheological properties and improved printability. Biologically, these scaffolds promoted increased cell viability and induced osteogenic differentiation of aBMSCs. These results support their potential as biomaterials for tissue engineering applications in bone regeneration.

https://doi.org/10.1016/j.dental.2026.03.041

30

High-Filled 3D-Printed Composites with Niobium Silicate Fillers

G de Souza Balbinot *[1], M Borba [2], L Brasil [2], N Silikas [2], F Collares [1]

[1] *Federal University of Rio Grande do Sul, Porto Alegre, Brazil*
[2] *University of Manchester, Manchester, United Kingdom*

Purpose / Aim: This study aimed to investigate the impact of niobium silicate fillers in nanohybrid, high-filled 3D printed resins designed for long-term dental restorations.

Materials & Methods: A UDMA/BisEMA/TEGDMA resin blend was prepared and filled with 60 wt% of inorganic particles. Experimental groups were defined based on filler composition: G20 contained 35 wt% barium silicate glass, 20 wt% niobium silicate glass, and 10 wt% silica nanoparticles; G10 contained 45 wt% barium silicate glass, 10 wt% niobium silicate glass, and 5 wt% silica nanoparticles; and GC (control) was formulated with 55 wt% barium silicate glass and 5 wt% silica nanoparticles. Specimens were printed using a DLP printer (Asiga Max) and post-cured for 40 minutes at 60 °C. The materials were evaluated for degree of conversion, water sorption and solubility, and optical properties after 28 days of aging. Martens hardness and flexural strength were tested immediately and after 14 days of water storage.

Results: The addition of niobium silicate did not affect the degree of conversion. After 28 days, all groups showed increased color change (ΔE00), with values exceeding the acceptability threshold. Translucency was reduced in the niobium-containing groups compared to the control. Martens hardness was highest in the G20 group, while the indentation modulus was greater in the GC group. Immediate flexural strength ranged from 125.34 MPa to 147.72 MPa; however, after 14 days of water storage, all groups exhibited a decrease in strength, with values dropping below 100 MPa.

Conclusions: The incorporation of niobium silicate into high-filled composites maintained their properties, yielding adequate physicochemical performance for 3D-printed long-term dental restorations.

https://doi.org/10.1016/j.dental.2026.03.042

31

Optical Properties and Light Curability of BNNS-Reinforced RBC

J Fan *[1,2], J Gough [2,3], N Silikas [1], DC Watts [1,4]

[1] *Division of Dentistry, School of Medical Sciences, The University of Manchester, Manchester, UK*
[2] *Henry Royce Institute, The University of Manchester, Manchester, UK*
[3] *Department of Materials, School of Natural Sciences, The University of Manchester, Manchester, UK*
[4] *Photon Science Institute, The University of Manchester, Manchester, UK*

Purpose / Aim: Two-dimensional (2D) boron nitride nanosheet (BNNS) possesses unique optical features including a white colour, a high and anisotropic refractive index and minimal light absorption in the visible range associated with its ultrawide band gap. This study aimed to investigate the optical properties and light curability of resin-based composite (RBC) reinforced with BNNS.

Materials & Methods: BNNS particle size distribution was characterised with Zetasizer Nano DLS and atomic force microscopy (AFM). Experimental RBC formulated with varying BNNSs loadings (0-10.0 wt%) and glass fillers (40 wt%) was prepared via ultrasonication, SpeedMixing and vacuum degassing. Filler morphology and dispersion was evaluated by Scanning electron microscopy (SEM). Optical properties including light transmittance and translucency parameters were measured using a MARC™ Light Collector and a reflectance spectrophotometer. Depth of cure (DoC) was analysed via Vickers hardness (HV) indentation mapping at 0.5 mm intervals, with the DoC defined as the depth corresponding to 80% HVmax. Degree of conversion (DC) was measured up to 24h post-irradiance with Fourier Transform Infrared Spectroscopy (FTIR). Data was analysed using one-way ANOVA with Tukey's post hoc tests (α = 0.05).

Results: BNNSs exhibited a 2D platelet-like structure, with an average lateral size of 1.6 μm and a thickness of 5.4 nm. SEM images revealed uniform dispersion and random isotropic orientation of BNNS up to 0.5 wt%, while agglomeration and voids formation were observed at higher loadings. Increasing BNNS content led to an exponential decline ($R^2 > 0.99$) in both light transmittance and translucency, with near complete opacity observed at 10.0 wt%. While top surface HV increased with BNNS loading, this was accompanied by a significant reduction in DoC. At 80% HVmax, DoC remained clinically acceptable up to 0.5 wt% (2.16 ± 0.22 mm) but declined to < 0.9 mm at 10.0 wt%. DC24h peaked at 0.5 wt% and remained above the clinical threshold of 65% up to 5.0 wt%, but dropped notably to 30.4% at 10.0 wt%.

Conclusions: BNNS incorporation enhanced top surface microhardness but adversely impacted light transmittance, translucency, and DoC. Low BNNS loadings (≤ 0.5 wt%) enhanced DC while maintained clinically acceptable DoC for opaque-shade restorative materials, highlighting the narrow loading window of BNNS suitable for clinical uses. Optimising the optical properties, loading level, dispersion quality, and orientation of BNNS is essential to balance mechanical reinforcement with light-curing efficiency, particularly to achieve the desired shade and opacity required for specific clinical applications.

https://doi.org/10.1016/j.dental.2026.03.043

32

Tetric plus Fill: A Balanced Bulk-Fill Composite

P Bielec *, H Bronner, T Bock

Ivoclar, Schaan, Liechtenstein

Purpose / Aim: Modern bulk-fill composites are designed to meet a wide range of clinical requirements, including mechanical strength, curing efficiency, low polymerization shrinkage, aesthetic integration, and good handling. However, these properties are often interrelated in complex ways-improving one can sometimes compromise another. Therefore, clinical efficacy depends on achieving a well-balanced combination of all relevant properties, rather than maximizing any single metric. This study evaluates the performance of a new (Tetric plus Fill) and established bulk-fill materials (Filtek One Bulk Fill, SimpliShade Bulk Fill, Omnichroma).

Materials & Methods: The study used ISO 4049-relevant parameters and other clinically important metrics to compare bulk-fill composites suitable for placement in increments greater than 3 mm. The materials tested were: Tetric plus Fill (TPF, A3 plus), Filtek One Bulk Fill (OBF, A3), SimpliShade Bulk Fill (SHBF, universal), and Omnichroma (OC, universal). All were evaluated for flexural strength, water sorption, water solubility, radiopacity, and sensitivity to ambient light. Additional tests included incremental thickness (using Vickers hardness profiling), volume shrinkage (using gas pycnometry), and translucency. Curing was performed according to each manufacturer's instructions with a Bluephase PowerCure light.

Results: While TPF exhibited the lowest sensitivity to ambient light, curing TPF for 3s at 3050 mW/cm^2 resulted in a reliable depth of cure up to 4 mm, and a moderate volume shrinkage of 2.3%. This combination of high depth of cure and low final translucency (12.6% after polymerization, down from 36.3% unpolymerized) suggests that TPF is suitable for anterior restorations. All tested materials' mechanical and physico-chemical properties (flexural strength, water sorption, solubility and radiopacity) were consistent with established and clinically proven standards for bulk-fill composites (Table 1).

Conclusions: All tested materials met established and clinically proven standards for mechanical and physicochemical properties, including flexural strength, volumetric shrinkage, water sorption, solubility, and radiopacity. Tetric plus Fill also offered practical advantages, such as extended working time under ambient light and a final translucency suitable for anterior restorations. Although these results were obtained under controlled in-vitro conditions, the findings indicate that TPF delivers both reliable performance and the ease of use needed for efficient, high-quality dentistry.

Table 1. Usability and stability related parameter of TPF, OBF, SHBF and OC

Material	Curing conditions	Incremental thickness (mm)	Translucency (unpoly -> poly) (%)	Light Sensitivity @2900 lx (s)	Light Sensitivity @15000 lx (s)	Volume Shrinkage (%)	Flexural Strength (MPa)	Water Sorption (µg/mm^3)	Water Solubility (µg/mm^3)	Radiopacity (% Al)
TPF	3s @3050 mW/cm^2	4.7 ± 0.1^b	36.3 -> 12.6	470	70	2.3 ± 0.1^c	133 ± 10^b	21.0 ± 0.5^c	2.1 ± 0.7^a	236^b
OBF	20s @1200 mW/cm^2	5.9 ± 0.1^a	13.2 -> 11.1	170	20	2.5 ± 0.1^b	157 ± 6^a	32 ± 1.5^a	1.1 ± 0.5^{ab}	325^a
SHBF	10s @1200 mW/cm^2	4.7 ± 0.2^b	11.8 -> 15.8	180	20	2.2 ± 0.1^c	135 ± 13^b	25.5 ± 0.3^b	0 ± 0.2^b	294^b
OC	10s @800 mW/cm^2	4.9 ± 0.1^b	7.2 -> 34.2	190	30	3.3 ± 0.1^a	91 ± 15^c	17.9 ± 0.6^d	1.9 ± 0.6^a	134^c

same letters denominate comparable values (ANOVA, Tukey B, p<0.05)

https://doi.org/10.1016/j.dental.2026.03.044

33

Effect of universal adhesives-containing silane on bond strength to 3D-resins

M Salum-Serrano *[1], V Zamora-Gutiérrez [1], A Beniscelli-Vasquez [1], R Aliaga-Gálvez [1], AD Longuercio [2], D Murillo [2], MF Gutiérrez [1]

[1] *Universidad de los Andes, Santiago, Chile*
[2] *State University of Ponta Grossa, Ponta Grossa, Brazil*

Purpose / Aim: To evaluate the effect of incorporating silane into universal adhesives on the microshear bond strength (µSBS) to 3D printing resins for permanent restorations.

Materials & Methods: Fifty 3D-printed reins blocks were assigned into 10 groups based on two factors: *i) 3D printing resin: 1) Crowntec (Saremco) and 2) Varseosmile Crown Plus (Bego) and ii) Cementation protocol: 1) Ambar Universal APS (without silane) + Allcem veneer; 2) Ambar Universal APS Plus (with silane) + Allcem veneer, 3) Scotchbond Universal (without silane) + Relyx veneer; 4) Scotchbond Universal Plus (with silane) + Relyx veneer, 5) Prosil silane + Allcem veneer.* After each surface treatment, nine transparent Tygon tubing molds were positioned on each resin block. Each mold was filled with the respective resin cement and light-cured for 40s. Specimens were stored in water for 24h before undergoing µSBS test. Data were analyzed using one-way ANOVA and Tukey's test ($\alpha = 0.05$).

Results: For Crowntec, statistically higher µSBS values were observed with Ambar Universal APS Plus compared to Ambar Universal APS, Scotchbond Universal and Prosil silane. For Varseosmile Crown Plus, Ambar Universal APS Plus also showed significantly higher µSBS values compared to Scotchbond Universal Plus. Crowntec showed significantly higher µSBS values than Varseosmile Crown Plus only when Scotchbond Universal Plus was used.

Conclusions: The incorporation of silane into the formulation of universal adhesives enhanced microshear bond strength to 3D-printed resins compared to universal adhesive without silane or silane used separately. However, this improvement was observed only for Ambar Universal APS Plus

Funding: This project was funded by ANID through Initiation Fondecyt grant number 11221070

https://doi.org/10.1016/j.dental.2026.03.045

34

Monomeric and polymeric properties of low viscosity monourethanes

A Gartner, A Salazar, J Stansbury *

University of Colorado School of Dental Medicine, Aurora, USA

Purpose / Aim: Due to the mechanical property advantages associated with urethane-urethane noncovalent interactions, polymers based on reactive urethane oligomers and monomers are

extensively utilized including as components of several types of dental materials. However, the beneficial urethane hydrogen bonding effects in these polymers complicate resin formulation with high viscosity that is typically addressed by adding reactive diluents that then compromise polymer performance potential. A solution to minimize resin viscosity and maintain high urethane content is monourethane monomers that have inherently low viscosities without dilution. This study highlights how structural differences in novel monourethane monomers affect viscosity and polymeric mechanical properties compared with urethane dimethacrylate (UDMA).

Materials & Methods: A structurally diverse array of monourethane monomers with either mono- or di-(meth)acrylate reactive groups were synthesized and characterized. Viscosity measurements were conducted at room temperature. A UV photoinitiator was added to these liquid monomers and the degree of conversion in irradiated disc specimens was measured by near-IR and then optionally were post-cured to higher conversion. Three-point bend bars were photocured and tested to obtain flexural modulus and strength results.

Results: The monomers with molecular weights ranging from <200 to >500 g/mol demonstrated viscosities that spanned from 28 to 350 mPa.s with most being well below 100 mPa.s while for comparison, the viscosity of UDMA is ~8900 mPa.s. The photocured degree of conversion for the homopolymers was 48-97% and this range increased to 75-100% conversion after post cure. For reference, UDMA homopolymer produced conversion values of 68 and 88%, respectively. The flexural modulus of the monourethane homopolymers that were both photocured and photo/thermal post cured was 2.8-4.1 GPa as compared with UDMA at 3.1 GPa. Flexural strength was highly structure dependent with the monourethanes ranging between 102 and 158 MPa with three of these being statistically equivalent to UDMA homopolymer at 158 MPa.

Conclusions: Mechanical properties of UDMA homopolymer are quite good although this is an impractical photopolymerizable formulation due to viscosity. Dilution of UDMA with TEGDMA to a viscosity of 55 mPa.s, which is similar to many of the monourethane monomers here, drops the flexural modulus and strength to 2.8 GPa and 136 MPa, respectively. Monourethane homopolymers can match mechanical properties of UDMA while offering viscosities approximately two-orders of magnitude lower. Besides potential use without need for comonomer dilution, these new monourethane monomers provide interesting options as reactive diluents for UDMA or BisGMA formulations that maintain high noncovalent reinforcement without high viscosity.

https://doi.org/10.1016/j.dental.2026.03.046

35

Curing Unit and Exposure Time Effects on Dentin Bond Strength

M Giannini *[1], V Araújo-Neto [1], T Rifane [1], C André [2], R Price [3]

[1] *University of Campinas, Piracicaba, Brazil*
[2] *Federal University of Minas Gerais, Belo Horizonte, Brazil*
[3] *Dalhousie University, Halifax, Canada*

Purpose / Aim: This study aimed to evaluate the effects of light-curing units (LCUs) and exposure times on dentin bond strength (DBS) of restorative materials.

Materials & Methods: A multi-peak LED LCU (Bluephase Power Cure/BPC, Ivoclar) and a diode laser (Monet, AMD Lasers) were used to photopolymerize two restorative materials (adhesive and resin composite): Tetric N-Bond Universal and Tetric Power Fill (TNTP, Ivoclar), and Ambar Universal and Opus Bulk Fill APS (AMOB, FGM). For the TNTP restorative material, the adhesive was light-cured for 1s (using Monet) and 3s, 10s or 30s using BPC (composite for 10s). For AMOB, the adhesive was light-cured for 1s (using Monet) and 3s, 10s or 30s using BPC (composite for 30s). Sixty-four extracted third molars were used for DBS test ($n=8$). The adhesives were applied to dentin, according to the manufacturers' instructions and a block of composite was incrementally built-up on bonded dentin surface. Samples were serially sectioned to obtain the specimens for DBS test (1.0 mm^2 cross-sectional area), which were tested after 24 hours and after one year of water-storage. The DBS data were analyzed using a three-way ANOVA (factors: type of adhesive, adhesive exposure time, and storage time) and post-hoc Tukey test ($\alpha=0.05$).

Results: The exposure time of 1 second using Monet laser yielded the lowest DBS, followed by 3-seconds light-curing with BPC. The longest exposure times (10s and 30s) yielded the highest DBS values, which did not differ from each other and regardless the restorative material. DBS did not reduce after one-year water-storage.

Conclusions: The results suggest that shorter exposure times (1s and 3s) produce low DBS. Optimal exposure time for light curing of the adhesives was 10s. DBS remained stable for both restorative materials after one year.

https://doi.org/10.1016/j.dental.2026.03.047

36

Bond strength of resin cements to Zirconia

R Nakagawa *[1], V Neto [2], R Albuquerque [1], C André [1], M Gianinni [2]

[1] *Universidade Federal de Minas Gerais, Belo Horizonte, Brazil*
[2] *Universidade de Campinas, Piracicaba, Brazil*

Purpose / Aim: To evaluate the bond strength (BS) of five resin cements to 5Y-PSZ zirconia after 24 hours and one-year post-cementation.

Materials & Methods: 5Y-PSZ plates (14x4x3mm, Katana UTML) were sandblasted with aluminum oxide, cleaned in an ultrasonic bath for 5 min, and divided into the following groups ($n=8$): Superbond (Sun Medical), Set PP (SDI), Estecem II (Tokuyama); Panavia V5 (Kuraray) and RelyX Universal (Solventum). Adhesives or primers were applied to 5Y-PSZ zirconia plates and their respective resin cements were bonded to plates. Samples were tested for shear BS after being stored in distilled water at 37°C for 24 hours and one year. The BS data were analyzed using two-way ANOVA and post-hoc Tukey test ($\alpha=0.05$).

Results: No significant differences among Estecem II andPanavia V5 were found, which showed higher BS results than those obtained for Superbond and Set PP, regardless the evaluation time. RelyX Universal showed the intermediate results. The BS of Superbond and Set PP to 5Y-PSZ zirconia reduced after one year.

Conclusions: The cementing systems presented different BS values to 5Y-PSZ zirconia and those that showed the lowest initial BS values showed a reduction in BS after one year.

https://doi.org/10.1016/j.dental.2026.03.048

37

Bond strength of universal adhesives containing silane to feldspathic ceramic

A Vásquez *[1], R Gálvez [1], D Melendez [2], N Weiss [1], AD Loguercio [2], MF Gutierrez [1]

[1] *Universidad de los Andes, Santiago, Chile*
[2] *State University of Ponta Grossa, Ponta Grossa, Brazil*

Purpose / Aim: To evaluate the effect of incorporating silane into universal adhesives on the microshear bond strength (μSBS) to feldspathic ceramic.

Materials & Methods: Thirty feldspathic ceramic blocks were randomly assigned to six groups according to the cementation protocol: 1) Ambar Universal APS (without silane) + Allcem veneer; 2) Ambar Universal APS Plus (with silane) + Allcem veneer; 3) Prosil silane + Allcem veneer; 4) Scotchbond Universal (without silane) + Relyx veneer; 5) Scotchbond Universal Plus (with silane) + Relyx veneer, 6) Prosil silane + Relyx veneer. All ceramic surfaces were etched with 10% hydrofluoric acid for 60 seconds. After the respective cementation protocol, nine transparent Tygon tube molds were positioned on each ceramic block. Each mold was filled with the respective resin cement and light-cured for 40s. Specimens were stored in distilled water at 37°C for 24h prior to the μSBS test. Data were analyzed using one-way ANOVA and Tukey's test ($\alpha = 0.05$).

Results: The group treated with Prosil silane + Allcem veneer showed significantly higher μSBS values compared to all other groups ($p < 0.05$). No significant difference in μSBS values was observed between Ambar Universal APS and Ambar Universal APS Plus ($p > 0.05$). However, Scotchbond Universal Plus showed significantly higher μSBS values than Scotchbond Universal ($p < 0.05$), and similar μSBS values to Prosil silane + Relyx veneer.

Conclusions: Incorporating silane into universal adhesives may enhance microshear bond strength to feldspathic ceramic compared to silane-free versions, despite inferior results when compared to use of silane dedicated bottle. However, this benefit was only evident with Scotchbond Universal Plus.

Funding: This project was funded by ANID through Initiation Fondecyt grant number 11221070 and FAI (Fondo de Apoyo a la Investigación) doctoral scholarship, Universidad de los Andes.

https://doi.org/10.1016/j.dental.2026.03.049

38

Adhesive impact on bond strength of treated ceramics: systematic review

R de Souza *[1], LC Freitas [2], L Araújo [2], C Lima [2], T Pires [2], T Costa [2], R Barra [2], F Leite [2], S Butler [1]

[1] *Western University, London, Canada*
[2] *Federal University of Juiz de Fora, Juiz de Fora, Brazil*

Purpose / Aim: This systematic review aimed to evaluate whether the application of an adhesive layer on glass ceramic restorations, after hydrofluoric acid (HF) etching and silane treatment, improves bond strength and clinical reliability. The motivation for this study arises from the controversy regarding the real benefits of including this additional step in the cementation protocol for glass ceramics, especially considering its potential impact on long-term mechanical performance.

Materials & Methods: A comprehensive search was conducted in six electronic databases (PubMed, Scopus, Web of Science, Cochrane Library, LILACS, and SciELO) following the PRISMA guidelines. The search strategy combined descriptors related to dental materials, surface treatment, adhesive application, adhesive cementation, and glass ceramics. Laboratory in vitro studies were selected if they evaluated adhesion to glass ceramics and compared protocols with and without adhesive application following HF etching and silanization. Studies were required to use standardized mechanical tests, such as microtensile bond strength, shear bond strength, biaxial flexural strength, fatigue resistance, and analysis of failure modes. Two reviewers independently screened the articles, extracted data, and assessed the risk of bias, with a third reviewer consulted in cases of disagreement.

Results: From 834 initial records, 18 studies met the eligibility criteria and were included in the analysis. The results indicate that adhesive application after HF and silane does not consistently improve the bond strength of glass ceramics to resin cements. Most studies reported no statistically significant difference between groups with or without adhesive, and some investigations demonstrated reduced mechanical performance, particularly in fatigue resistance and load-bearing capacity. Universal adhesives also failed to show superior results compared to silane alone. In contrast, surface conditioning with HF (5–10%) followed by silanization consistently provided effective micromechanical retention and chemical bonding. Enhanced wettability and durable adhesion were confirmed through various analytical methods, including Raman spectroscopy, SEM/EDS, and mechanical testing.

Conclusions: Current evidence does not support the routine use of adhesive application after HF and silane conditioning for glass ceramic restorations. The conventional protocol with HF and silane alone is sufficient to achieve reliable and durable adhesion. Eliminating the adhesive step can streamline the clinical workflow, reduce potential technique sensitivity, and maintain high-quality bonding. Further clinical trials and standardized in vitro studies are still needed to reinforce these findings.

https://doi.org/10.1016/j.dental.2026.03.050

39

Three-Dimensional Roughness in Prosthetic Bases: PMMA, Polyamides, and 3D- printing

D Martinez-Torres, A Buitrago-Osuna, M Sarmiento-Delgado *

Universidad Nacional de Colombia, Bogota, Colombia

Purpose / Aim: To evaluate the three-dimensional surface roughness of different materials used in the fabrication of bases for dental prostheses through optical profilometry, and to determine the influence of the manufacturing method on the obtained topographic characteristics.

Materials & Methods: An in vitro experimental study was conducted using four types of materials: thermopolymerizable acrylic resin (PMMA), prepolymerized PMMA milled using CAD/CAM technology, photopolymerizable resin for 3D printing, and polyamide injected. For each group, ten circular samples measuring 10 mm in diameter and 3 mm in thickness were fabricated according to the technical specifications of each method. Surface roughness was measured using an Alicona InfiniteFocus G5 optical profilometer (Bruker, Austria) with a 50X lens, capturing data at the center and three equidistant points per sample. The qualitative evaluation was performed through three-dimensional isometric reconstruction. Three-dimensional surface roughness parameters, as defined by the ISO 4287-4288 standard (Sa, Sz, Sdr, Sk, Spk, and Svk), were quantified. A total of 120 readings were processed. Statistical tests for normality, Kruskal-Wallis, and post hoc comparisons using Dunn's test were applied. A significance level of $p < 0.05$ was established.

Results: Milled PMMA exhibited the lowest roughness (Sa = 0.42 ± 0.13 μm), followed by thermopolymerizable PMMA (Sa = 0.44 ± 0.14 μm), 3D-printing resin (Sa = 0.65 ± 0.34 μm), and polyamide (Sa = 2.18 ± 1.63 μm). Regarding the developed surface ratio (Sdr), the polyamide material showed the highest value (9.54 ± 24.02%), indicating a surface with greater topographical complexity (Table 1). In contrast, the Milled (0.30 ± 0.32%) and Conventional (0.34 ± 0.15%) materials presented significantly lower values, suggesting fewer irregular surfaces. The printed material showed an intermediate value (0.47 ± 0.5%), indicating slightly greater surface complexity compared to the Conventional and Milled materials, but considerably less than the polyamide material. Statistically significant differences were found between all groups ($p < 0.05$). Abbott-Firestone curves indicated that milled materials showed lower initial wear and reduced fluid retention capacity, whereas polyamide displayed a topography characterized by prominent peaks and deep valleys.

Conclusions: The manufacturing method has a decisive effect on the surface roughness of materials used for prosthesis bases. CAD/CAM milling provides more homogeneous and smoother surfaces, which may enhance biocompatibility and reduce bacterial accumulation. In contrast, 3D printing and polyamide result in rougher surfaces, which could compromise long-term clinical performance.

Table Roughness Parameters: S

			Pos Hoc Dunn		
	Sa(μm)	3D-printing		Polyamide	Milled
Conventional	0,44 ± 0,14		0.075	p < 0.05*	0.73
3D-printing	0.65 ± 0.34			p < 0.05	p < 0.05
Polyamide	2.18 ± 1.63				p < 0.05*
Milled	0.42 ± 0.13				
Kruskal-Wallis	p < 0.05*				
	Sz(μm)	3D-printing		Polyamide	Milled
Conventional	12.6 ± 13.04	0.82		p < 0.05	p < 0.05
3D-printing	10.9 ± 5.62			p < 0.05	0.062
Polyamide	32.5± 19.1				p < 0.05*
Milled	7.78 ± 4.27				
Kruskal-Wallis	p < 0.05*				
	Sdr(%)	3D-printing		Polyamide	Milled
Conventional	0.34 ± 0.15			p < 0.05	
3D-printing	0.47 ± 0.5			p < 0.05*	
Polyamide	9.54± 24.02				
Milled	0.30 ± 0.32				
Kruskal-Wallis	p < 0.05*				
	Sk(μm)	3D-printing		Polyamide	Milled
Conventional	1.24 ± 0.32	p < 0.05		p < 0.05*	0.74
3D-printing	1.82 ± 0.85			p < 0.05	0.067
Polyamide	6.39 ± 4.56				p < 0.05*
Milled	1.31 ± 0.46				
Kruskal-Wallis	p < 0.05*				
	Spk(μm)	3D-printing		Polyamide	Milled
Conventional	0.72 ± 0.24	0.23		p < 0.05	0.29
3D-printing	0.66 ± 0.39			p < 0.05*	0.89
Polyamide	3.51 ± 3.9				p < 0.05*
Milled	0.65 ± 0.24				
Kruskal-Wallis	p < 0.05*				
	Svk(μm)	3D-printing		Polyamide	Milled
Conventional	1.0 ± 0.75	p < 0.05		p < 0.05	p < 0.05
3D-printing	1.6 ± 1.1			p < 0.05	p < 0.05
Polyamide	3.51 ± 1.89				p < 0.05*
Milled	0.6 ± 0.18				
Kruskal-Wallis	p < 0.05*				

https://doi.org/10.1016/j.dental.2026.03.051

Friday, October 3rd

'Clinical properties'

40

Modeling structural relaxation in veneering dental porcelains via FEM

P Shelar, S Butler *

Western University, London, Canada

Purpose / Aim: This study investigated the influence of thermal gradients on structural relaxation in dental porcelains and explored the underlying mechanisms contributing to the development of thermal stresses. These stresses, particularly in the subsurface regions of veneered ceramics, have been widely associated with clinical failures. While thermal stresses are a known issue in multilayered dental restorations, the contribution of structural relaxation, especially under varying cooling rates and veneer thicknesses, remains insufficiently understood. This research addresses this gap by evaluating how different thermal conditions influence stress formation and offers insights into optimizing fabrication protocols and improvements in the design to enhance the longevity of dental restorations

Materials & Methods: A Finite Element Method (FEM) framework was developed to simulate thermo-mechanical behavior during the cooling phase of veneered dental ceramics. Custom user subroutines (UEXPAN and UTRS) were written and integrated into the FEM solver to account for temperature-dependent thermal expansion and structural relaxation effects. Validation of the model was performed through both qualitative and quantitative comparisons with experimental observations. The simulations involved a standardized framework made of 3Y-TZP zirconia with a constant thickness of 0.5 mm, combined with veneering porcelains (VM9 and Empress 2) of varying thicknesses (0.7 mm, 1.4 mm, and 2.1 mm). Cooling rates ranging from 30°C/min to 300°C/min were applied to assess their influence on thermal gradients and stress profiles.

Results: The results revealed that increasing the cooling rate significantly elevated thermal gradients within the veneer layer, leading to deviations in fictive temperature evolution and suppression of structural relaxation. Under these conditions, high transient and residual tensile stresses were observed in the subsurface of the veneer. Conversely, slower cooling rates facilitated structural relaxation, resulting in compressive subsurface stresses that are considered desirable for mechanical stability. The study also showed that greater veneer thickness amplified these effects: thick veneers cooled rapidly exhibited the highest levels of tensile stress, whereas thin veneers subjected to slow cooling developed more favorable stress profiles due to enhanced relaxation.

Conclusions: This evaluation highlights the critical role of structural relaxation in the stress development of veneering porcelains during cooling. Both veneer thickness and cooling rate significantly influence the resulting stress state. By optimizing these parameters, it is possible to promote compressive stresses that improve clinical performance. These findings provide valuable guidance for the design and fabrication of veneered restorations, enabling better control of stress development and contributing to improved long-term outcomes in restorative dentistry.

https://doi.org/10.1016/j.dental.2026.03.052

41
In situ evaluation of EGCG-chitosan dentifrices on dentin loss

L Franco *[1], K Pintado-Palomino [2], R Scatolin [3], L Gusmão [4], A Tedesco [4], M Owasawara [5], R Garcia [6], T Scaramucci [6], S Corona [1]

[1] *School of Dentistry of Ribeirão Preto, University of São Paulo, Ribeirão Preto, Brazil*
[2] *School of Dentistry, Federal University of Minas Gerais, Belo Horizonte, Brazil*
[3] *Herminio Ometto University Center, School of Dentistry, Araras, Brazil*
[4] *Department of Chemistry, Center of Nanotechnology and Tissue Engineering- Photobiology and Photomedicine Research Group, University of Sao Paulo, Ribeirão Preto, Brazil*
[5] *Pharmacognosy Laboratory, Faculty of Pharmaceutical Sciences of Ribeirão Preto, University of Sao Paulo, Ribeirão Preto, Brazil*
[6] *Department of Restorative Dentistry, University of Sao Paulo, São Paulo, Brazil*

Purpose / Aim: The aim of this study was to evaluate, in situ, the effect of applying experimental dentifrices containing chitosan nanoparticles loaded with epigallocatechin-3-gallate (EGCG) on dentin surface loss.

Materials & Methods: For this purpose, the experimental protocol was divided into five phases of five days each, with seven-day washout periods. Eighty dentin discs (Ø 4 mm × 1 mm) were obtained from bovine teeth and treated with 0.5 M EDTA to expose the dentinal tubules. Eight volunteers used custom-made mandibular intraoral appliances containing two bovine dentin samples on each side, with dentinal tubules previously exposed with 0.5 M EDTA. The samples underwent extraoral erosion (0.3% citric acid, pH 2.6, four times daily) and intraoral brushing with the tested dentifrices (15 seconds, twice daily) for five days, according to the following experimental groups: placebo (PL), chitosan nanoparticles (NCh), chitosan-encapsulated EGCG (NCh + EGCG), free EGCG, and Elmex Sensitive (ES). After the experimental period, dentin surface loss was assessed with a profilometer (2100 Proscan 3D, USA). The specimen surfaces were scanned, covering the permeable area (T1, after tubule exposure) and the treated areas (T2, after erosion and dentifrice treatment), and analyzed using Proscan Application software v. 2.0.17. Data were subjected to one-way ANOVA statistical analysis.

Results: The results indicated no statistically significant difference ($p = 0.885$) among the tested dentifrice groups regarding dentin surface loss.

Conclusions: The formulations containing active agents (NCh, NCh + EGCG, EGCG, and ES) did not influence dentin surface loss among the experimental groups, demonstrating that all dentifrices produced similar wear on the dentin surface.

Filing of patent application Nº. BR 10 2025 009040-6.

Funding: CNPq - Research Productivity Grant (Process #308735/2023-4) Fapesp (Process 2024/12845-0)

https://doi.org/10.1016/j.dental.2026.03.053

42
Ex-vivo study of pulpal inflammation under blue and red lights

D Oliveira *, M Rocha, S Reinhard, S Wallet

University of Florida, Gainesville, USA

Purpose / Aim: Assess the inflammatory responses of the pulpal tissue to the use of blue- and red-light irradiation.

Materials & Methods: 108 healthy human pre-molars extracted as part of normal clinical care for orthodontic reasons were used in a human tooth ex-vivo model (IRB202201548). Class V restorations (n = 12/group) were performed in a single increment using a commercial self-cured adhesive and a resin-based composite formulation (Stela, SDI) and exposed to red-light, blue-light, or no-light. Light exposures were performed for 20 s using experimental curing lights emitting either blue- (460nm) or red-light (620nm) (Ultradent). All restored teeth were kept in the culture medium for either 24h (n = 12/group), 7d (n = 12/group), or 14d (n = 12/group), with media exchange every 3 days. At each time point, culture supernatants and pulpal tissues were collected to assess indicative markers of cellular function using qPCR and inflammation with a focus on cytokine and chemokines using targeted (Luminex) approaches to define the responsive immune signatures. Data were analyzed using ANOVA and Tukey's tests.

Results: Red-light exposure resulted in lower pro-inflammatory cytokine expression compared to blue-light exposure ($p < 0.05$); and promoted a more favorable immune response, with increased anti-inflammatory cytokine expression ($p < 0.05$), indicating a potential wound healing benefit. At 24 hours, blue light-induced an acute inflammatory response characterized by elevated IL-6 and TNF-α, whereas red light showed a more moderated profile. By day 7, red-light-treated samples exhibited increased expression of wound-healing markers, such as type I collagen and alkaline phosphatase, with continued suppression of oxidative stress signals. By day 14, red-light groups demonstrated a stable anti-inflammatory cytokine profile (e.g., IL-10, TGF-β), suggesting resolution of inflammation and progression toward tissue homeostasis. In contrast, blue light groups showed persistent pro-inflammatory signals and delayed regenerative response.

Conclusions: Red light was demonstrated to be a safer alternative to blue light improving immunological outcomes

https://doi.org/10.1016/j.dental.2026.03.054

43
Reducing Biofilms in the Oral Microbiome

D Nair *, M Schurr, H Escobedo, C Puranik, D Danforth, J Stansbury

University of Colorado Anschutz Medical Campus, Aurora, USA

Purpose / Aim: Pathogenic biofilm formation in the microbiome contributes to oral dysbiosis. In this work, we evaluate polymers that can selectively eliminate caries-causing bacteria and repeatedly disrupt biofilm formation in both, in vitro and in vivo studies.

Materials & Methods: An acrylated polyphenol (Acrylated HydroxyAzobenzenes- AHA) was synthesized and incorporated within highly crosslinked resin-based restorations and dentures. Fourier Transform- Infrared Spectroscopy (FTIR) was used to ascertain the samples' double-bond conversion, while the films' biocompatibility was also established (ISO-10993 protocol) and were sent for external evaluation. In the in vitro studies, cariogenic biofilms from human saliva were formed on substrates for over 16 hours, and subsequently irradiated with multiple wavelengths of visible light sources to induce the mechanical disruption of biofilms. Biofilms (CFU/mL) were quantified via serial dilutions with 3 technical replicates seeded on BHI agar plates. For the in vivo studies, a murine cariogenic model with/without AHA in which mice were fed a 70% sucrose diet was conducted. At six weeks, the mice were swabbed for 16S rRNA targeted sequencing and microbiome was analyzed

Results: The AHA, which was incorporated within resin formulations at different concentrations, achieved > 95% double-bond

conversion. The cytocompatibility of AHA-resins also enabled the reduction of both Streptococcus mutans and Candida albicans biofilms. In in vivo studies, the AHA-based resins eliminated caries when compared to control mice, which showed 70% caries.

Conclusions: Polymers that can be incorporated within dental resins and dentures can selectively inhibit cariogenic biofilms in both in vitro and in vivo studies. Our future studies will focus on the long-term efficacy and the long-term impacts on the oral microbiome.

https://doi.org/10.1016/j.dental.2026.03.055

44

AI-Driven Design Boosts Fatigue Resistance in Narrow Dental Implants

R dos Santos *[1], A Della Bona [1], J Griggs [2], U Lenz [1]

[1] *University of Passo Fundo, Passo Fundo, Brazil*
[2] *University of Mississippi Medical Center, Jackson, USA*

Purpose / Aim: To evaluate the mechanical performance of prosthetic components supported by narrow-diameter dental implants through a multidimensional design optimization strategy powered by artificial intelligence.

Materials & Methods: A narrow-diameter dental implant (3.0 mm) with Morse taper connection, along with its corresponding abutment and fixation screw, was scanned via micro-computed tomography (micro-CT). High-resolution digital models were reconstructed using grayscale thresholding (Simpleware, Synopsis). Six key geometric parameters of the internal connection were extracted. Using reverse engineering in SolidWorks, a 3D assembly was built, and systematic dimensional variations (±20%) of these six parameters were introduced following a design of experiments (DOE++, Reliasoft) based on a Taguchi orthogonal array. Twenty-seven modified assemblies were analyzed under static loading through finite element analysis (FEA) in ABAQUS, following ISO 14801:2016 geometry. Fatigue behavior was estimated with Fe-safe software, and parameter sensitivity was assessed via DOE++. The dataset was used to train an artificial neural network (ANN) to predict fatigue limits of intermediate designs. A genetic algorithm (GA) was subsequently applied to evolve the design toward maximized fatigue strength.

Results: The initial design exhibited a fatigue limit of 193 N. Multidimensional optimization increased this value to 294 N. The ANN + GA-derived design achieved a fatigue limit of 304 N, reflecting a 57.5% improvement over the original configuration.

Conclusions: The proposed AI-assisted methodology enables precise optimization of the implant-abutment interface in narrow-diameter systems. This approach significantly enhances mechanical resistance, supporting the development of more durable prosthetic designs and contributing to the long-term clinical success of implant-supported rehabilitations.

https://doi.org/10.1016/j.dental.2026.03.056

45

Development of a fully automatic staining apparatus for accelerated aging

AC Ionescu *[1,2], D Berri [1]

[1] *University of Milan, Milan, Italy*
[2] *IRCCS Ca' Granda Ospedale Maggiore Policlinico, Milan, Italy*

Purpose / Aim: Several staining protocols for dental materials are available in the literature, with poor standardization and comparability of the results. We aimed to develop an easily programmable, fully automatic staining apparatus to meet any requirement for simulating clinically significant staining cycles in an accelerated way in vitro.

Materials & Methods: A robotic arm (4 degree-of-freedom RoArm-M2-S with ESP32 main control unit, TOPONE Electronics, Shenzhen, China) was programmed to cycle a holder containing 4 specimen-filled sleds. Each sledge exposed 6 disks of RBC, HVGIC, and enamel. The cycle included bathing in mouthwashes for 1 min, one for each sled, containing 0.2% chlorhexidine [CHX], 0.2% CHX + ascorbic acid as anti-staining [CHX+VitC], 0.2% CHX + N-acetylcysteine as anti-staining [CHX+NAC], or artificial saliva as negative control [CTRL]. Then, cycles were performed in a coffee bath for 2 min, followed by washout for 5 min in artificial saliva. Cycles simulated exposure to coffee from 2 to 5/day. Another mouthwash exposure followed by a 30 min washout in artificial saliva completed the simulation of a daily routine in an accelerated way. We performed up to 30 consecutive routines in triplicate for each condition. Staining was documented with macrophotography and a spectrophotometer (CIELab approach, Konica Minolta CM-2500c). Statistical analysis included multi-way ANOVA and Tukey's test, $p < 0.05$.

Results: Routines ranging from 2 coffees/day up to 5/day and up to 30 consecutive routines (1-month simulations) were successfully performed. The 2 coffees/day routine best allowed observing differences between treatments, starting from #3 and reaching the maximum difference between treatments at #14. ΔE was lowest for RBC (Fig. 1) and higher for HVGIC and enamel. CHX led to the biggest increase in ΔE in all groups, while both antistaining formulations were effective in reducing staining, albeit not reaching the level of artificial saliva (negative control).

Conclusions: A fully automatic staining apparatus was successfully developed and programmed to simulate clinically significant staining routines in an accelerated way in vitro. This apparatus provided reliable data that were comparable to the existing body of data in the literature. It helped evaluate how effective two anti-staining agents were at reducing the known staining caused by CHX-containing mouthwashes.

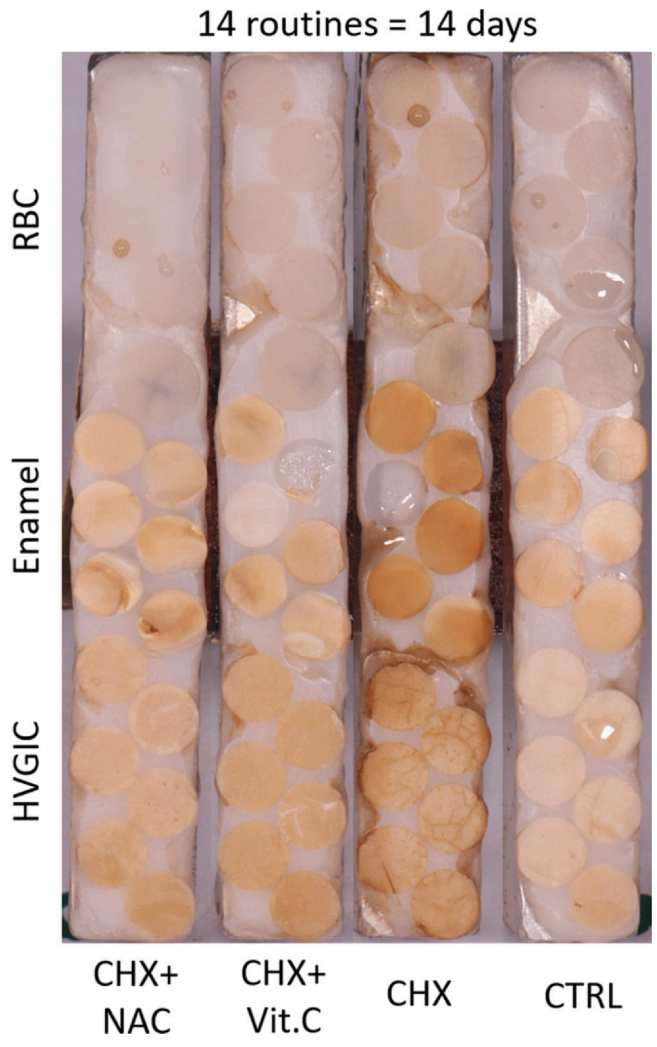

https://doi.org/10.1016/j.dental.2026.03.057

46

Polycystin-1 Activator-loaded Injectable Hydrogel for Periodontal Regeneration

I De Souza Araujo *[1], R Perkins [2], G Huang [2], Z Xiao [2], W Zhang [2]

[1] *University of Saskatchewan, College of Dentistry, Saskatoon, Canada*
[2] *University of Tennessee Health Science Center, Memphis, USA*

Purpose / Aim: Polycystin-1 is a mechanosensitive protein involved in osteoblastic response to mechanical forces. Polycystin-1 activator zinc01442821 (MS) and its analog MS2 have demonstrated the ability to stimulate osteogenesis. The aim of this study is to incorporate MS and MS2 into a collagen-based hydrogel for local delivery and polycystin-1 activation for periodontal regeneration.

Materials & Methods: Type I collagen solution 10 mg/mL was prepared in 0.1M acetic acid under stirring and neutralized using 1M NaOH. MS (10 μM, 20 μM, and 50 μM) and MS2 (10 μM, 20 μM, and 50 μM) were added to the collagen gel and mixed overnight at 4 °C under stirring. Cylinder-shaped samples (10 x 3 mm) were prepared to test drug release (n = 3/group). Each sample was placed into vials with 5 mL of PBS and aliquots of 500 μL were collected at multiple time points up to 14 days. The amount of drug released was verified using high-performance liquid chromatography. Cytotoxicity of MS- and MS2-loaded hydrogels was verified after culturing human periodontal ligament stem cells (PDLSCs) on top of the gels (n = 4/group) using Alamar Blue assay at 1, 3, and 7 days. PDLSCs growing on pristine collagen gel was the control. The osteogenic markers RUNX2, OCN, BSP, and ALP expressions were tested using RT-qPCR after culturing PDLSCs on top of MS- and MS2-loaded hydrogels for 7 and 14 days. ALP protein quantification was performed on days 7 and 14. Two-way ANOVA was used with Tukey post hoc ($\alpha = 0.05$) for statistical comparisons.

Results: Release profiles indicated a peak of release occurring from 1h to 6h in all concentrations of MS and MS2. A decrease in the release is evident for both MS and MS2 at 50 μM for up to 7 days, while the other concentrations presented a more consistent profile. No cytotoxicity was evidenced for the tested concentrations of MS and MS2. PDLSC viability significantly increased at day 7 for all groups ($p < 0.05$). MS- and MS2-loaded hydrogels significantly increased ALP expression after 7 days ($p < 0.05$). MS2 upregulated BSP and OCN expressions while MS evidenced a down-regulatory activity for those genes ($p < 0.05$). MS- and MS2-loaded hydrogels significantly increased ALP protein levels after 14 days ($p < 0.05$).

Conclusions: Local delivery of polycystin-1 activator MS and its analog MS2 through collagen hydrogels demonstrated controlled release up to 14 days. The molecules did not induce toxicity, and MS2-loaded hydrogels positively influenced the osteogenic differentiation of PDLSCs for periodontal regeneration.

https://doi.org/10.1016/j.dental.2026.03.058

47

New etching protocols, prism orientation, resin composition: enamel-bonding effects

M Canadas *[1,2,3], T Stape [1,2,4], F Panzeri [3], A Tezvergil-Mutluay [1,2,4]

[1] *Institute of Dentistry, University of Turku, Turku, Finland*
[2] *Adhesive Dentistry Research Group, Biomaterials, and Medical Device Research Program, Biocity, Turku, Finland*
[3] *Ribeirao Preto School of Dentistry, University of Sao Paulo, Ribeirao Preto, Brazil*
[4] *Turku University Hospital, TYKS, University of Turku, Turku, Finland*

Purpose / Aim: Proper bonding is essential for the durability of composite fillings. Although there is in vivo and in vitro evidence supporting the general concept that bonding to enamel is reliable and predictable on the long-term, the anisotropic structure of enamel and resin composition affect bonding outcomes. Furthermore, the earliest signs of clinical failures for composite fillings are identified at the enamel-adhesive interface indicating that there is still need for improvements. The aim of this study was to evaluate whether enamel prism orientation, etching protocols or the composition/application modes of methacrylate- based resins would affect resin-enamel bonding

Materials & Methods: A total of 180 enamel surfaces were be obtained from sound human third molars and randomly divided into 18 groups (n = 10) based on (i) “bonding resins”: a mild universal adhesive (Scotchbond universal plus, 3M ESPE), a neat bonding resin (Scotchbond Multipurpose adhesive, 3M Oral Care) and their combination; (ii) “etching protocol”: self-etch application, 37%H3PO4 (30s) or 20%phytic acid etching (30s) and (iii) “prism orientation”: perpendicular or parallel to bonded interfaces. After bonding, one cylindrical composite buildup (0.8 mm diameter and 2 mm high) was performed on each enamel surface. Samples were stored in (i)

artificial saliva for 24h. A micro-shear test was performed in a universal testing machine to assess resin-enamel bond strengths (MPa). Shear tension was applied to each specimen at a crosshead speed of 0.5 mm/minute until fracture using a thin wire (diameter 0.20 mm) looped around the base of the composite cylinder. Data were analyzed by factorial ANOVA and Tukey test ($\alpha = 0.05$).

Results: The interaction between "etching protocol and prism orientation" had significant effects on micro-shear tension ($p < 0.01$), as well as the interaction between "bonding resin and etching protocol" ($p < 0.01$). After 37%H3PO4 and 20%phytic acid, bonding to perpendicularly oriented prisms produced significantly higher values compared to those parallelly oriented ($p < 0.05$). No significant differences were identified between 20%phytic acid and 37% H3PO4 etching between corresponding groups ($p > 0.05$). The neat bonding resin produced comparable bond strengths to solvated adhesive regardless of etching agent ($p > 0.05$).

Conclusions: The use of phytic acid may be a viable alternative for etching enamel. Additionally, using a neat bonding resin may be a feasible mode of application, as long as there is prior enamel etching. Improving bonding performance of resin-enamel interfaces may contribute to extended longevity of composite fillings.

https://doi.org/10.1016/j.dental.2026.03.059

48

Beyond Milling: in-vitro Evaluation of 3D Printed Long-Term Dental Restoratives

F Schmidt *, J Yassine, E Prause, F Beuer

Charité Universitaetsmedizin Berlin, Berlin, Germany

Purpose / Aim: This study aimed to evaluate the in-vitro performance of a 3D printed, ceramic-filled dental resin intended for long-term restorative use. Additive manufacturing via vat photopolymerization (VPP) enables design flexibility and material efficiency, but independent data on the mechanical behavior and bonding performance of these materials remain limited. We assessed structural, mechanical, and adhesive properties and compared them to two widely used CAD/CAM-milled restorative materials.

Materials & Methods: One 3D printed resin and two milled hybrid materials were analyzed. Microstructural properties were examined using high-resolution Micro-CT. Flexural strength and fatigue resistance were assessed according to ISO 4049 and staircase methods. Shear bond strength (SBS) to dual-cure resin cements was tested following various pretreatment protocols. Statistical analysis was performed using ANOVA ($\alpha = 0.05$).

Results: The 3D-printed resin exhibited the lowest initial biaxial flexural strength and fatigue resistance among the tested materials. Specifically, it showed a 9–15% higher relative strength degradation compared to the milled nanohybrid composite resin (NHC) and polymer-infiltrated ceramic network (PICN) materials. Fractographic analysis revealed that areas of nonhomogeneous microstructure in the 3D-printed resin served as potential fracture origins. Micro-CT imaging indicated that the 3D-printed resin had a more irregular filler distribution and visible layered macrostructure, whereas the milled materials demonstrated more uniform microstructures. Shear bond strength (SBS) testing showed no significant differences among the three materials. However, the pretreatment strategy significantly influenced SBS values. Sandblasting and silane application enhanced bond strength across all materials, while hydrofluoric acid etching resulted in the lowest SBS, particularly for the 3D-printed resin.

Conclusions: The tested 3D printed resin demonstrated adequate in-vitro performance and reliable bonding when appropriate pretreatment was applied. While mechanical endurance was slightly lower than for milled materials, especially under fatigue, the adhesive and structural results support its potential for clinical use in selected indications. Ongoing developments in material composition and printing strategies may further improve its suitability for long-term restorations.

https://doi.org/10.1016/j.dental.2026.03.060

49

Physicochemical properties of adhesives associated with S-PRG and 0.1% hydroxyapatite

G Zabeu *, M Costa, F Zordan, C Rodrigues, M Giacomini, L Wang

Bauru School of Dentistry, University of São Paulo, Bauru, Brazil

Purpose / Aim: Adhesive systems present complex chemical compositions, varying in the type and concentration of monomers and solvents, which directly influence their clinical performance. Solvents such as water, ethanol, and acetone play a critical role in the volatilization and dispersion of adhesive components, thereby affecting the interaction with moisture present in the dentin substrate. Consequently, the hydrophilicity of an adhesive system is largely determined by its formulation, which impacts water sorption and its susceptibility to hydrolytic degradation. In addition, the incorporation of bioactive agents has been explored due to their potential to enhance bonding performance and material durability by promoting remineralization and chemical interaction with the dentin matrix. Thus, the aim of this study was to evaluate the physicochemical behavior of adhesive systems containing bioactive particles associated with the incorporation of 0.1wt% hydroxyapatite (HA), focusing on their water sorption (S), solubility (SB), and wettability (contact angle, CA).

Materials & Methods: The experimental design included two factors: (1) adhesive system at five levels—Adper Scotchbond Multipurpose (MP), Clearfil SE Bond (SE), FL Bond II (FL), Adper Single Bond Universal (SU), and BeautiBond Xtreme (BX); and (2) condition at two levels—control (unmodified adhesives, C) and adhesives with 0.1 wt% HA incorporationH). For S and SB analysis, disc-shaped specimens ($n = 10$) were prepared using a custom mold (0.8×4mm), and mass measurements were recorded in three steps: initial desiccation (m1), water immersion (m2), and final desiccation (m3). Results were expressed in $\mu g/mm^3$. For wettability analysis, droplets of each adhesive ($n = 6$) were deposited onto glass slides, and contact angles were measured. Data were analyzed using two-way ANOVA, followed by Tukey's post-hoc test ($p < 0.05$).

Results: The results showed that the universal adhesive SU exhibited the highest values for both sorption and solubility, suggesting greater water interaction due to its hydrophilic nature. Additionally, HA incorporation led to increased sorption values for all materials. In terms of wettability, the inclusion of HA reduced the contact angle for all adhesives, except for BX, which remained stable.

Conclusions: In conclusion, the addition of bioactive particles did not significantly alter the hydrophilicity of the adhesive systems. Although the incorporation of hydroxyapatite increased sorption and solubility, it enhanced the wettability of the tested adhesive materials.

https://doi.org/10.1016/j.dental.2026.03.061

50
In-vitro characterization and clinical survival of bulk-fill-composites: A systematic review

F von Knobloch [1], J Selbertinger [1], F Pfefferkorn [2], A Schedle *[1]

[1] *Medical University of Vienna, University Clinic of Dentistry, Vienna, Austria*
[2] *Dentsply DeTrey GmbH, Konstanz, Germany*

Purpose / Aim: The objectives of this study were to investigate the longevity and quality of restorations placed with bulk-fill composites compared to conventional composites. Both material categories were characterized by in-vitro properties (part I) and by their longevity in short and long-term clinical studies (part II).

Materials & Methods: Part I: All bulk-fill composites had a flexural strength well above 80 MPa and can therefore be used in the posterior region including occlusal surface in accordance with ISO 4049. Despite higher volume shrinkage compared to conventional composites, bulk-fill flowables achieved the significantly lowest shrinkage stress which enables the use in lager increments compared to conventional composites.

Part II: Four different databases PubMed, MEDLINE via Ovid, Embase and Cochrane Library were used for a systematic literature retrieval of clinical trials regarding the longevity of bulk-fill composites in comparison to conventional composites, structured according to the PRISMA flow diagram. Included studies were evaluated in terms of esthetic, functional and biological properties and a calculation of the mean annual failure rate (mAFR) was performed.

Results: Part I: All bulk-fill composites had a flexural strength well above 80 MPa and can therefore be used in the posterior region including occlusal surface in accordance with ISO 4049. Despite higher volume shrinkage compared to conventional composites, bulk-fill flowables achieved the significantly lowest shrinkage stress which enables the use in lager increments compared to conventional composites.

Part II: Both material types showed acceptable mean mAFRs with a slightly lower mean mAFR for bulk-fill composites (0.78%) compared to conventional composites (1.33%). The findings of the short-term studies (< 2 years) indicated the following sequence of reasons for failures of bulk-fill materials, ranging from most to least significant: Retention > marginal staining > fractures. The order for long-term studies (> 2 years) was: Color stability and translucency > anatomic form > marginal adaption > tooth integrity > recurrence of caries, erosion and abfraction > marginal staining. Bulk-fill composites showed slightly higher Alpha and Bravo scores, and lower Charlie scores compared to conventional composites.

Conclusions: This study shows that the investigated flowable and viscous bulk-fill composites have a flexural strength comparable to conventional composites and significantly lower shrinkage stress. Their mAFR is lower than that of conventional composites. These results suggest that flowable and viscous bulk-fill composites, which allow fewer increments to place a filling, lead to clinical outcomes comparable to conventional composites.

https://doi.org/10.1016/j.dental.2026.03.062

51
Experimental adhesive loaded with fluoride-containing bioactive particles and biomimetic analogue

N Carvalho [1], P Ferreira [1], F Gomes [1], S Abreu [1], T Oliveira [1], A Loguercio [2], J Bauer *[1]

[1] *UFMA, São Luís, Brazil*
[2] *UEPG, Ponta Grossa, Brazil*

Purpose / Aim: To develop and characterize experimental self-etching adhesive systems loaded with fluoride-containing bioactive particles and polyacrylic acid as a biomimetic analogue.

Materials & Methods: Different concentrations of non-silanized fluoroaluminosilicate glass particles and polyacrylic acid were added to the hydrophobic phase of experimental self-etching adhesive systems. The evaluated properties included: cohesive strength, alkalinizing activity (pH), ion release of fluoride (F^-), calcium (Ca^{2+}), and phosphate (PO_4^{3-}), cell viability, and formation of hydroxyapatite nanoprecursors. Surface analyses were performed using scanning electron microscopy/energy-dispersive spectroscopy (SEM/EDS) and X-ray diffraction (XRD) after 28 days of storage at 37°C in phosphate-buffered saline. Data were analyzed using one-way ANOVA and the Holm-Sidak post hoc test ($\alpha = 0.05$).

Results: The adhesive systems containing fluoroaluminosilicate particles were able to alkalinize the solutions at all evaluated time points. The addition of 10% fluoroaluminosilicate and polyacrylic acid increased the release of F^-, Ca^{2+}, and PO_4^{3-} ions. The cohesive strength and elastic modulus of the experimental adhesives showed values comparable to the control group ($p > 0.05$). The incorporation of these particles contributed to the formation of hydroxyapatite nanoprecursors. All experimental groups demonstrated similar biocompatibility values and were not cytotoxic to the cells. Moreover, the formation of hydroxyapatite precursor nanodeposits enhanced cell viability.

Conclusions: The incorporation of polyacrylic acid as a biomimetic analogue, in combination with fluoroaluminosilicate bioactive particles, appears to be a promising strategy for enhancing self-etching adhesive systems. This combination demonstrates the ability to neutralize pH, increase ionic release and cell viability, and promote the formation of hydroxyapatite nanoprecursors, without compromising the mechanical properties of the adhesive

https://doi.org/10.1016/j.dental.2026.03.063

52
Effects of Calcium Polyphosphate Bleaching Gels on Eroded Enamel

C Barbosa *[1], M Guanipa-Ortiz [1], J Andrade [1], W Vieira-Junior [1], K Rischka [2], F Aguiar [1], D Lima [1]

[1] *Faculdade de Odontologia de Piracicaba, Piracicaba, Brazil*
[2] *Fraunhofer Institute for Manufacturing Technology and Advanced Materials IFAM, Bremen, Germany*

Purpose / Aim: This in vitro study aimed to evaluate the changes in physical properties of dental enamel after bleaching using gels with different compositions followed by an erosive challenge.

Materials & Methods: Bovine enamel specimens (4 × 4 × 2 mm; n = 12/group) stored in artificial saliva were treated with bleaching gels containing carbamide peroxide (CP) or hydrogen peroxide (HP) with or without calcium polyphosphate (CaPP) followed by an erosive challenge. In Experiment 1, 10% commercial CP (CPC), CPC + 2% NaF, 10% manipulated CP (CPM), CPM + 2% NaF, 10% CP + 0.5 wt% CaPP, 10% CP + 1.5 wt% CaPP, manipulated gel without CP, or no bleaching were applied for 14 days. In Experiment 2, CP was switched with 35% HP, and all gels were applied for two sessions. Thereafter, all samples were subjected to a 5-day erosive challenge using 1% citric acid (pH 3.5) for 120 s. Enamel surface loss was assessed using contact profilometry and scanning electron microscopy (SEM). Statistical analysis was performed using a generalized linear model ($\alpha = 0.05$).

Results: Compared with that in the CP + 0.5% CaPP and HP + 0.5% CaPP groups, enamel loss was significantly greater in the CPM and CPC groups and HPM and HPC groups in Experiments 1

and 2, respectively. SEM analysis showed lesser organic-matrix dissolution in the groups containing 0.5% CaPP. Both low- and high-concentration bleaching gels containing 0.5% CaPP improved enamel preservation after an erosive challenge compared to that with gels without CaPP.

Conclusions: Thus, the addition of CaPP may help minimize enamel damage during bleaching by reducing mineral loss.

https://doi.org/10.1016/j.dental.2026.03.064

53

Multifactorial Analysis of Universal Composite Shade Matching

A AlShabib *, T Aloraini, A Alwazzan, F Alhelal, M Alselmi, H Algamaiah

King Saud University, Riyadh, Saudi Arabia

Purpose / Aim: This study aimed to evaluate the shade-matching accuracy of five Universal-shade resin composites in anterior and posterior teeth. Additionally, it investigated factors such as cavity depth and digital shade-matching devices (OptiShade and Easyshade) on color matching performance

Materials & Methods: Five universal one-shade composites (Omnichroma, Omnichroma Flow, Omnichroma Bulk Flow, Vitra APS Unique, and Charisma Bulk Flow ONE) were tested. Four extracted human teeth (two upper central incisors and two premolars) from a single donor were used, each serving as a natural tooth mold. Standardized non-retentive cavities (5 mm diameter; depth 2 mm or 3 mm) were prepared in each tooth. Cavities were restored in one increment with the assigned composite, using a clear matrix and a custom index to ensure a flush surface, then light-cured for 40 s (Fig. 1). Pre- and post-restoration tooth color was measured with two calibrated digital shade devices (OptiShade and VITA Easyshade V), recording CIE L*, a*, b* values. Color differences between the restored and baseline color were computed using the CIEDE2000 formula. All data were statistically analyzed ($\alpha = 0.05$) to identify significant effects of material, cavity location, and depth.

Results: ΔE2000 color differences ranged from approximately 1.3 (minimal mismatch) to 6.8 (pronounced mismatch) across all tested conditions, indicating that shade matching performance varied widely. Overall, shallow anterior restorations showed the lowest ΔE2000 values (better shade match), whereas deeper posterior restorations yielded the highest ΔE2000 values (poorer match). Statistical analysis confirmed significant effects of composite material, tooth location (anterior vs. posterior), and cavity depth on color matching ($p < 0.05$). Among the composites, Charisma Bulk Flow ONE exhibited the smallest mean ΔE2000 (generally < 4), indicating more consistent shade adaptation, while Omnichroma showed the largest ΔE2000 values in deep restorations (up to ~6.7), indicating visibly perceptible mismatches. The other one-shade materials (Omnichroma Flow, Omnichroma Bulk Flow, and Vitra APS Unique) showed intermediate performance, with generally better matching in anterior teeth.

Conclusions: Within the limitations of this study, one-shade resin composites showed promise for simplifying shade selection and minimizing the need for multiple composite shades. They generally produced acceptable esthetic results in small anterior restorations, but color matching was less predictable in larger or posterior restorations, with performance varying among different products. These findings indicate that one-shade composites can improve clinical efficiency and reduce material inventory, supporting more sustainable restorative practices, but clinicians should consider cavity size, location and material-specific capabilities to ensure optimal esthetic outcomes.

Figure 1

https://doi.org/10.1016/j.dental.2026.03.065

54

Impact of Silver Nanoparticles on Alginate: Microbiological and Mechanical Analysis

A Costa *[1,2], A Facury [3], E Franco [2], G Borges [3], J Neves [2], L de Figueiredo [1], L Correr-Sobrinho [2]

[1] *Herminio Ometto Foundation (FHO), Araras, Brazil*
[2] *Piracicaba Dental School - State University of Campinas (FOP-UNICAMP), Piracicaba, Brazil*
[3] *University of Uberaba (UNIUBE), Uberaba, Brazil*

Purpose / Aim: This study assesses the antimicrobial activity and physical alterations of alginate impression material mixed with silver nanoparticle (AgNP) solutions.

Materials & Methods: The samples were assigned to five groups according to type of alginate and mixing solution: (G1) Avagel + distilled water; (G2) Jeltrate + distilled water; (G3) Jeltrate + 0.2% chlorhexidine digluconate solution; (G4) Jeltrate + 0.2% silver nanoparticle solution; and (G5) Jeltrate + 1% AgNP. Silver nanoparticles (AgNPs) were synthesized from fungus Trichoderma reesei. Fifty impressions were made ($n = 10$) from a metal matrix, from which plaster models were fabricated. Surface detail reproduction and dimensional stability were analyzed under a light microscope. Surface detail reproduction results were obtained by observing the replication of a 50 μm line on the plaster model. Dimensional stability (in percentage) was calculated by subtracting the measurements between X' and X'' from the matrix and plaster model. The antimicrobial effect was assessed independently based on the formation of zones of inhibition between the alginate molds ($n = 3$) and the agar medium containing Streptococcus mutans and Candida albicans. Dimensional stability values were subjected to ANOVA and Tukey's post-hoc test ($\alpha = 0.05$).

Results: G3 yielded the highest dimensional stability and showed significant differences from the other groups ($p < 0.05$) (Table 1). A 50 μm line was reproduced in plaster for all tested groups, regardless of the impression material and antimicrobial solution.

Conclusions: AgNPs incorporated into the alginate mixture did not produce dimensional changes in the alginate mold. G1 and G3 exhibited antimicrobial potential, as evidenced by bacterial inhibition. Jeltrate or Avagel, regardless of the concentration of AgNP solution, did not demonstrate antimicrobial activity.

Funding: PIC - FHO 2024/2025.

Table. Mean values ± standard deviation of dimensional stability (%).

GROUPS	DIMENSIONAL STABILITY (%)
G1 – Avagel + water (AW)	99.6 ± 0.06 b
G2 – Jeltrate + water (JW)	99.2 ± 0.08 b
G3 – Jeltrate + CHX (J.CHX)	100.0 ± 0.15 a
G4 – Jeltrate + 0.2% AgNP (JAgNP_0.2%)	99.5 ± 0.09 b
G5 – Jeltrate + 1% AgNP (JAgNP_1%)	99.4 ± 0.09 b

Note: A – Avagel; J – Jeltrate; CHX – 0.2% chlorhexidine digluconate; and AgNP – silver nanoparticle. **Avagel composition:** potassium alginate, calcium sulfate, tetrasodium pyrophosphate, potassium fluotitanate, polyethylene glycol, magnesium oxide, diatomaceous earth, flavoring, chlorhexidine, anhydrous alcohol, and phenolphthalein (data provided by the manufacturer). **Jeltrate composition:** potassium alginate, calcium sulfate, tetrasodium pyrophosphate, potassium fluotitanate, polypropylene glycol, magnesium oxide, diatomaceous earth, pigments, flavoring (data provided by the manufacturer).

https://doi.org/10.1016/j.dental.2026.03.066

55

Influence of different fluoride varnishes on dentin tubule occlusion

M Barros *, J Figueiredo, AB Borges, CRG Torres

Institute of Science and Technology, Sao Paulo State University - UNESP, São José dos Campos, Brazil

Purpose / Aim: The aim of this study was to evaluate the effect of six different fluoride varnishes on the dentin tubule occlusion.

Materials & Methods: Sixty dentin specimens were obtained from bovine incisors. They were cleaned with ultrasonic bath, completely dried and analyzed in a scanning electron microscope, obtaining images with an original magnification of 5,000X (Phenom XL, Thermo Scientific). The area occupied by the lumen of dentin tubules was calculated using the ImageJ software. The specimens were divided into 6 groups according to the treatments applied (n = 10): PRO- 5%NaF varnish (Profluorid, Voco); PBM- 5%NaF + BioMin varnish (Profluorid BioMin, Voco);BIF- 5%NaF + 5%CaF2 varnish (Bifluoride 10, Voco); CC –2.1%NaF + calcium phosphate (Clinpro Clear, 3M); CW - 5%NaF varnish (Clinpro White, 3M); EFV – 2.4%NaF experimental fluoride varnish (Voco). The specimens were immersed for 24h into artificial saliva and the varnishes removed with acetone, being immersed again in artificial saliva for 7 days. After this time the varnish application was repeated, as well the immersion in saliva for an additional 7 days. After that, new images were obtained and the area of the dentin tubules measured again. The reduction percentage of the area occupied by the dentin tubules was calculated. The data were analyzed using one-way ANOVA and Tukey test.

Results: ANOVA showed significant differences among the groups (p = 0.001). The results of Tukey test were: CW-94.91(3.10) a, EFV-96.84(2.72)ab, PB-96.98(1.33)ab, CC-97.63 + (2.23)b, PRO = 98.97(0.70)b, BIF-99.04(0.64)b. Groups followed by different letters do not present significant differences.

Conclusions: All varnishes tested showed high levels of tubule occlusion, although it was smaller for Clinpro White in relation to some products. The other materials were not statistically different.

https://doi.org/10.1016/j.dental.2026.03.067

56

Recycled Zirconia: Influence of Low-Temperature Degradation on Wear Resistance

L Alves *[1], E Benalcazar-Jalkh [1], T Campos [2], E Bergamo [1], E Oliveira [1], S Tebscherani [3], C dos Santos [4], Y Zhang [5], E Bonfante [1]

[1] *University of São Paulo - Bauru School of Dentistry, Bauru, Brazil*
[2] *Federal University of Pelotas (UFPel), Pelotas, Brazil*
[3] *Federal University of Technology, Parana, Brazil*
[4] *University of Rio de Janeiro State, Volta Redonda, Brazil*
[5] *School of Dental Medicine, University of Pennsylvania, Philadelphia, USA*

Purpose / Aim: To evaluate the influence of low-temperature degradation on the wear resistance and translucency parameter of recycled zirconia relative to commercially available 3Y-TZP and 5Y-PSZ.

Materials & Methods: Recycled zirconia powder was obtained from 3Y block remnants through high-intensity orbital milling. The powder was calcined at 900ºC and sieved. Twelve discs of recycled 3Y (diameter: 12 mm; thickness: 1.2 mm) were obtained by uniaxial pressing and sintered (1550ºC – 2h). As controls, discs of commercial zirconia 3Y and 5Y (Ceramill Zi and Ceramill Zolid fx, Amanngirrbach GmbH) were obtained and sintered (1450ºC – 2h). Half of the specimens of each group underwent hydrothermal aging (134˚C, 20h, 2.2 bar). A sliding wear test was performed using a spherical zirconia antagonist (100 N load, 1,250,000 cycles in water). The wear area was assessed using optical microscopy and quantified with ImageJ software. Wear characteristics were assessed by scanning electron microscopy (SEM). Crystalline phases were identified through X-Ray Diffraction (XRD). Translucency Parameter (TP) was evaluated before and after aging. Data from wear and TP measurements were analyzed using ANOVA followed by Tukey's post hoc test.

Results: Aging and material significantly influenced the wear area ($p = 0.01$ and $p = 0.00$, respectively). 3Y and recycled 3Y aged groups exhibited similar wear areas, both significantly larger than those of the other groups. In contrast 3Y immediate demonstrated the lowest wear area, which was comparable to the 5Y groups, regardless of aging condition. SEM revealed larger wear scars after aging for both 3Y and recycled 3Y, while 5Y did not demonstrated influenced of the aging on the wear characteristics. XRD showed a predominance of tetragonal phase in 3Y and recycled 3Y, with the presence of monoclinic peaks after aging. In contrast, 5Y predominantly exhibited a stable cubic phase, unaffected by aging. The highest TP was observed for 5Y, followed by 3Y, while recycled 3Y exhibited the lowest TP, regardless of aging condition ($p = 0.001$). Aging reduced TP only for 5Y ($p = 0.001$).

Conclusions: Recycled 3Y exhibited wear resistance comparable to 3Y, however lower translucency. These findings suggest that recycled zirconia represents a viable and sustainable alternative for applications prioritizing wear resistance over translucency.

https://doi.org/10.1016/j.dental.2026.03.068

57

Influence of Printing Temperature on Accuracy and Strength of Crowns

A Correr *, U Monteiro, G Baccaro, A Rios, L Correr-Sobrinho

Piracicaba Dental School - UNICAMP, Piracicaba, Brazil

Purpose / Aim: This study aimed to evaluate the effect of printing temperature on the linear dimensional accuracy and flexural strength of resin composite crowns fabricated using 3D printing technology.

Materials & Methods: Full-contour crowns were designed (Exocad, DentalCAD 3.2) and printed with a photopolymerizable resin composite (SmartDent, Vitality; 58 wt% glass filler) at three different temperatures: 25 °C, 37 °C, and 50 °C (n = 10), using a Photon Mono 2 LCD printer (Anycubic). A 3D printing Heater Air (Anycubic) device was used during the printing of heated groups. Both the crowns and flexural bars were washed in isopropyl alcohol for 5 minutes and post-cured under violet light for 10 minutes in a Wash&Cure unit (Anycubic). Dimensional accuracy was assessed in four anatomical regions: mesiodistal length (MDL), buccolingual width (BLW), mesial cusp height (MCH), and buccal wall thickness (BWT), using an STM Measuring Microscope (Olympus). To measure BWT, the crowns were bisected buccopalatally using a diamond disc on a cutting machine. To ensure standardization, a 1 mm spherical protuberance was added to each measurement site during the crown design (CAD) phase, serving as a reference point for accurate and consistent dimensional analysis. Flexural strength was evaluated according to ISO 4049 using a three-point bending test (n = 10). Data were analyzed using one-way ANOVA and Tukey's post-hoc test (α = 0.05).

Results: Printing temperature significantly influenced BLW (p = 0.0222), with the highest accuracy observed at 37 °C (98.3 ± 1.5%) and the lowest at 25 °C (96.6 ± 1.6%). The group printed at 50 °C showed intermediate accuracy (97.9 ± 0.9%) and was statistically similar to both. No significant differences were found for MDL (p = 0.749), MCH (p = 0.947), or BWT (p = 0.117). Accuracy ranged from 97.6% to 97.9% for MDL, 96.3% to 96.6% for MCH, and 95.5% to 96.9% for BWT (Table 1). Flexural strength was also significantly affected by temperature (p = 0.0133). The highest mean flexural strength was obtained at 37 °C (181.82 ± 6.89 MPa), followed by 50 °C (175.54 ± 6.89 MPa) and 25 °C (153.27 ± 6.50 MPa). Statistically significant differences were found between 25 °C and 37 °C (p = 0.0149).

Conclusions: Printing temperature plays a critical role in optimizing both the dimensional accuracy and mechanical performance of 3D-printed crowns. The temperature of 37 °C provided the best balance between precision and strength, suggesting it as a favorable setting for clinical applications.

Table 1. Adjusted means (± SD) of linear accuracy (%) of 3D-printed crowns and flexural strength (MPa) of 3D-printed bars at different temperatures, followed by the statistical grouping.

Temperature	MDL (%)	BLW (%)	MCH (%)	BWT (%)	Flexural Strength (MPa)	
25	97.6 ± 0.9 A	96.6 ± 1.6 B	96.3 ± 1.9 A	96.8 ± 2.1 A	153.27 ± 6.50	B
37	97.9 ± 0.6 A	98.3 ± 1.5 A	96.4 ± 2.2 A	95.5 ± 1.6 A	181.82 ± 6.89	A
50	97.8 ± 1.0 A	97.9 ± 0.9 AB	96.6 ± 1.9 A	96.9 ± 0.9 A	175.54 ± 6.89	AB

https://doi.org/10.1016/j.dental.2026.03.069

58

Evaluation of cusp coverage approaches for structurally compromised teeth

L Bernal *[1,2], G Ojeda [3], M Ernst [4]

[1] *Facultad de Odontología, Universidad San Sebastian, Puerto Montt, Chile*
[2] *Escuela de doctorado Universidat Internacional de Catalunya, Barcelona, Spain*
[3] *Facultad de Odontología, Universidad de los Andes, Santiago, Chile*
[4] *Facultad de Odontologia Universidad de Concepcion, Concepcion, Chile*

Purpose / Aim: This study aims to evaluate the mechanical resistance of endodontically treated maxillary premolars by comparing two direct and one indirect restorative techniques for cusp coverage.

Materials & Methods: Thirty freshly extracted, intact maxillary premolars of standardized dimensions were selected. Standardized MOD cavities involving both cusps were prepared. The teeth were randomly assigned to three groups: Group 1, restored with Bulk Fill resin and an overlay restoration (RBD) (n = 10); Group 2, rehabilitated with Ribbond and resin on the cavity floor plus a resin overlay (RIB) (n = 10); and Group 3, restored with Bulk Fill resin and a lithium disilicate ceramic overlay (e.max) (n = 10). Restored teeth were stored in distilled water at 37 °C for 60 days. A monotonic axial load was then applied until fracture. Fracture load data were analyzed using one-way ANOVA and Tukey's post-hoc test for multiple comparisons (α = 0.05). Fracture initiation and propagation were examined using stereomicroscopy and scanning electron microscopy.

Results: Differences in fracture resistance were observed among the e.max, RBD, and RIB groups. The e.max group demonstrated the highest resistance, while the RBD group exhibited the lowest. In the RBD group, fracture initiation and propagation primarily occurred within and through the restoration. In contrast, the fiber-reinforced (RIB) group showed a shift in fracture patterns toward the external surfaces of the restoration. Evidence of crack deflection and bridging around the polyethylene fibers was observed in the RIB group.

Conclusions: The incorporation of polyethylene fibers in extensive resin-based overlay restorations for endodontically treated premolars reduced the incidence of cohesive fractures within the restorative material, limited crack propagation, and enhanced fracture resistance compared to composite resin restorations without fiber reinforcement. However, this approach did not reach the level of protective performance observed in glass-ceramic restorations.

https://doi.org/10.1016/j.dental.2026.03.070

59

Development and characterization of a photoresponsive silver vanadate dental resin

J Tardelli *[1,2,3], ML Leite [1,4], A Costa [1], M Schiavon [5], A Reis [3], R Carvalho [2], A Manso [1]

[1] *Department of Oral Health Sciences, The University of British Columbia, Vancouver, Canada*
[2] *Department of Oral Biological and Medical Sciences, The University of British Columbia, Vancouver, Canada*
[3] *Department of Dental Materials and Prosthodontics, University of São Paulo, Ribeirão Preto, Brazil*
[4] *Department of Operative Dentistry and Dental Materials, University of Saskatchewan, Saskatoon, Canada*

[5] *Department of Natural Sciences, Federal University of São João del-Rei, São João del-Rei, Brazil*

Purpose / Aim: The aim of this study was to develop and evaluate new experimental dental resin blends (RB) loaded with silver vanadate (SV) salt on their chemical and physical properties, as well as their antimicrobial and cytotoxic effects associated or not with blue light antimicrobial photodynamic therapy (aPDT), immediately and after storage.

Materials & Methods: The experimental RB (70% Bis-EMA/30% TEEGDMA) was mixed with either 0.5w% or 1.0w% SV to establish the following groups: RB (control), RB + 0.5SV, and RB + 1SV. The RBs were initially assessed for their degree of conversion (DC). Next, resin discs (6 mm diameter by 1 mm thickness) were formed in a metallic mold and photocured (40 s on each side) at ~850 mW/cm^2 for contact angle (CA) (n = 6), water sorption (WS) and solubility (SL) (n = 9). Flexural strength (FS) bars (25 × 2 × 2 mm) were fabricated, photocured for 360 s in total at 850 mW/cm^2, and randomly stored in water for 1-, 7- or 30-day period (n = 12). Additional bars (n = 12) were produced for SV release. The antimicrobial activity of the RBs was assessed on the surface of resin discs against a dual-species cariogenic biofilm (S. mutans and C. albicans) and determined by CFU assays, immediately and after 30-day water storage, under dark and blue light treatment conditions (450 nm; 40.5 J/cm^2) (n = 9). A viability test was performed on gingival epithelial cells (MTT), associated or not with blue light (450 nm; 40.5 J/cm2) (n = 8). Data were analyzed by ANOVA and Tukey; a = 5%.

Results: The incorporation of SV at either 0.5% or 1.0% did not compromise the DC, WS, SL, and FS values compare to the controls ($p > 0.05$). However, SV-loaded resins presented significantly higher CA values than RB control ($p < 0.05$). Water storage resulted in a significant increase in FS for all RBs after 7 and 30 days ($p < 0.05$), while SV release decreased over time. Immediate antimicrobial effects were observed for RB + 1SV in dark conditions, plus all experimental groups associated with aPDT. After 30-day water storage, the antimicrobial activity was sustained and comparable to immediate values for RB + 0.5SV and RB + 1SV with aPDT ($p < 0.05$). Only RB + 1SV combined with light treatment reduced cell viability ($p < 0.05$).

Conclusions: The addition of SV did not negatively impact physicochemical and mechanical properties of the experimental RBs. Furthermore, the experimental RB loaded with 0.5% SV presented as non-cytotoxic while sustaining antimicrobial effects against dual-species biofilms after 30-day water storage, when associated with blue light PDT.

https://doi.org/10.1016/j.dental.2026.03.071

60

Low-peroxide bleaching gel with BioS_Nb_2O_5 activated by violet LED

G Santos *[1], I Matos [1], M Souza [2], E Zanotto [2], V Leitune [3], V Cavalli [1]

[1] *University of Campinas - UNICAMP, Piracicaba, Brazil*
[2] *Federal University of São Carlos (UFSCar), São Carlos, Brazil*
[3] *Federal University of Rio Grande do Sul (UFRGS), Porto Alegre, Brazil*

Purpose / Aim: Despite its proven efficacy, in-office tooth bleaching with 35% hydrogen peroxide (HP) is associated with adverse effects on dental structure and pulp tissue. Therefore, reducing HP concentration is desirable to minimize these side effects without compromising bleaching efficacy. This study aimed to evaluate the bleaching efficacy and enamel surface effects of experimental gels containing 3% and 6%HP and a combination of biosilicate / niobium pentoxide (BioS_Nb), irradiated by violet LED, in order to determine the optimal Nb_2O_5 concentration.

Materials & Methods: Bovine enamel–dentin blocks were stained with black tea (pH = 7.0), and randomly assigned to nine groups (n = 5/group): 3%HP + BioS (1.5, 2.0 and 2.5 wt% Nb), 6% HP + BioS (1.5, 2.0 and 2.5 wt% Nb), 3%HP, 6%HP, and 35%HP (commercial – control group). All groups were irradiated with violet LED, except the control. Three bleaching sessions (30 minutes each, with 7-day intervals) were performed. Color change and whiteness index (ΔE_{00} and ΔWID) were assessed using the parameters L*, a*, b*. Surface microhardness (KHN, %SHR) and surface roughness (ΔRa) were also evaluated. Analyses were performed at baseline (T0), 24 h (T1) and 14 days (T2) after the final bleaching session. Data were analyzed using two-way ANOVA followed by Tukey or Bonferroni post hoc tests (α = 5%).

Results: At T1, the 3%HP + BioS_1.5%Nb and 3%HP groups showed significantly lower ΔE_{00} values compared to the control and their respective groups within both factor (particle and HP). At T2, all groups showed no difference compared to the control. Both 3%HP and 6%HP gels containing BioS_2%Nb showed no statistical difference from each other or the 35%HP, whereas other groups exhibited significant reduction in ΔWID at T1. At T2, only the 3%HP + BioS_1.5%Nb and 3%HP groups showed a significant reduction in ΔWID compared to 35%HP. The 3%HP + BioS_2%Nb group demonstrated a significantly higher ΔWID compared to its respective particle concentration groups at both T1 and T2. No significant differences were observed among all groups over time for KHN, ΔRa, or %SHR values ($p > 0.05$).

Conclusions: Experimental bleaching gels containing 3% or 6% hydrogen peroxide combined with Biosilicate® and 2%Nb, and activated by violet LED irradiation, delivered bleaching efficacy without compromising the physical properties of dental enamel.

https://doi.org/10.1016/j.dental.2026.03.072

61

Spray-Dried Tea-Tree and Eucalyptus Essential-Oil Microcapsules for Antimicrobial Dental Applications

FP Rodrigues *[1], L de Paula [2], S Brignone [3], S Palma [3], M Marczewski [4], S Raghu [5], M Killian [5]

[1] *University of Leeds, Leeds, UK*
[2] *Paulista University-UNIP, Sao Paulo, Brazil*
[3] *University of Cordoba, Cordoba, Argentina*
[4] *Łukasiewicz-PIT, Poznan, Poland*
[5] *University of Siegen, Siegen, Germany*

Purpose / Aim: To synthesise and characterise spray-dried tea tree and eucalyptus essential oils microcapsules for incorporation into dental materials where antimicrobial activity and formulation stability are desired, such as varnishes, oral hygiene products, and temporary restorative materials.

Materials & Methods: Essential oil-loaded microcapsules were prepared via spray-drying using two encapsulating systems: gum arabic/maltodextrin (GA/MDX) and hydroxypropyl methylcellulose/maltodextrin (HPMC/MDX). The aqueous phase was made by dissolving HPMC or GA under magnetic stirring for 12 h and MDX for 5 min. Commercial tea tree and eucalyptus essential oils (DoTerra®, USA) were added to aqueous-polymer dispersions and homogenised at 18,000 rpm for 30 min (Ultra-Turrax T25 IKA-Works, USA). The emulsions were atomised using hot-air-jet in the drying-chamber (160 °C inlet and 100 °C outlet temperatures, Q-flow was 600L/h; 10% vacuum, 100% aspiration) using a spray-dryer

(Büchi-B-290-Labortechnik-AG-Flawil, Switzerland). Five formulations were prepared using a 1:1 (emulsion base:oil phase) (1) HPMC + MDX + Eucalyptus; (2) GA + MDX; (3) GA + MDX + Eucalyptus; (4) GA + MDX + Tea Tree; and (5) HPMC + MDX. Characterisations were performed including X-ray diffraction (XRD) (Malvern-PANalytical, UK) to assess crystallinity (λ = 1.524Å; 40kV; 15mA), and ageing effects at 0 and 2-week storage in room temperature, with 2θ = 10–100°, Cu-Kα radiation; Zeta potential analysis (Malvern-Nano-Zetasizer, Germany) of 15 mg of powders dispersed in 2.5 mL of PBS to assess the suspension stability and particle dispersion (pH 7.4, 25 °C); and Scanning electron microscopy (Hitachi-4800, Japan) to assess morphology and surface integrity.

Results: Essential oil-based microcapsules presented expected spray drying process spherical morphology (0.5–15 μm), with low crystallinity and amorphous structure confirmed by broad XRD peaks for all groups. The peak between 15° and 25° was broad and of low-intensity, which corresponds to the low-level of powder-crystallinity. No structural changes were observed after ageing, however, the addition of both eucalyptus and tea tree led to a more electronegative zeta potential ($p = 0.996$), enhancing stability. The particles in these powders had a negative surface charge, indicating repulsion between particles, preventing their aggregation when suspended in a solvent. However, SEM of all groups revealed concave surfaces morphologies, and minimal, but some aggregation. HPMC reduced the formation of depression.

Conclusions: Spray-drying produced stable-spherical microcapsules suitable for incorporation into dental materials. Both essential-oils contributed to improved colloidal stability and may support long-term dispersion and antimicrobial action, with potential for future use in dental materials targeting biofilm control.

https://doi.org/10.1016/j.dental.2026.03.073

62

Niobium Calcium Phosphate in Experimental Resin Endodontic Sealer Properties

R Tomasi, E Gaviolli, V Leitune *

Federal University of Rio Grande do Sul, Porto Alegre, Brazil

Purpose / Aim: To synthesize calcium phosphate particles with niobium, incorporate them into an experimental resin-based endodontic sealer, and evaluate their properties.

Materials & Methods: Calcium phosphate particles with niobium were synthesized by mixing NaCl, KCl, Na_2HPO_4, KH_2PO_4, $CaCl_2$, and $NbCl_5$, by precipitation synthesis method. A dual-cure experimental endodontic sealer was formulated using UDMA, BISEMA, and GDMA, with camphorquinone, DHEPT, and benzoyl peroxide as activator/initiator. The particles were added to the sealer at three concentrations: 10 wt.%, 20 wt.%, and 30 wt.%. A control group without particles was used for comparison. The evaluated properties included radiopacity, degree of conversion, flexural strength, flow, and film thickness. Data were analyzed by one-way ANOVA and Tukey.

Results: Groups with particle addition showed higher radiopacity and lower degree of conversion compared to the control group ($p < 0.05$). The control group exhibited the highest flexural strength, while groups with particle addition showed a significant reduction ($p < 0.05$). Regarding flow, groups with particle addition had lower flow values, with no statistical difference between the 20 wt.% and 30 wt.% addition groups. Film thickness was higher in groups with particle addition ($p < 0.05$).

Conclusions: It was possible to successfully synthesize calcium phosphate particles with niobium. The addition of particles at concentrations of 10%, 20%, and 30%, by weight, reduced flexural strength, degree of conversion, and flow, while increasing film thickness and radiopacity of experimental sealers.

https://doi.org/10.1016/j.dental.2026.03.074

63

Light attenuation through varying lithium disilicate thicknesses and opacities

N Zubair [1], M Dawoudzai [1], E Omoto [2], M Queiroz [2], J da Silva [3], A Maluly-Proni [2], T Fagundes [2], PH Dos Santos *[1]

[1] *University of Toronto, Toronto, Canada*
[2] *Sao Paulo State University - UNESP, Aracatuba, Brazil*
[3] *University of Campinas, Piracicaba, Brazil*

Purpose / Aim: This study evaluated the influence of thickness and opacity of lithium disilicate (LD) ceramics on their optical properties—translucency, contrast ratio (CR), and light attenuation—as well as on the degree of conversion (DC) and mechanical properties (nanohardness and elastic modulus) of light-cured resin cements

Materials & Methods: A total of 128 LD ceramic specimens (IPS emax CAD, 6 × 6 mm) were fabricated in four thicknesses (0.5, 1.0, 1.5, and 2.0 mm) and four opacity levels: high translucency (HT), medium translucency (MT), low translucency (LT), and medium opacity (MO). Samples were processed using standardized cutting, sintering, and polishing protocols. Spectrophotometry was used to assess translucency and CR, while irradiance attenuation was measured with a MARC Patient Simulator under a polywave LED curing unit (1200 mW/cm^2). Light-cured resin cements were polymerized beneath the ceramic specimens, and their DC was analyzed via Fourier-transform infrared spectroscopy (FT-IR). Nanoindentation tests were conducted to evaluate nanohardness and elastic modulus.

Results: Ceramic thickness and opacity significantly affected translucency, CR, and light transmission. At thinner dimensions, HT and MT ceramics exhibited significantly higher translucency and lower CR values. However, at 2.0 mm thickness, differences among opacity levels became negligible. Light attenuation increased with thickness and opacity, leading to a significant reduction in DC and mechanical performance of resin cements, particularly under MO ceramics at 2.0 mm. Conversely, HT and MT ceramics at thinner thicknesses allowed for greater light transmission and improved resin cement polymerization and mechanical properties.

Conclusions: The optical and mechanical behavior of lithium disilicate ceramics is influenced by both thickness and opacity. Increased values reduce light transmission and resin cement performance, though optical differences diminish at greater thicknesses. Proper material selection and curing protocols are essential for optimal esthetics and long-term success.

https://doi.org/10.1016/j.dental.2026.03.075

64

Raman-AI models predict color and fatigue strength of zirconia crowns

MG Rocha *[1], IJ Daulton [1], A Delgado [1], E Kee [2], D Oliveira [1], J-F Roulet [1], P Zoidis [1], P Pereira [1]

[1] *University of Florida College of Dentistry, Gainesville, FL, USA*
[2] *Lousiana State University, New Orleans, LA, USA*

Purpose / Aim: To develop and validate Raman spectroscopy-based artificial intelligence models capable of predicting color properties and fatigue strength of zirconia crowns manufactured under different milling conditions.

Materials & Methods: Thirty central incisor crowns were manufactured using three distinct milling methods: dry milling (DM, n = 10), wet milling with distilled water (WM, n = 10), and wet milling with contaminated water (CM, n = 10). Chemical properties were analyzed using X-ray Diffraction and Confocal Raman Spectroscopy. Color analysis was performed with a spectrophotometer using the CIEDE2000 (ΔE00) formula. Specimens were cemented to standardized polyurethane dies and underwent stepwise fatigue testing. Statistical analyses (α = 0.05; β = 0.2) and artificial intelligence modeling were performed to correlate material composition with fatigue strength and color outcomes.

Results: CM specimens showed significantly higher cubic phase content (73.31 ± 1.31%) compared to DM (70.12 ± 1.05%) and WM (69.97 ± 0.89%). XRD revealed spectral shifts in WM samples indicating increased grain boundary stress. CM specimens exhibited significantly different L*, a*, b* values compared to DM and WM, while differences between DM and WM were predominantly in L* values. ΔE00 values were DM/WM: 0.93 ± 0.09; DM/CM: 3.20 ± 0.21 and WM/CM: 3.64 ± 0.29. The mean fatigue cycles were DM: 78,166 ± 2,138, CM: 72,894 ± 2,139, and WM: 68,347 ± 4,701, with Weibull moduli of 12.18 ± 3.03, 11.33 ± 2.86, and 4.86 ± 1.21, respectively. AI models for color prediction achieved R^2 values of 93.58% (L*), 76.58% (a*), and 91.35% (b*), while the fatigue prediction ensemble model reached R^2 = 82.48%.

Conclusions: CM significantly increased cubic phase content and produced clinically unacceptable color differences compared to DM and WM. DM demonstrated optimal performance with the highest fatigue resistance and lowest variability, while WM showed compromised mechanical properties despite acceptable color match to DM. The developed artificial intelligence system successfully identified complex relationships between crystallographic structure and material performance through specific Raman spectral features, establishing a promising tool for predicting zirconia properties based on manufacturing conditions.

https://doi.org/10.1016/j.dental.2026.03.076

65

Multi-acrylamide-based adhesives preserve dentin bond strength after radiotherapy

L Correr-Sobrinho *[1], A Colombino [1], A Correr [1], F Tsuzuki [1], A Costa [2,1], C Pfeifer [3]

[1] *State University of Campinas - UNICAMP, Piracicaba, Brazil*
[2] *Herminio Ometto Fundation, Araras, Brazil*
[3] *Oregon Health Science University - OHSU, Portland, USA*

Purpose / Aim: Patients undergoing head and neck radiotherapy often face compromised dentin bonding due to structural changes and increased degradation risk. Traditional methacrylate adhesives are prone to hydrolysis, limiting long-term performance. Multi-acrylamide monomers, which lack ester groups and offer enhanced crosslinking potential, may provide greater stability under these conditions. The aim of this in vitro study was to evaluate the effect of multi-acrylamides added to experimental adhesives on the microtensile bond strength (μTBS) of the dentin-composite interface before and after radiotherapy (RT).

Materials & Methods: Three experimental adhesives were formulated with UDMA (60 wt%) combined with 40 wt% of either TMAAEA (a tertiary triacrylamide), DEBAAP (a tertiary diacrylamide), or HEMA (hydroxyethyl methacrylate). Adper Single Bond (Adper SB; Solventum) was used as the commercial control. Specimens prepared from extracted human molars (n = 96) were allocated to four adhesive groups and further subdivided into three subgroups (n = 8) according to radiotherapy timing: Pre-RT, in which irradiation (70 Gy total; 2 Gy/day, 5 days/week for 7 weeks) was applied before adhesive procedures; Post-RT, where the same irradiation protocol was performed after bonding; and Control, with no irradiation. Microtensile sticks with 1 mm^2 cross-sectional area were prepared and tested to failure under tensile load (1.0 mm/min). Bond strength data were analyzed using ANOVA followed by Bonferroni post-hoc test (α = 0.05).

Results: Results are shown in Table 1. In the control condition (no irradiation), adhesives containing TMAAEA and Adper SB showed the highest bond strength values (μTBS), significantly higher than those with DEBAAP and HEMA ($p < 0.001$). After radiotherapy, both Adper SB and HEMA exhibited a significant reduction in μTBS when applied before or after irradiation ($p < 0.001$). In contrast, TMAAEA maintained high bond strength regardless of the timing of radiotherapy, with significantly better performance compared to the other adhesives, especially in the Post-RT group ($p < 0.001$). DEBAAP also showed consistent μTBS across all conditions, though without statistical superiority over Adper SB or HEMA. Overall, TMAAEA demonstrated the greatest resistance to radiotherapy-induced degradation.

Conclusions: The incorporation of multi-acrylamide monomers, particularly TMAAEA, into dental adhesives enhanced resistance to radiotherapy-induced degradation, maintaining bond strength across different clinical scenarios. These findings suggest that acrylamide-based adhesives represent a promising strategy for dental care in oncology patients.

Table – Means of microtensile bond strength (μTBS) ± Standard Deviation (MPa) for the adhesives modified with TMAAEA, DEBAAP, experimental control (HEMA), and for the commercial (Adper SB).

	μTBS (MPa)		
Silane	Control	Pre-RT	Post-RT
HEMA	23.6 ± 1.2 Ab	18.3 ± 2.7 Bb	20.1 ± 2.8 ABb
DEBAAP	23.2 ± 2.4 Ab	22.5 ± 7.4 Ab	23.1 ± 2.6 Aab
TMAAEA	31.1 ± 5.3 Aa	29.9 ± 3.6 Aa	27.6 ± 3.4 Aa
Adper SB	30.7 ± 2.1 Aa	19.3 ± 5.1 Bb	24.3 ± 5.4 Bab

Pre-RT: specimens received 70 Gy of radiotherapy (2 Gy/day, 5 days/week for 7 weeks) before restoration.
Post-RT: specimens were restored prior to receiving the same radiotherapy protocol.
Control: no radiotherapy applied.
Values followed by the different lower-case subscript within the same column and upper-case superscript in the same row are statistically different (α = 5%).

https://doi.org/10.1016/j.dental.2026.03.077

66

In vitro evaluation of single application of two-bottle bleaching gels

M Teixeira [1], L Condolo [2], L Barbosa [2], K da Cruz [1], A Reis [2], A Loguercio [2], T de Paris Matos [1], M Favoreto *[1]

[1] *Tuiuti University of Parana, Curitiba, Brazil*
[2] *State University of Ponta Grossa, Ponta Grossa, Brazil*

Purpose / Aim: To evaluate, in vitro, the hydrogen peroxide permeability into the pulp chamber, bleaching efficacy, and physicochemical properties (pH and initial concentration) of a new pH neutral two-bottle in-office bleaching gel, applied in a single session, in comparison to acidic products.

Materials & Methods: Sixty sound human premolars were randomly assigned into six groups (n = 10) according to the in-

office bleaching protocol: DSP White Clinic 35%, DSP [DWCL], Whiteness HP, FGM [WTHP], Whiteness HP Maxx, FGM [WTMX], Pola Office Powder, SDI [PLOF], Potenza Bianco 35%, PHS [PZBC], and the new Total Blanc One Step, DFL [TBOS]. All gels were applied in three 30-min sessions, with a seven-day interval between applications. Hydrogen peroxide permeability (μg mL^{-1}) into the pulp chamber was determined using UV-Vis spectrophotometry. Bleaching efficacy was assessed by CIEDE2000 (ΔE00) and the Whiteness Index for Dentistry (ΔWID) using a digital spectrophotometer. The pH of the gels was monitored using a digital pH meter, and HP concentration was determined by titration. Statistical analysis was performed using two-way ANOVA (gel vs. time) and Tukey's post-hoc test ($\alpha = 0.05$).

Results: All bleaching gels allowed hydrogen peroxide diffusion into the pulp chamber, with statistically significant differences between groups ($p = 0.0001$). PLOF exhibited the highest diffusion ($p < 0.01$), while TBOS showed the lowest ($p < 0.01$). All gels demonstrated progressive bleaching over the sessions ($p < 0.0001$), with no significant differences among the groups ($p > 0.05$). Most gels exhibited an acidic pH during application, whereas TBOS maintained a neutral pH throughout the 30-min application. The hydrogen peroxide concentration of all gels decreased after 30 min of application but remained above 30% active hydrogen peroxide.

Conclusions: A single 30-min application per session of the tested bleaching gels was sufficient to promote bleaching efficacy in all groups. However, only the TBOS exhibited significantly lower hydrogen peroxide diffusion into the pulp chamber, likely due to its more neutral pH compared to the other gels evaluated.

https://doi.org/10.1016/j.dental.2026.03.078

67

Dentinal moisture level in cervical restorations: 6-month randomized clinical trial

M Rodríguez *[1], A Echeverria [1], A Beniscelli-Vasquez [1], R Aliaga-Galves [1], AD Loguercio [2], MFe Gutiérrez [1]

[1] *Universidad de Los Andes, Santiago, Chile*
[2] *State University of Ponta Grossa, Ponta Grossa, Brazil*

Purpose / Aim: To evaluate the effect of wet and oversaturated dentin on the 6-month clinical performance of two universal adhesive systems applied in the etch-and-rinse mode in non-carious cervical lesions (NCCLs).

Materials & Methods: The study protocol and informed consent form were reviewed and approved by the local scientific ethics committee. A total of 120 restorations were randomly assigned to 30 participants (14 male and 16 female), divided into four groups (n = 30): AMP-wet (Ambar Universal APS Plus adhesive applied to wet dentin); AMP-overwet (AMP applied to oversaturated dentin); PBA-wet (Prime&Bond Active adhesive applied to wet dentin); PBA-overwet (PBA applied to oversaturated dentin). In all groups, enamel and dentin were etched for 15s. Adhesives were light-cured for 10s at 1,000 mW/cm^2. A resin composite was applied in three increments, each cured for 20s at 1,000 mW/cm^2. Restorations were finished immediately with fine diamond burs and spiral polishers. Evaluations were conducted at baseline and after 6 months using the FDI criteria. The following outcomes were evaluated: retention/material fracture, marginal staining, marginal adaptation, postoperative sensitivity and recurrence of caries. Differences among groups were analyzed using the Friedman repeated-measures analysis of variance rank ($\alpha = 0.05$).

Results: The recall rate at 6 months was 100%. Three restorations were lost during this period: one each in the AMP-overwet, PBA-wet and PBA overwet. The retention rates (95% confidence interval) were: 100% (84.6-100) for AMP-wet and 96.7% (95% CI: 83.4-99.4) for AMP-overwet, PBA-wet and PBA-overwet. Minor marginal staining was observed in seven restorations (three in AMP-wet, one in AMP-overwet, two in PBA-wet and one in PBA-overwet). Seventeen restorations showed minimal marginal adaptation defects (six in AMP-wet, three in AMP-overwet, four in PBA-wet and four in PBA-overwet). No significant differences were found amongthe groups for any of thel clinical parameters evaluated ($p > 0.05$).

Conclusions: The clinical performance of the two universal adhesives was not affected by the moisture level of dentin when applied using the etch-and-rinse technique. Both adhesives performed similarly on wet or oversaturated dentin after 6 months.

Funding: This project was funded by ANID through Initiation Fondecyt grant number 11221070.

https://doi.org/10.1016/j.dental.2026.03.079

68

Effect of the dentin thickness on the intrapulpal calcium penetration

C Rossini *, F Berger, AB Borges, CRG Torres

Institute of Science and Technology, Sao Paulo State University - UNESP, Sao Jose dos Campos, Brazil, São José dos Campos, Brazil

Purpose / Aim: The aim of this study was to evaluate the influence of remaining dentin thickness on the pulpal penetration of calcium ions after application of different pulp capping agents.

Materials & Methods: Dentin discs with thicknesses of 0.5 mm, 1.0 mm, and 1.5mm were obtained from the labial surface of bovine incisors. The smear layer was removed by acid etching, and the specimens were assembled in artificial pulpal chambers, filled with ultrapure water, to simulate pulpal fluid and to collect of calcium ions released by the tested materials. The pulp capping agents evaluated were CH – calcium hydroxide cement (Dycal-Dentsply); W/MTA – white MTA (Angelus); B/MTA – blue MTA (Voco); F/MTA – Endo-Eze MTA Flow (Ultradent); CS – regular calcium silicate cement (Biodentine, Septodont); and RMCS – resin-modified calcium silicate (TheraCal LC, Bisco). Calcium concentration in the simulated pulpal fluid was measured after 24h and 48h. Data were analyzed using 3-way ANOVA (Material x Thickness × Moment of evaluation) and Tukey test, with a significance level of 5%.

Results: The results of Tukey test were: MATERIAL= CH-3.46 (2.14)a, RMCS-4.24(2.19)a, W/MTA -5.50(4.09)b, F/MTA-5.58 (4.37)b, B/MTA-5.87(4.38)b, CS-17.05(8.61)c. THICKNESS= 1.5mm-4.02(3.21)a, 1mm-6.04(5.40)b, 0.5mm-10.78(8.29)c. The calcium release increased with time for all materials, with exception to CS.

Conclusions: The smaller remaining dentin thickness resulted in higher calcium penetration. Calcium hydroxide cement and the resin modified calcium silicate showed the smaller calcium release than MTA based materials. The regular calcium silicate cement showed the higher calcium release.

https://doi.org/10.1016/j.dental.2026.03.080

69

Er: YAG Laser Influence on Dentin Bond-Strength and Enzymatic Activity

G Chagas, N Gomes, M Rocha, K Yui, F Feitosa, C Pucci *

Sao Paulo State University – UNESP, Institute of Science and Technology, São Jose dos Campos, Brazil

Purpose / Aim: The objective of this study was to evaluate the impact of Er:YAG laser treatment on dentin surfaces regarding the bond strength of direct restorations in previously bleached teeth, along with its effect on matrix metalloproteinase enzymatic activity by in situ zymography technique, and the fracture pattern analysis and scanning electron microscopy (SEM) analysis of the dentin structure were also carried out.

Materials & Methods: 60 healthy bovine incisors were used for the microtensile bond strength test (μTBS), which had the enamel on the buccal surface worn away in a circular polisher until the dentin exposure. The samples were divided into six groups, according to the type of treatment, where: CP: positive control (no treatment); CN: negative control (bleaching with 35% hydrogen peroxide); L1: Er: YAG laser (5W); L2: Er:YAG laser (7.5W); CL1: whitening and Er: YAG laser (5W); and CL2: whitening and Er:YAG laser (7.5W). Specimens from all groups were then restored with a universal adhesive in a self-etching manner, under simulated pulp pressure of 15 cm of H2O. The fracture pattern of the specimens was analyzed under a stereomicroscope, and those that showed adhesive failure were analyzed under SEM. Additional specimens (n = 18) were taken to in situ zymography technique to analyze the enzymatic activity of extracellular matrix metalloproteinase (MMPs). The data were statistically analyzed for normality and homoscedasticity, and ANOVA one-way and Tukey's post-hoc test (5%) were conducted.

Results: The μTBS data, in MPa, showed significant differences between the groups ($p < 0.000$): CP $(33.7 \pm 1.6)^{A}$, L1 $(32.5 \pm 1.6)^{A}$, CL1 $(31.9 \pm 2.1)^{AB}$, L2 $(28.64 \pm 3.9)^{AB}$, CL2 $(27.7 \pm 3.9)^{B}$ and CN $(17.7 \pm 1.6)^{C}$. The predominant fracture pattern between the groups was adhesive failure. SEM images revealed that the laser-treated dentin showed exposed dentinal tubules, without a smear layer. The pixel count in Image J software of in situ zymography data ($p = 0.765$) showed no significant difference for all groups: CP (4,8 ±2,4)^{A}, CN (9,4 ± 2,9)^{A}, L1 (4,7 ± 1,1)^{A}, L2 (2,3 ± 7)^{A}, CL1 (4,9 ± 2,9)^{A}, CL2 (4,8 ± 4,1)^{A}.

Conclusions: The Er:YAG laser proved capable of nullifying the harmful effects of bleaching on bond strength.

https://doi.org/10.1016/j.dental.2026.03.081

70

Zirconia crown-abutment interface evaluation following different cementation protocols

C Mazzitelli *[1], C D'Alessandro [1], T Maravic [1], E Baena [2], S Fanton [1], Ed Mancuso [1], L Ceballos [2], L Breschi [1], A Mazzoni [1]

[1] *University of Bologna, Bologna, Italy*
[2] *Universidad Rey Juan Carlos, Madrid, Spain*

Purpose / Aim: To evaluate the zirconia crown–abutment interface in terms of linear roughness (Ra), surface roughness (Rs), and residual resin cement mean height (Pmean) after different cementation protocols.

Materials & Methods: A sound maxillary premolar was prepared with a circumferential chamfer to receive a zirconia crown (Katana Zirconia STML, Kuraray Noritake). A digital scan of the tooth was obtained (VirtuoVivo, Straumann Group), and 25 resin tooth replicas were 3D-printed (Sonic Mega 8KS, Phrozen). Crowns were cemented on resin replicas with Panavia SA Universal (Kuraray Noritake) in self-adhesive mode applying a constant load of 10 N. Specimens were divided into five experimental groups (n = 5) based on cementation protocol: (SC + sc + SC)-Initial self-cure (SC, 6 min to achieve a gel-phase), cement removal with a scaler (sc), and final SC (6 min in the dark); (SC + sc + LC)-Initial SC, sc, and final light-cure (LC, 10s per surface using a LED lamp); (mBr + LC)-Immediate cement removal with a microbrush (mBr) followed by LC; (TC + sc + SC): Tack-cure (TC 3s), sc, and final SC; (TC + sc + LC)-TC, sc, and final LC. Cement excess was removed until no longer visible to the naked eye. Three-dimensional images of the buccal portion of the crown-abutment interface of the specimens were evaluated using a digital optical microscope (Keyence). Ra, Rs and Pmean were quantified by averaging 5 measurements per specimen before and after polishing with silicon rubber using the microscope software. Data were statistically analyzed ($p < 0.05$).

Results: Cementation protocols and their interaction with polishing significantly affected Ra and Rs ($p < 0.05$). Specifically, TC groups (TC + sc + LC and TC + sc + SC) exhibited significantly higher roughness values compared to mBr + LC and SC + sc + LC, both before and after polishing ($p < 0.05$). Cementation protocols also significantly influenced Pmean ($p < 0.05$). When an initial SC was performed (SC + sc + SC and SC + sc + LC) the highest residual cement mean heights was obtained, while TC and mBr groups (TC + sc + SC, TC + sc + LC and mBr + LC) demonstrated lower Pmean values ($p < 0.05$). Polishing significantly reduced peak height across all groups ($p < 0.05$).

Conclusions: Tack-curing of the universal resin cement tested resulted in the lowest Pmean and in the highest surface roughness compared to cementation protocols involving conventional removal techniques (i.e. the use of a microbrush or a scaler after a SC polymerization). The initial SC was related to higher amount of resin cement excess.

https://doi.org/10.1016/j.dental.2026.03.082

71

Measuring Bruxing-induced Aligner Wear Rate Using Optical Coherence Tomography (SS-OCT)

B Van Heel *, S Ong, A Fok, HP Chew

MDRCBB, University of MN, Minneapolis, USA

Purpose / Aim: To evaluate the use of Swept-Source Optical Coherence Tomography (SS-OCT) for measuring wear of orthodontic aligners over time in a simulated bruxism model.

Materials & Methods: STL files of a maxillary and mandibular left-quadrant were used to create both milled zirconia and 3D-printed models. The zirconia models were mounted in a chewing simulator (Artificial Resynthesis Technology, MDRCBB, MN, USA) to simulate bruxing under a maximum force of 31 N and lateral movement of 3 mm (6 mm per cycle). Aligners were thermoformed using plastic sheets (Essix Plus™, Dentsply Sirona, Charlotte, NC, USA) on the 3D-printed models, then installed on the zirconia models and subjected to a total of 12,500 bruxing cycles. The aligners were placed on the 3D printed model and the upper and lower canines were scanned using SS-OCT (IVS-2000, Santec, Komaki, Japan) at baseline and at intervals of 2,500 cycles. A frame with the thinnest remaining aligner material, identified on the scan of the final time point, was designated as the region of interest (ROI) and corresponding frames from previous time points were subsequently extracted. Material loss at each time point was quantified using a customized algorithm (MATLAB v2024b, Mathworks, Natick, MA, USA). A Micro-Computed Tomography (Micro-CT) System (XT-

H 225, Nikon Metrology Inc., Brighton, MI, USA) was also used to scan the aligners at the end of the 12,500 cycles, and they were compared with the SS-OCT results for validation.

Results: Evident gradual wear was observed at the cusp tip of the maxillary and mandibular canine after every 2,500 cycles. After 10,000 cycles, both SS-OCT and Micro-CT showed a hole on the maxillary canine as illustrated in Fig. 1. The increase in wear depth ranged from 0.05 to 0.21 mm throughout the intervals until the point of puncture (10,000 cycles).

Conclusions: Use of the chewing simulator to simulate bruxing together with SS-OCT enables a reliable and efficient approach of monitoring wear over time and to evaluate the performance of aligner materials.

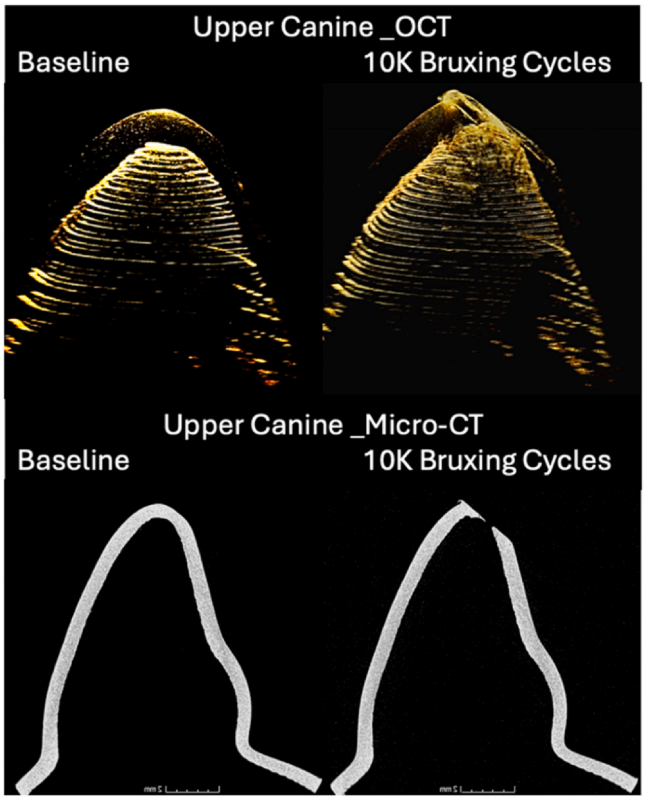

Figure 1

https://doi.org/10.1016/j.dental.2026.03.083

72

Antibacterial and Radiopaque Core-Shell Particles for Dental Materials

N Aslankoohi *, C Stewart

Mesosil Inc, Toronto, Canada

Purpose / Aim: Dental materials releasing antimicrobial compounds into marginal micro-gaps between restoration and surrounding tooth structure may prevent secondary caries formation and enhance the durability of the restoration. Ideally, the provision of antimicrobial properties should not affect other key properties of restoratives, such as mechanical properties, radiopacity, translucency, and aesthetics. We developed spherical core-shell particles loaded with an antimicrobial compound whose framework contains silica, and zirconia or titania. Herein, we demonstrate that particles incorporated into a restoration maintain or improve pre-existing restoration properties, including radiopacity and translucency, by tuning the refractive index of the filler particles.

Materials & Methods: Tetraethyl orthosilicate (TEOS) as the precursor of silica, amphiphilic antimicrobial compound (octenidine dihydrochloride (OCT)), NaOH as base catalyst and water were mixed, and the reaction proceeded to form solid mesoporous core particles. Alkoxide precursors of shell (TEOS, zirconium (IV) propoxide as the precursor of zirconia, or titanium (IV) butoxide as the precursor of titania) were added, and the reaction proceeded to form core-shell particles. Morphology and elemental mapping of the particles were visualized by STEM-EDX (Hitachi HF-3300 and Bruker silicon-drift EDS detector). Release of OCT was measured after immersion in PBS at 37°C by UV-Visible spectrophotometry (Cytation3 imaging reader). Particles were incorporated in the dental composite, and the radiopacity of the final composite was measured according to ISO 13116:2014.

Results: Highly spherical particles having silica, and zirconia or titania in their composition, additionally loaded with OCT during the synthesis, were obtained using the synthesis described. OCT formed 20-25 wt% of particle composition and was released in a sustained manner, without particle degradation that was previously seen from metal-SiO2-OCT particles. This spherical morphology, high loading content, and stability were possible as the less stable and more irregular titania or zirconia phase was applied to an established scaffold with the desired properties. Radiopacity of the composite containing core-shell particles was significantly higher than silica alone, owing to the titania or zirconia shell.

Conclusions: Mesoporous core-shell particles having antimicrobial-silica as the core and antimicrobial-silica-zirconia or silica-titania as the shell were synthesized via 1-pot synthesis. Core antimicrobial-silica properties were retained, while the presence of zirconia or titania provided the opportunity to modulate the refractive index of filler particles and endow them with radiopacity. Particles with ternary compositions such as silica-zirconia-titania may also be synthesized using this method.

https://doi.org/10.1016/j.dental.2026.03.084

73

Bonding-performance of different time-of-action of single-double-bottle silanes on lithium-silicates-CAD-CAM ceramics

F Murillo-Gómez *[1], R Urcuyo [2]

[1] *School of Dentistry, University of Costa Rica, San Jose, Costa Rica*
[2] *School of Chemistry, University of Costa Rica, San Jose, Costa Rica*

Purpose / Aim: Evaluate the effect of single/double bottle silane-primers and two silane action-times (1/5min) in the bond strength of two lithium silicate-based CAD/CAM ceramics.

Materials & Methods: Plates (6x3x2mm) of lithium disilicate-reinforced ceramic (IPS e. max CAD, Ivoclar/Vivadent) and zirconia reinforced lithium silicate ceramic (Suprinity, VITA) were cut and divided into 4 groups: 1. One-bottle/silane, 1 min of action-time (1B1m); 2. One-bottle/silane, 5 min (1B5m); 3. 2B1m; 4. 2B5m. All groups were etched with 5%HF for 20s. Resin-cement cylinders (n = 15; 1mm-diameter) were bonded to the plates according to manufacturer, stored in distilled water (37°C/3 months), and subjected to microshear bond-strength (μSBS) test using a universal-testing machine (Electropuls E3000-Instron; 1mm/min). Data were analyzed with two-way ANOVA and Tukey's post-hoc test ($\alpha = 0.05$). Surface micromorphology (n = 3) was evaluated using a scanning electron microscope (SEM, H-3700-Hitachi), and chemical

composition: (n = 3) was analyzed using Raman (Alpha/300-WITec) and FTIR spectroscopies (Nicolet/6700-Thermo-Scientific).

Results: For μSBS data only material*treatment interaction was statistically significant (p = 0.001). ZLS-2B/5m group (12.07 ± 6.04MPa) showed the highest values, statistically outperforming ZLS-2B1m (5.98 ± 2.91MPa), ZLS-1B5m (5.30 ± 4.69MPa) and LD-1B1m (6.30 ± 4.02MPa). No other significant differences were observed. FTIR analysis showed the typical spectrum for both materials, with the appearance of additional bands (1640/1715cm^{-1}) in all silanated groups. Raman spectroscopy revealed typical spectra for the control groups and 2B LD groups, while 1B groups exhibited additional bands between 1200-3110cm^{-1} corresponding to organic compounds in the silane primers. SEM analysis revealed greater silane coverage in 1B-treated groups (especially 1m), where the etched surfaces were less visible compared to 2B-treated groups.

Conclusions: One-bottle silane primer and 1min of action produce thicker silane layers, as confirmed by spectroscopic and SEM analysis. However, the adhesive performance is material-dependent. For lithium disilicate, the best results were achieved with 1B5m and 2B treatments, while for zirconia-reinforced lithium silicate, 2B5m and 1B1m treatments performed best.

https://doi.org/10.1016/j.dental.2026.03.085

74
Two-year clinical evaluation of cluster shades composite in anterior teeth

CRG Torres *, G da Silva Chagas, G Leon, V Bottesini, M Mailart, AB Borges

Institute of Science and Technology, Sao Paulo State University - UNESP, Sao Jose dos Campos, Brazil

Purpose / Aim: The aim of this prospective study was to compare the clinical performance of restorations performed with a regular resin composite versus a cluster shade material.

Materials & Methods: Thirty patients received two class III or IV restorations (n = 60), one with a regular two levels of translucency composite (Amaris - Voco) and the other with a cluster shade material with a single level of translucency (Admira Fusion 5 – Voco). The materials were applied using up to 2mm thick layers. For all restorations, the self-etching adhesive system Futurabond U (Voco) was used. All restorations were evaluated using the FDI criteria after 7 days, 12 and 24 months postoperatively by two calibrated examiners.

Results: After 24 months, 26 patients attended the recall and 52 restorations were evaluated. The Fisher's exact test showed no significant differences between the materials for all parameters analyzed (p > 0.05). In relation to the overall scores, all restorations were esthetically and biologically acceptable after 24 months. For the functional scores, 3,57% were not acceptable for both groups. Considering all properties, the success rates were 96,43% for both materials.

Conclusions: After two years of clinical service, both materials tested presented good clinical behavior for all properties analyzed, without significant differences.

https://doi.org/10.1016/j.dental.2026.03.086

75
Bibliometric Analysis of In Vitro Properties of Calcium Silicate Cements

V Rosa *, CF Sabino

National University of Singapore, Singapore, Singapore

Purpose / Aim: This study aimed to perform a bibliometric analysis of the research landscape of calcium silicate cements (CSCs) in dentistry based on in vitro studies published over the last decade. The objective was to identify the frequency, co-occurrence, and evolution of key research themes related to CSCs' mechanical, chemical, and physical properties.

Materials & Methods: A structured literature search was conducted using Scopus, PubMed, and Web of Science for articles published between 2014 and 2024. Boolean queries combined terms related to CSC types (e.g., "calcium silicate cement," "tricalcium silicate") with properties of interest (e.g., "compressive strength," "ion release," "setting time") and relevant experimental contexts. A total of 2,989 records were screened, and 381 in vitro studies met the following inclusion criteria: standardized methodology, reported sample conditions, and at least one quantitative property measurement. References were managed in EndNote, de-duplicated, and exported in CSV format for bibliometric analysis in VOSviewer (v1.6.20). Co-authorship, Co-occurrence, Citation, Bibliographic Coupling, and Co-citation analyses were performed. Links and Total Link Strength attributes were applied to quantify relationships. Term frequency and citation thresholds were iteratively optimized for clarity and cluster resolution.

Results: Calcium ion release, volume change, and bioactivity emerged as the most frequent and interconnected topics, forming dense clusters that indicate a strong research focus. Other prominent terms included radiopacity and solubility reflecting the continued interest in mechanical and physicochemical properties. Temporal mapping revealed a shift in research themes over time. Earlier studies (average publication ~2014–2016) focused on core parameters, such as pH analysis, setting time and porosity. More recent topics (2020–2024) include flowability, diametral tensile strength, nanoparticles, and antibacterial activity, suggesting a growing interest in handling characteristics and biological properties. The network structure demonstrated a high connectivity across the mechanical, chemical, and physical domains. Bridging terms such as water–powder ratio and the presence of modifying additives reflect integrated efforts to understand how compositional variables influence in vitro performance.

Conclusions: This bibliometric analysis highlights the evolution of scientific interest in CSC research within in vitro studies. While foundational topics remain central, recent trends emphasize bioactivity and evaluation of additional functional properties. These findings provide a structured overview of the shifting research priorities in the study and development of calcium silicate-based cements.

https://doi.org/10.1016/j.dental.2026.03.087

76
Machine Learning Regression Models for Color Prediction of CAD-CAM materials

B Mascaro *[1], M Tejada-Casado [2], R Conejo [2], R Ghinea [2], R Fonseca [1], J Reis [1], M del Mar Pérez [2]

[1] *Sâo Paulo State University (UNESP), School of Dentistry, Araraquara, Brazil*
[2] *University of Granada, Granada, Spain*

Purpose / Aim: This study aimed to predict the color coordinates of different CAD-CAM materials at varying thicknesses against tooth-colored backgrounds.

Materials & Methods: Lava Ultimate, Grandio Blocs, VITA Enamic, and VITA Mark II with thicknesses of 0.5, 1.0, and 1.5 mm were studied. Spectral reflectance data were obtained using a spectroradiometer to determine CIELAB coordinates of each specimen against a standard black background and nine tooth-colored backgrounds (ND1-ND9). Three approaches were used for predictive model development based on the input variables: material, thickness, and L*a*b* values. A leave-one-out cross-validation (LOO-CV) strategy was used for model development and evaluation, and Partial Least Squares (PLS) regression was applied to predict the color coordinates. CIEDE2000 color differences (ΔE00) between measured and predicted data were calculated, and the accuracy of the method was evaluated by comparing ΔE00 values with corresponding 50:50% perceptibility (PT00) and acceptability (AT00) thresholds.

Results: In the first approach, the mean ΔE00 value of the predicted versus the measured data was 1.04, which is clinically acceptable. For all materials, ΔE00 values predicted in the second approach remained below the acceptability threshold, with VITA Mark II exhibiting imperceptible values (ΔE00 < 0.8). In the third approach, only the 0.5 mm VE did not result in imperceptible ΔE00, but it was still considered acceptable.

Conclusions: The color of monolithic CAD-CAM materials with different thicknesses against tooth-colored backgrounds could be predicted with clinically acceptable color differences using automatic machine learning regression models.

https://doi.org/10.1016/j.dental.2026.03.088

77

Turmeric Oil Cellulose Nanocrystal/Xyloglucan Pickering Emulsions for Oral Care

A Fernandes *, A Costa, E Scopel, B Zakani, A Manso, E Cranston

University of British Columbia, Vancouver, Canada

Purpose / Aim: Untreated dental caries remains the most prevalent global health condition, disproportionately affecting vulnerable populations. Although treatments like fluoride varnishes and chlorhexidine are effective, their use is limited to those with access to dental care. Curcumin, the major bioactive compound in turmeric oil, has been studied as a photosensitizer for antimicrobial photodynamic therapy (aPDT) in dentistry. However, poor water solubility restricts its application in water-based delivery systems. The purpose of this study was to develop and characterize turmeric oil Pickering emulsions; and evaluate their antimicrobial properties associated with blue light treatment (aPDT) against cariogenic species.

Materials & Methods: Pickering emulsions of turmeric oil-in-water (20/80) were prepared using cellulose nanocrystals (CNCs) to stabilize the oil-water interface, and xyloglucan (XyG) to adjust the viscosity, establishing four experimental groups (0, 14, 142, and 521 mg XyG/mg CNC). Droplet size and droplet stability, rheology, and phase separation were tested and monitored over a 14-day period. The most stable formulation was then selected for further antimicrobial testing against Streptococcus mutans and Candida albicans under dark or blue light conditions (l = 440–460 nm; Valo at 830 mW/cm^2). Minimum inhibitory concentration (MIC), minimum bactericidal concentration (MBC), and minimum fungicidal concentration (MFC) were determined. First, serial dilutions were incubated for 24 hours (C. albicans) or 48 hours (S. mutans), and microbial growth was assessed by spectrophotometry. Next, MBC and MFC effects were confirmed by culturing onto agar plates. Each sample was run in triplicate (n = 3). Control groups included turmeric oil alone and CNC-XyG alone.

Results: CNC-XyG turmeric oil emulsions showed smaller droplet sizes and greater stability. Rheology and emulsion stability to the ratio between CNC and XyG were key parameters for selecting the optimal Pickering-emulsion formulation. The selected 20/80 turmeric oil-in-water emulsion stabilized with 142 mg XyG/mg CNC reduced S. mutans growth by 60% under light exposure. Additionally, this formulation was able to inhibit the growth of C. albicans under both light and dark conditions. Control samples without oil or light showed minimal microbial reduction.

Conclusions: CNC-XyG-stabilized emulsions favoured a homogeneous distribution of turmeric in the delivery system and enabled antimicrobial activity through photodynamic and light-independent mechanisms. These findings demonstrated that the combination of CNC and XyG can serve as a delivery platform for turmeric oil emulsions targeting oral care applications. These findings bring an alternative approach toward the development of more accessible, over-the-counter oral care products.

https://doi.org/10.1016/j.dental.2026.03.089

78

$CaTiO_3$-catalyzed at-home bleaching-gel: color alteration, cytotoxicity, and enamel microhardness

F Mon *[1], R de Oliveira Ribeiro [1], V Peruchi [1], DG Soares [2], L de Oliveira Fernandes [1], IM Soares [1], M Pires [1], J Oliveira [1], J Hebling [1], CA de Souza Costa [1]

[1] *São Paulo State University, Araraquara, Brazil*
[2] *University of São Paulo, Bauru, Brazil*

Purpose / Aim: This study assessed the bleaching efficacy and cytotoxicity (CT) of a 22% carbamide peroxide (CP22%) bleaching gel containing different concentrations of calcium titanate ($CaTiO_3$), as well as the effects of these formulations on enamel microhardness.

Materials & Methods: Standardized enamel/dentin discs were fitted into artificial pulp chambers and allocated into the following groups: G1: no treatment (negative control), G2: CP22%, G3: CP22% + 2 mg/mL $CaTiO_3$, G4: CP22% + 6 mg/mL $CaTiO_3$, G5: CP22% + 10 mg/mL $CaTiO_3$. In all bleached groups, gels were applied onto the enamel surface for 60 minutes. The extracts (culture medium + bleaching gel components diffused through the discs) were collected and then applied to MDPC-23 odontoblast-like cells, which were evaluated concerning their viability (Alamar Blue, n = 8; Live/Dead, n = 4), oxidative stress (carboxy-H_2DCFDA probe, n = 8), and morphology (SEM, n = 4). The amount of H_2O_2 diffused was also determined (leuco crystal violet/peroxidase assay, n = 8). Additional enamel/dentin discs were used for enamel microhardness analysis (Knoop microhardness; baseline, and 5-, 10-, and 15-days post-bleaching; n = 8), surface morphology (SEM/EDS/mapping, n = 4), and bleaching efficacy (ΔE_{00} and ΔWID; n = 8). Data were analyzed by ANOVA/Tukey (cell viability), ANOVA/Sidak (bleaching efficacy), and ANOVA/Bonferroni (enamel microhardness), with a significance level set at 5%.

Results: Among the bleached groups, G5 showed the highest bleaching efficacy and cell viability ($p < 0.05$), as well as the lowest H_2O_2 diffusion and oxidative stress ($p < 0.05$). Increased enamel microhardness was observed in all groups in which $CaTiO_3$ was added to the bleaching($p < 0.05$).

Conclusions: In conclusion, the incorporation of $CaTiO_3$ into 22% carbamide peroxide enhances the bleaching efficacy and enamel microhardness, as well as reduces the trans-amelodentinal cytotoxicity of the esthetic therapy. These data suggest that such innovative catalytic strategy may be relevant for developing safer and more effective bleaching protocols.

https://doi.org/10.1016/j.dental.2026.03.090

79
Enhanced In-Office Bleaching with TiF4-containing Polymeric Primers

V Peruchi *[1], R de Oliveira Ribeiro [1], IP Soares [1], L de Oliveira Fernandes [1], J Oliveira [1], M Pires [1], F Wu Mon [1], J Hebling [1], DG Soares [2], CA de Souza Costa [1]

[1] *São Paulo State University, Araraquara, Brazil*
[2] *University of São Paulo, Bauru, Brazil*

Purpose / Aim: The effect of an innovative bleaching strategy combining a polymeric primer (Ppol) containing titanium tetrafluoride (TiF4) with a bleaching gel commonly used for in-office bleaching therapy was evaluated regarding esthetic efficacy, trans-amelodentinal cytotoxicity, and enamel microhardness.

Materials & Methods: For this purpose, the following groups were established: CN (no treatment – negative control), CP (commercial bleaching gel with 35% H_2O_2), 2TiF4 (2 mg/mL Ppol TiF4 + commercial 35% H_2O_2 bleaching gel), 6TiF4 (6 mg/mL Ppol TiF4 + commercial 35% H_2O_2 bleaching gel), and 10TiF4 (10 mg/mL Ppol TiF4 + commercial 35% H_2O_2 bleaching gel). Standardized enamel/dentin discs were obtained and stained with black tea. For trans-amelodentinal cytotoxicity assessment, the discs were individually adapted to artificial pulp chambers. The enamel surface was coated or not with the Ppol containing the different concentrations of TiF4, and then the commercial 35% H_2O_2 bleaching gel was applied for 45 minutes. The extracts (culture medium + components of the bleaching gel diffused across the discs) were collected and immediately applied to cultured MDPC-23 odontoblast-like cells. Following, the cells were evaluated concerning their viability (Alamar Blue, n = 8; Live/Dead, n = 3) and oxidative stress (carboxy-H2DCFDA probe, n = 8). The amount of H_2O_2 diffused through the enamel/dentin discs was also determined (leuco crystal violet/peroxidase, n = 8) for all bleached groups. Other standardized enamel-dentin discs were used to evaluate the esthetic efficacy (ΔE_{00} and ΔWID, n = 8), as well as microhardness (Knoop, n = 8), superficial morphology, and composition (SEM/EDS, n = 4) of the enamel exposed to the treatments. Data were submitted to ANOVA/Tukey test with a significance level of 5%.

Results: In all bleached groups, cells showed reduced viability compared to CN ($p < 0.05$). Among the bleached groups, 10TiF4 presented the highest cellular viability and bleaching efficacy, as well as the lowest oxidative stress and H_2O_2 diffusion ($p < 0.05$). The enamel microhardness was significantly increased in Group 10 TiF4 ($p < 0.05$).

Conclusions: It is concluded that covering the enamel surface with Ppol containing TiF4 before application of a bleaching gel with 35% H_2O_2 enhances the microhardness of this hard dental tissue, improves the esthetic outcomes, and reduce the trans-amelodentinal cytotoxicity caused by the conventional in-office bleaching therapy. The Ppol containing 10 mg/mL of TiF4 was the most promising product to be used in combination with a 35% H_2O_2 bleaching gel.

https://doi.org/10.1016/j.dental.2026.03.091

80
12-Month Evaluation of a Chemically-Cured Bulk-Fill Composite in Posterior Restorations

A Barrientos *[1], AD Loguercio [2], B Carpio-Salvatierra [2], R Ñaupari-Villasante [2], M Wendlinger [2], S Cavagnaro [1], A Leon [1], R Aliaga-Galvez [1], F Gutierrez [1]

[1] *Universidad de los Andes, Santiago, Chile*
[2] *State University of Ponta Grossa, Ponta Grossa, Brazil*

Purpose / Aim: To evaluate the clinical performance of posterior restorations using a new chemically-cured bulk-fill composite (Stela Automix [AU] and Stela Capsule [CA], SDI) compared to a light-cured bulk-fill composite [BU] after 12 months.

Materials & Methods: Fifty-five participants with at least three posterior teeth requiring restoration were recruited, resulting in a total of 165 restorations. Following the application of Stela Primer, the chemically-cured composite (AU or CA) was inserted. In the BU group, a universal adhesive was applied, followed by the light-cured composite (Scotchbond Universal/Filtek One, Solventum). Participants were evaluated at baseline, 7 days, 6-, and 12-month using the updated FDI criteria. Differences in the proportions among groups were analyzed using Cochran's test ($\alpha = 0.05$).

Results: All participants completed the study across all recall periods. No significant changes were observed after 12 months in functional properties, including: F1: Fracture of material and retention; F2: Marginal adaptation; F3: Contact point/food impact; F4: Form and contour; F5: Occlusion and wear. Similarly, no changes were observed in biological properties: B1: Recurrence of caries; B2: Dental Hard tissues defects at the restoration margin. For esthetic properties, surface luster and texture (A1): Restorations were rated as 'good' in 18% (AU), 25% (CA), and 11% (BU) of cases ($p > 0.05$); Marginal staining (A2): 'Good' ratings were observed in 9% (AU), 11% (CA), and 11% (BU) of restorations ($p > 0.05$); and Color match (A3): Restorations were rated as 'good' in 14% (AU), 13% (CA), and 31% (BU) of cases ($p > 0.05$). When comparing baseline to the 12-month evaluation, significant differences were observed only for marginal staining (A2) across all groups ($p < 0.05$). No restorations were classified as 'clinically unsatisfactory' or 'clinically poor' during the 12-month period.

Conclusions: Chemically-cured composites, whether applied as Automix or Capsules, demonstrated similar clinical performance to a light-cured composite after 12 months of clinical service.

Funding: This project was funded by ANID through Initiation Fondecyt grant number 11221070.

https://doi.org/10.1016/j.dental.2026.03.092

81
Ninety-Month Clinical Evaluation of a Universal Adhesive Using Different Strategies

I Arnes-Ávila *[1], R Ñaupari-Villasante [2], B Carpio-Salvatierra [2], T Matos [3], M Barceleiro [4], AD Loguercio [2], MF Gutierrez [1]

[1] *Universidad de los Andes, Santiago, Chile*
[2] *State University of Ponta Grossa, Ponta Grossa, Brazil*
[3] *Tuiuti University of Paraná, Curitiba, Brazil*
[4] *Fluminense Federal University, Rio de Janeiro, Brazil*

Purpose / Aim: The aim of this study was to evaluate the clinical performance of a universal adhesive (Futurabond U, Voco) in restorations of non-carious cervical lesions (NCCLs) using different adhesive strategies after 90 months.

Materials & Methods: A total of 200 restorations were performed in 50 volunteers with at least four NCCLs, randomly assigned to four groups (n = 50): self-etch (SEE), selective enamel etching (SET), etch-and-rinse with dry dentin (ERDry), and etch-and-rinse with moist dentin (ERWet). Restorations were evaluated using the FDI criteria at baseline and after 6, 12, 36, 60 and 90 months. Data were analyzed using the Kaplan-Meier survival test for retention rate and the Kruskal-Wallis test for secondary outcomes ($\alpha = 0.05$).

Results: After 90 months of clinical performance, 135 restorations were re-evaluated (SEE = 33; SET = 34; ERDry = 34; ERWet = 34). Thirty-two restorations were lost (SEE = 9; SET = 8; ERDry = 8; ERWet = 7), and the retention rates were 72.7% for SEE, 76,5% for both SET and ERDry, and 79,4% for ERWet ($p > 0.05$). Sixteen restorations (SEE = 7, SET = 5, ERDry = 2, ERWet = 2) showed slight marginal discoloration, 28 restorations (SEE = 12, SET = 5, ERDry = 5, ERWet = 6) exhibited minimal marginal adaptation defects ($p > 0.05$). No significant differences were found among for the secondary outcomes ($p > 0.05$).

Conclusions: The clinical behavior of the universal adhesive in NCCLs was satisfactory after 90 months, regardless of the adhesive strategy used.

https://doi.org/10.1016/j.dental.2026.03.093

82

AI-Assisted Design of Step-Stress Accelerated Lifetime Tests

J Griggs *

University of Mississippi Medical Center, Jackson, USA

Purpose / Aim: To determine (1) the effects of the rates of load increase (aggressive, moderate, and mild) on the precision and accuracy failure probability estimates made using step-stress accelerated lifetime testing (SSALT) and (2) the most efficient number of neurons to use in training a feedforward artificial neural network (ANN) to predict the precision of failure probability estimates.

Materials & Methods: The Simumatic tool of Reliasoft Suite (HBK) was used to conduct monte carlo simulations of SSALT experiments. The population parameters ($\beta = 2.58$, $\alpha 0 = 40.24$, $\alpha 1 = -4.78$) were taken from a previous SSALT of dental implants (Duan et al., 2018). In each simulation, the Simumatic was instructed to use 1000 SSALT experiments to estimate the failure probability at 2M cycles under a load amplitude of 171 N (true answer, Pf = 5%), and the span of the 95% confidence interval of the 1000 experiments (the uncertainty) was noted. A full-factorial 3x3x3 design was used to explore the effects of the 3 loading rates, where each loading rate had 3 initial settings. ANNs with different numbers of neurons (3-10) in the single hidden layer were trained on the data in Matlab, and a genetic algorithm guided each ANN in search of the combination of loading rates corresponding to minimum uncertainty. The genetic algorithm 'bred' the best 2 solutions in each generation using a random crossover point between their genomes, and occasional offspring had point mutations in their genomes. The algorithm evolved the best combination of loading rates over 100 generations with 125 offspring per generation.

Results: Failure probability estimates had a negative bias (1% too low) for all loading rate combinations. The loading rates for aggressive, moderate, and mild load profiles all had significant ($p \leq 0.05$) main effects and interactive effects on the uncertainty of failure probability estimates. Least uncertainty resulted from the fastest rate for the aggressive profile in combination with the slowest slowest rate for the mild profile. ANNs with more neurons than necessary were overly optimistic about the performance of the load profiles that they recommended, and they never did find the optimal combination. Smaller ANNs quickly and accurately solved the optimization problem, although they spent longer training using the TRAINLM command in Matlab compared to the larger ANNs (Fig. 1).

Conclusions: The most efficient SSALT experiment design had aggressive and mild load profiles with loading rates that were as disparate as possible. Smaller ANNs (3 neurons in 1 hidden layer) were better at solving this design optimization problem.

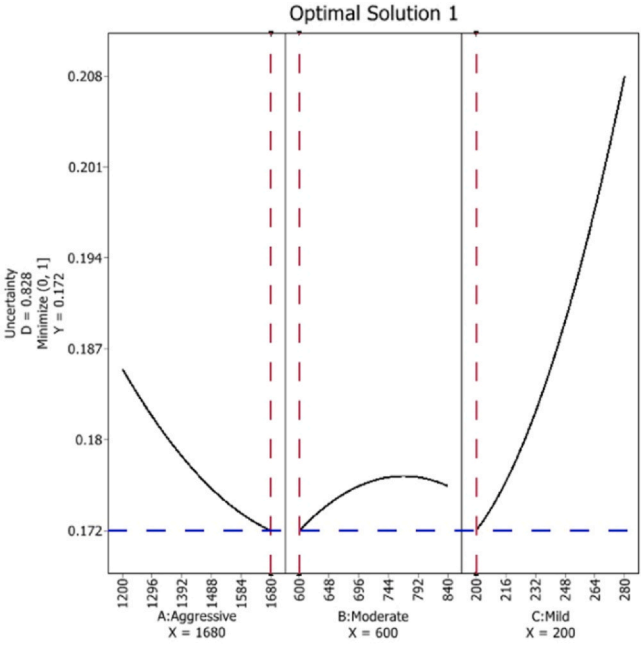

https://doi.org/10.1016/j.dental.2026.03.094

83

Prolonged solvent evaporation of adhesives in cervical restorations: 24-month follow-up

V Zamora-Gutierrez *[1], M Salum-Serrano [1], AD Loguercio [2], S Cavagnaro [1], A León [1], R Aliaga-Gálvez [1], MF Gutierrez [1]

[1] *Universidad de los Andes, Santiago, Chile*
[2] *State University of Pontagrossa, Ponta Grossa, Brazil*

Purpose / Aim: To evaluate the effect of prolonged solvent evaporation time on the 24-months clinical performance of an ethanol-water solvent vs an acetone-base universal adhesive systems used as selective enamel etching application mode in non-carious cervical lesions (NCCLs).

Materials & Methods: The local scientific ethics committee reviewed and approved the study's protocol and consent form (protocol CEC2022129). 148 restorations were randomly placed in 28 subjects (13 male and 15 female) according to the following groups: SUP5 (Scotchbond Universal Plus adhesive [ethanol-water solvent] evaporated for 5 seconds); SUP25 (Scotchbond Universal Plus adhesive evaporated for 25 seconds); GBU5 (Gluma Bond Universal adhesive [acetone solvent] evaporated for 5 seconds); GBU25 (Gluma Bond Universal adhesive evaporated for 25 seconds). All groups were light-cured for 10s/1,000 mW/cm^2. A resin composite was placed by applying three increments, each one was light cured for 20s/1,000 mW/cm^2. The restorations were finished immediately with fine diamond burs and polishers. The restorations were evaluated at baseline and after 24 months by using the updated FDI criteria. The following outcomes were evaluated: retention, marginal staining, marginal adaptation, post-operative sensitivity and recurrence of caries. The differences among the groups were

calculated using Friedman's repeated measures analysis of variance rank ($\alpha = 0.05$).

Results: The recall rate was 100% at 24-months. Eight restorations were lost at twenty-four months (eight SUP-5, two for SUP-25 and two for GBU-25). According to FDI criteria, the 24-month retention rates (95% confidence interval) were 79% (63%-89%) for SUP-5, 95% (83%-99%) for SUP-25, 100% (91%-100%) for GBU-5, and 95% (83%-99%) for GBU-25, with statistical difference among SUP-5 when compared to all groups ($p < 000.1$). Sixty restorations were considered to have minor discrepancies in their marginal adaptation at the 24-month recall using the FDI criteria (16 for SUP-5, 14 for SUP-25, 17 for GBU-5, and 13 for GBU-25). No significant difference was detected between any pair of groups at the 18-month recall ($p > 0.05$). Marginal staining was observed in 25 restorations (seven for SUP-5, six for SUP-25, eight for GBU-5, and four for GBU-25). No significant difference was detected between any pair of groups at the 24-month recall for all secondary parameters evaluated ($p > 0.05$).

Conclusions: The prolonged solvent evaporation time (25 s) of a universal adhesive only improve its clinical performance in NCCLs after 24-months when only an ethanol-water-based adhesive was applied.

Funding: This project was funded by ANID through initiation Fondecyt grant number 11221070

https://doi.org/10.1016/j.dental.2026.03.095

84

Double layer application of universal adhesives in cervical restorations:18-month follow-up

J Pancetti *[1], R Zaviezo [1], Z Maureira [1], M Rodriguez [1], R Gálvez [1], R Saavedra [1], AD Loguercio [2], MF Gutierrez [1]

[1] *Universidad de los Andes, Chile, Faculty of Dentistry, Santiago, Chile*
[2] *State University of Ponta Grossa, School of Dentistry, Ponta Grossa, Brazil*

Purpose / Aim: To evaluate the effect of a double layer application of auniversal adhesive systems on the 18 months clinical performance used as etch-and-rinse and selective enamel etching application mode in non-carious cervical lesions (NCCLs).

Materials & Methods: The local scientific ethics committee reviewed and approved the study protocol and consent form (protocol CEC2024050). 144 restorations were randomly placed in 36 subjects (16 male and 20 female) according to the following groups (n = 36): ER1 (one layer of Scotchbond Universal Plus adhesive applied as etch-and rinse mode); ER2 (double layer of Scotchbond Universal Plus adhesive applied as etch and-rinse mode); SEE1 (one layer of Scotchbond Universal Plus adhesive applied as selective enamel etching); SEE2 (double layer of Scotchbond Universal Plus adhesive applied as selective enamel etching). All groups were light-cured for 10s/1,000 mW/cm^2 only after final layer. A resin composite was placed by applying three increments and each one was light cured for 20s/1,000 mW/cm^2. The restorations were finished immediately with fine diamond burs and polishers. The restorations were evaluated at baseline and after 18 months by using the updated FDI criteria. The following outcomes were evaluated: retention, marginal staining, marginal adaptation, post-operative sensitivity and recurrence of caries. The differences among the groups were calculated using Friedman repeated measures analysis of variance rank ($\alpha = 0.05$).

Results: The recall rate was 100% at 6- and 18-months. Threerestorations were lost at six months (one for ER1, two for SEE1). After 18-month recall, additionally, one restoration was lost (one for ER1). According to FDI criteria, the 18-month retention rates (95% confidence interval) were 94.4% for ER1, 100% for ER2, 94.4% for SEE1 and 100% for SEE2. Ten restorations (five for ER1, two for ER2, three for SEE2) showed minor marginal staining, and 38restorations (eight for ER1, ten for ER2, ten for SEE1 and ten for SEE2) presented minimal marginal adaptation defects. No significant differences among the groups were observed in retention rates, as well as all secondary parameters evaluated ($p > 0.05$).

Conclusions: The double layer application of a universal adhesive systems did not improve the clinical performance of resin restorations in NCCLs after 18 months.

Funding: This project was funded by ANID through Initiation Fondecyt grant number 11221070.

https://doi.org/10.1016/j.dental.2026.03.096

85

Development of an automated deep-learning model for fractographic analysis

L Ortega [1], J Vergara [2], V Caro [3], M Wendler *[1]

[1] *Faculty of Dentistry, Universidad de Concepcion, Concepcion, Chile*
[2] *Instituto Profesional Virginio Gomez, Concepcion, Chile*
[3] *Facultad de Ingenieria, Universidad de Concepcion, Concepcion, Chile*

Purpose / Aim: Fractographic analysis—the study of fracture surface patterns in materials—has emerged as a critical diagnostic tool in understanding the failure mechanisms of dental biomaterials. Despite its relevance, this process remains highly dependent on expert interpretation, limiting its scalability and objectivity. The proposed research seeks to overcome these limitations by developing and validating an automated deep learning (DL) model capable of performing fractographic analysis on images of fractured dental materials.

Materials & Methods: Bar-shaped specimens ($2 \times 2 \times 20$ mm^3) were fabricated from various commercial materials, including lithium disilicate, direct resin-based composites, and 3D printing resins, and fractured using a three-point bending test. Fractured surfaces were imaged using both a stereomicroscope and a scanning electron microscope. A calibrated panel of experts manually annotated the fractographic features—such as mirror and mist regions, hackle, and compression curls-using Roboflow Inc. tools to generate ground truth data for model training. The YOLOv11 architecture (Ultralytics) was employed for object detection, instance segmentation, and fine-grained classification of fracture features. To improve generalizability, data augmentation strategies were applied, including adaptive histogram equalization, geometric transformations, and color/exposure perturbations. Model performance was evaluated using precision, recall, and F1-score metrics. Cohen's Kappa coefficient was calculated to assess the level of agreement between human and AI-generated annotations.

Results: The developed model demonstrated high performance in object detection (1.00) and instance segmentation (0.91). Detection of mirror–mist regions and compression curls yielded the highest accuracy. In contrast, other fractographic features such as hackle marks and arrest lines showed less consistent results, likely due to high intra-class variability and a limited number of annotated instances. Additionally, the high Cohen's Kappa coefficient (0.85) indicated strong agreement between the AI model and expert human analysis.

Conclusions: This preliminary study highlights the potential of deep learning to support objective and scalable fractographic analysis. Future efforts will focus on expanding the annotated dataset,

refining class definitions, and incorporating advanced preprocessing techniques to improve the visibility of fracture patterns—especially those that are frequent yet diffuse.

https://doi.org/10.1016/j.dental.2026.03.097

86
Synthesis and characterization of bilayer zirconia-systems based on recycled 3Y-TZP

E Bonfante *[1], T Campos [2], S Claudinei [3], L Alves [1], E Bergamo [1,4], S Tebcherani [5], L Witek [4,6], P Coelho [7,8], G Thim [9], S Yamaguchi [10], E Sousa [1], G Marcolino [1], EB Benalcazar-Jalkh [1]

[1] *University of Sao Paulo - Bauru School of Dentistry, Bauru, Brazil*
[2] *Universidade Federal de Pelotas, Pelotas, Brazil*
[3] *Faculty of Technology, Rio de Janeiro State University, Rezende, Brazil*
[4] *Biomaterials Division, New York University College of Dentistry, New York, USA*
[5] *Department of Production Engineering, Federal University of Technology, Ponta Grossa, Brazil*
[6] *Department of Biomedical Engineering, NYU Tandon School of Engineering, New York, USA*
[7] *Department of Surgery, University of Miami Miller School of Medicine, Miami, USA*
[8] *Department of Biochemistry and Molecular Biology, University of Miami Miller School of Medicine, Miami, USA*
[9] *Department of Physics, Aeronautics Technological Institute, São José dos Campos, Brazil*
[10] *Department of Dental Biomaterials, Osaka University Graduate School of Dentistry, Osaka, Japan*

Purpose / Aim: To synthesize and characterize the microstructure, phase content, optical and mechanical properties of bilayer zirconia systems based on pristine (Zpex, Tosoh) or recycled 3Y-TZP powder and ultra-translucent 5Y-PSZ (Zpex Smile, Tosoh).

Materials & Methods: Non-milled zirconia remnants were collected, grounded, and recycled by ball milling for 12 hours at 20 rpm. Subsequently, a fresh solution was prepared for binder addition (8g PVA) and grinded for another 4 hours. After drying, the recycled powder was sieved and weight for sample manufacture. Disk-shaped samples of bilayer zirconia were fabricated through progressive manual and uniaxial pressing of either pristine or recycled 3Y-TZP and a top layer of 5Y-PSZ. After sintering, microstructure and phase composition were analyzed using Scanning-Electron-Microscopy (SEM) and X-Ray Diffraction (XRD). Optical and mechanical properties were assessed via reflectance and biaxial flexural strength tests, followed by fractographic analysis. Optical and mechanical properties data were analyzed using two-way ANOVA and Tukey test, and Weibull statistics, respectively.

Results: The recycled powder exhibited a mean particle-size of 1.14μm. SEM revealed uniform surface morphology across both sintered groups. While tetragonal zirconia was identified as the predominant phase in pristine and recycled 3Y-TZP, characteristic peaks of tetragonal and cubic phases were observed in 5Y-PSZ at XRD evaluation. Lower translucency-parameter and higher contrast-ratio were observed for the recycled bilayers compared to its pristine counterpart. The pristine group presented higher strength (1138.6; 1179.4-1099,1 MPa) compared to bilayers based on recycled 3Y-TZP (882; 948.5-820.13 MPa). Fractographic features suggest that failures initiated at the tensile surface for both groups and propagated towards the compressive side with changes in direction at the interface of zirconia layers.

Conclusions: The synthesis of bilayered systems using recycled 3Y-TZP was successful, resulting in high strength (over 800-MPa) and homogeneous microstructure. Bilayers based on pristine powder presented higher translucency and strength compared to their recycled counterparts.

https://doi.org/10.1016/j.dental.2026.03.098

87
Open-access digital periodontal ligament generation from a computed-tomography using offset-tools

FA Shakhtour *[1,2], PJ Watson [1], N Austin [1], S Barber [1], A Altaie [1], FP Rodrigues [1]

[1] *University of Leeds, Leeds, UK*
[2] *University of Petra, Amman, Jordan*

Purpose / Aim: Accurate representation of the periodontal ligament (PDL) is essential for realistic digital modelling in Dentistry. However, the PDL is not easily visualised in cone-beam computed-tomography (CBCT) due to its small thickness and low contrast. This study aimed to develop, demonstrate, and validate a reproducible workflow for creating a digital PDL using offset-based modelling as a preparatory step for future dental simulations.

Materials & Methods: CBCT data of a human mandible was segmented using 3D Slicer ®v.5.8.1 (USA) to isolate individual teeth and alveolar bone generating a 3D master model. The resulting model was imported into Meshmixer ®v.3.5 (UK) where a consistent offset of 0.2 mm was applied to the root surfaces to generate a periodontal ligament layer, therefore generating two different models: with and without the PDL. For each tooth, the root region was selected, smoothened, and separated from the crown. A 0.2 mm negative offset was applied to the root surface, creating an inner shell that was duplicated. Both the outer and the first inner shells were combined. Smoothened edges were joined, resulting in periodontal ligament (PDL) volume. The second inner shells' normal vectors were flipped, and then both the crown and the inner shell were joined as one structure. Models were exported as binary STL files and imported into MeshLab® v2020.07 (Italy) for mesh size reduction. Pre and post processing were performed in Abaqus where the maximum principal stress distribution was evaluated for the comparison of the models generated.

Results: The comparison between the models highlighted the importance of the method as it clearly showed differences on the stress distribution at the cervical area between the teeth and the bone, with higher maximum principal stresses found for the model without the PDL. The offset technique enabled the successful creation of a continuous, anatomically plausible PDL layer surrounding each root surface. The method proved to be straightforward, reproducible, and compatible with further mesh refinement steps.

Conclusions: This study presents a simplified digital workflow for periodontal ligament generation from CBCT-derived models using offset tools. The comparison between the models highlighted the importance of the method and the potential to offset the PDL by any distance according to a specific research question. This approach improves the accuracy of future simulations and treatment planning in fields of Orthodontics, Restorative and Prosthetic Oral Rehabilitations.

https://doi.org/10.1016/j.dental.2026.03.099

88
Adjustment time, cost and satisfaction of conventional and digital splints

A Echeverría *[1], M Rodríguez [1], C Miranda [1], J Rivera [1], A Beniscelli- Vásquez [1], R Aliaga- Gálvez [1], C Vidal [1], AD Loguercio [2], MF Gutierrez [1]

[1] *Universidad de Los Andes, Santiago, Chile*
[2] *Universidade Estadual de Ponta Grossa, Ponta Grossa, Brazil*

Purpose / Aim: To evaluate differences in adjustment time, manufacturing cost, and patient satisfaction between conventional and digital occlusal splints.

Materials & Methods: The study protocol and consent form were reviewed and approved by the local ethics committee. Thirteen adult participants diagnosed with probable bruxism and requiring occlusal splint participated in this randomized crossover clinical trial. For conventional splints, gypsum models were fabricated, while for digital splints, models were scanned and processed using CAD/CAM technology. All patients received and used both types of splints and were divided into two groups based on the order of first splint delivery: (i) conventional followed by digital (CD); or (ii) digital followed by conventional (DC). The adjustment time for each splint was recorded on the day of installation. Manufacturing costs were calculated based on materials and production processes. Each splint was used for two weeks. After each period, participants completed two satisfaction questionnaires assessing comfort, usability, and overall experience. administered for each splint. A paired t-test was performed to compare manufacturing and adjustment times, as well as manufacturing cost. The Wilcoxon signed-rank test was used for the analysis of satisfaction data. Statistical analyses were performed using SPSS statistical software ($\alpha = 0.05$).

Results: Digitally manufactured splints required significantly less adjustment time than conventional splints ($p < 0.05$). The manufacturing costs was also significantly lower for digital splints compared to conventional ones ($p < 0.05$). No significant differences were found between splint types in any individual satisfaction or quality of life parameters ($p > 0.05$). However, overall participant acceptance was significantly higher for digital splints ($p < 0.05$).

Conclusions: Digital occlusal splints demonstrated advantages over conventional splints in terms of reduced adjustment time, lower manufacturing costs, and higher overall participant acceptance, while maintaining comparable quality of life and satisfaction levels.

Funding: This project was funded by ANID through Initiation Fondecyt grant number 11221070.

https://doi.org/10.1016/j.dental.2026.03.100

89
Comparative accuracy of four scanners under three lighting conditions

E Quintana [1], M Martínez *[2], G Nima [2], Y Gallardo [1]

[1] *Universidad Científica del Sur, Lima, Peru*
[2] *Universidad de los Andes, Santiago de Chile, Chile*

Purpose / Aim: To compare *in vitro* the effect of three different illuminance conditions on the accuracy of four intraoral scanners.

Materials & Methods: Accuracy (Trueness and Precision) of four intraoral scanners was evaluated: TRIOS 3 (TS), CS 3600 (CS), Helios 600 (HS) and Virtuo Vivo (VV), under three groups of different light conditions (500 lux, 1000 lux, and 6000 lux). Twelve scans were obtained from each device, resulting in 144 STL files, which were then compared to a reference STL file generated from a digitized maxillary master cast using an extraoral scanner. Geomagic software was used to calculate the accuracy of the scanners. Statistical analysis was perfomed using a generalized linear model (GLM). A two-way ANOVA (scanners x light source) and Tukey's post-hoc test ($\alpha = 0.05$) were conducted to compare light conditions.

Results: Among the scanners evaluated, VV demonstrated the highest trueness (29.16 ± 11.53 μm) and precision (28.95 ± 11.60 μm) across all illuminance conditions (Table 1). TS showed significant accuracy variations with increasing illuminance, while CS, HS, and VV exhibited no statistically significant differences in accuracy under the three lighting conditions.

Conclusions: Light conditions affect the scanning accuracy, depending on the intraoral scanner device. Although a decrease in the accuracy was observed between the four scanners tested, it was not significant for all of them. VV showed the best accuracy among all light sources and scanner types. CS had the lowest precision and VV had the best trueness.

		Trios 3	Carestream	Helios 600	Virtuo Vivo
Trueness	500 Lux	60.31 ± 14.34 Ab	89.16 ± 17.93 Ac	77.11 ± 4.80 Ac	29.16 ± 11.53 Aa
	1000 Lux	75.51 ± 17.16 Bb	91.75 ± 14.85 Ac	82.83 ± 8.39 Abc	29.64 ± 3.15 Aa
	6000 Lux	81.69 ± 26.50 Bb	98.62 ± 20.98 Ac	88.90 ± 8.88 Abc	32.18 ± 3.76 Aa
Precision	500 Lux	60.36 ± 14.68 Ab	82.50 ± 19.11 Ac	76.61 ± 5.02 Ac	28.95 ± 11.60 Aa
	1000 Lux	75.45 ± 17.18 Bb	83.52 ± 14.65 Ab	82.48 ± 8.45 Ab	29.37 ± 2.90 Aa
	6000 Lux	81.53 ± 26.43 Bb	90.16 ± 20.79 Ab	88.36 ± 9.03 Ab	31.91 ± 3.66 Aa

Table 1: Mean values ± standard deviations in μm for trueness and precision of the scanners under different light sources. Standard deviation followed by similar letters indicate no significant differences (Upper letters compare light sources for the same scanner, and lower letters compare scanners for the same light source) by two-way ANOVA and Tuckey's posthoc test ($p<0.05$). Lower values mean better trueness and precision.

https://doi.org/10.1016/j.dental.2026.03.101

Saturday, October 4th

'Biological properties'

90
Antimicrobial Synergy of Nanotubes and Visible Light in Glass Ionomer

K Kantovitz *[1,2], L dos Santos [2], E Bronze-Uhle [3], J Rangel-Coelho [2], L Teixeira [2], F Nociti-Jr [4], P Lisboa-Filho [3], A Segundo [2]

[1] *University of Maryland, Baltimore, USA*
[2] *Faculdade São Leopoldo Mandic, Campinas, Brazil*
[3] *Unesp, Bauru, Brazil*
[4] *American Dental Association, Chicago, USA*

Purpose / Aim: This study evaluated the antimicrobial effect of titanium dioxide nanotubes (nTiO2) incorporated into glass ionomer cement (GIC) and activated by LED light against Streptococcus mutans.

Materials & Methods: First, nTiO2 nanotubes were characterized for their absorption spectrum using a spectrophotometer and microbial inactivation dosimetry by colony-forming unit (CFU/mL) counts were obtained for Escherichia coli and Staphylococcus aureus at 10, 20, and 30 seconds of exposure. Subsequently, 0% and 5% by weight of nTiO2 (≈20 nm) were incorporated into GIC (Ketac Molar EasyMix®), and S. mutans ($1x10^8$ CFU/mL) were cultured on the cement disks. Cell viability (trypan blue), cell morphology (scanning electron microscope at 15 KV, 60X), and gene expression (vicR, covR) were assessed after 1, 6, and 7 days. Gene expression was analyzed through real-time PCR. Data were analyzed using Shapiro-Wilk, Kruskal-Wallis, and Dunn tests ($\alpha = 0.05$).

Results: The absorption spectrum of nTiO2 ranged from 400-450 nm, with the lowest CFU/mL observed at 30 s of exposure. The incorporation of nTiO2 into the GIC matrix significantly reduced the S. mutans count after 7 days ($p < 0.05$), although no synergistic effect between nTiO2 and LED light was observed ($p > 0.05$). The morphology of S. mutans remained unchanged, and a higher expression of vicR was detected at 72 h in the presence of nTiO2 ($p < 0.05$), while covR was not expressed.

Conclusions: In conclusion, no synergistic effect was found between the incorporation of nTiO2 into GIC and LED light activation against S. mutans. The incorporation of 5% nTiO2 reduced bacterial counts on the restorative material without altering S. mutans morphology.

https://doi.org/10.1016/j.dental.2026.03.102

91

Neutrophil-mediated enzymatic degradation of dentinal collagen

Y Peled *[1], A Ragheai [1], Z Gouveia [1,2], C Stewart [1,2], C Sun [1], J Barker [1], M Glogauer [1,3], Y Finer [1,2]

[1] *Faculty of Dentistry, University of Toronto, Toronto, Canada*
[2] *Institute of Biomedical Engineering, University of Toronto, Toronto, Canada*
[3] *Department of Dental Oncology, Maxillofacial and Ocular Prosthetics, Princess Margaret Cancer Centre, Toronto, Canada*

Purpose / Aim: Caries (tooth decay) is one of the most prevalent diseases and a leading cause of dental restoration's failure. This process involves dentinal demineralization (mineral removal) due to bacterial acid production, resulting in exposed demineralized collagen and tooth cavitation. Recently, neutrophils, innate immune cells, were found to degrade demineralized dentinal collagen in vitro. These abundant cells can travel from the gingival sulcus, near the teeth roots and bacterial biofilm (plaque), and cleave demineralized dentinal collagen. Such activity could compromise the tooth-restoration interface integrity clinically. We hypothesize that specific neutrophil-derived enzymes can degrade demineralized dentinal collagen. This may reveal significant mechanistic milestones, involving novel culprits in caries and restoration failure.

Materials & Methods: Dentin from extracted human teeth was sectioned into slabs, and demineralized. Isolated neutrophils collected from healthy donors' blood, and neutrophil-derived enzymes - neutrophil elastase (NE), cathepsin G (CG), neutrophil defensins, matrix metalloproteinases (MMP) -8, -9, neutrophil gelatinase-associated lipocalin, myeloperoxidase, and lactoferrin, were incubated with rat tail type-I collagen (RTC). Samples were analyzed using ultra-performance liquid chromatography/mass spectroscopy (UPLC/MS) to detect type-I collagen fragments. Enzymes that demonstrated collagenolytic activity towards RTC were then incubated with demineralized dentin slabs (DDS) under similar conditions and analyzed with UPLC/MS as described. Statistical analysis was conducted using ANOVA with Tukey's HSD post-hoc test ($n = 3$, $p < 0.05$).

Results: NE, CG, and MMP-8 demonstrated (Fig. 1) significant collagenolytic activity against RTC ($p < 0.05$). Subsequently, only NE and CG showed significant degradation of the more complex dentin matrix in DDS ($p < 0.05$), indicating their specific relevance to the dentin microenvironment. This discrepancy likely reflects the complexity of the dentin structure compared to isolated type-1 collagen, as well as the broader degradative spectrum of NE and CG, the serine proteases. Structural analyses of these enzymes are ongoing to further elucidate potential degradative mechanisms.

Conclusions: These findings highlight NE and CG as key contributors to dentin degradation, with potential implications for restoration failure via degradation of the tooth-restoration interface. By targeting these neutrophil-derived enzymes, novel anti-degradative therapies could be developed to complement traditional antimicrobial strategies, potentially enhancing restoration longevity and clinical outcomes. To further support this, in-silico analysis of the 3D structure of enzyme catalytic sites involved in DDS degradation will be conducted to characterize the interaction between the enzymes and type-1 collagen. This may identify key molecular interactions that will enable targeted inhibitor development or protective strategies to reduce demineralized dentinal collagen degradation.

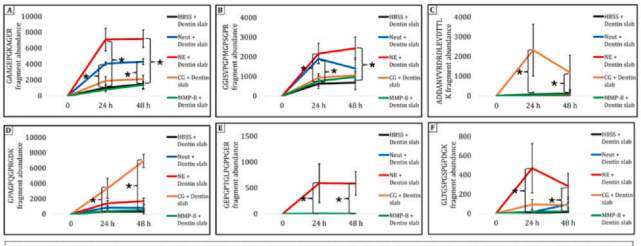

Figures A-F – Collagen fragments levels are differentially changed following the incubation of demineralized dentin slabs with and without human neutrophils (Neut), or neutrophil-derived enzymes – neutrophils elastase (NE), cathepsin G (CG), and matrix metalloproteinase (MMP)-8. Demineralized dentin slabs were incubated for up to 48h at 37°C, 5% CO_2, pH=6.8 with HBSS alone, with and without 1-5X10^6 cells/mL Human neutrophils, 10 µg/ml NE, 10 µg/ml CG, and 1 ug/ml MMP-8. Neutrophil-derived enzyme NE have increased 4 collagen fragments (Fig. A, B, E, F), and CG have increased 2 (Fig. C, D) after 24h and/or 48h, as compared to the control. Collagen fragment levels are expressed as arbitrary units of abundance, based on mass spectrometry signal intensity (n=9). * = P>0.05.

https://doi.org/10.1016/j.dental.2026.03.103

92

Lab-on-a-Chip to ultrasensitive cortisol biosensing based on LIG/MIP

N Carreño *, L Gonçalves, R Balboni, B Lopes, S Khan, R Vaucher

UFPel, Pelotas, Brazil

Purpose / Aim: Cortisol is the primary glucocorticoid responsible for regulating human metabolism. This steroid hormone, produced in the adrenal glands, acts as a metabolic regulator of blood glucose levels, enabling rapid energy supply to muscles and enhancement of brain functions (KUO, 2015). Monitoring cortisol levels in the body is essential for assessing hypothalamic-pituitary-adrenal (HPA) axis function and diagnosing hormonal disorders such as depression, anxiety, and Cushing's syndrome. Current techniques for cortisol measurement include enzyme-linked immunosorbent assay (ELISA) and liquid chromatography tandem mass spectrometry (LC-MS/MS) (ZHANG, 2016). An alternative approach for cortisol monitoring involves electrochemical sensors. demonstrated the sensor's reliable detection capability throughout this physiological range. This study employed cyclic voltammetry (CV) to evaluate laser-induced graphene molecularly imprinted polymer (LIG MIP) sensors for cortisol detection across clinically relevant concentrations (0-60 µg/dL).

Materials & Methods: An alternative approach for cortisol monitoring involves electrochemical sensors. Laser-induced graphene (LIG) electrodes have demonstrated high sensitivity and selectivity for hormone detection, making them functional for clinical environments and rapid diagnostic applications (RABTI, 2015). This study employed cyclic voltammetry (CV) to evaluate laser-induced graphene molecularly imprinted polymer (LIG MIP) sensors for cortisol detection across clinically relevant concentrations (0-60 µg/dL).

Results: The electrochemical analysis demonstrated the sensor's reliable detection capability throughout this physiological range.

Laser-induced graphene (LIG)-based sensors have demonstrated high sensitivity and selectivity for cortisol.

Conclusions: Thus, this work contributes to the advancement of biomedical sensing technologies, supporting the feasibility of LIG-MIP sensors as an efficient and accessible tool for cortisol assessment and the diagnosis of stress-related metabolic conditions.

https://doi.org/10.1016/j.dental.2026.03.104

93

Laser-Induced Graphene Sensor for Multiplexed Detection of Catecholamines and Tyrosine

R Lund *, N Carreño, L Goncalves, R Balboni, B Lopes, S Khan, B Noremberg, G Maron

UFPel, Pelotas, Brazil

Purpose / Aim: The hormones epinephrine (EP) and norepinephrine (NE) are neurotransmitters in the central and peripheral nervous systems, synthesized from the amino acid tyrosine (TY). They act as regulators of heart rate, mobilize glucose, and modulate blood flow to the muscles. Monitoring these hormones is critical in clinical and research settings, as abnormal levels may be associated with conditions such as hypertension, vasoconstriction, neurological disorders, and cardiovascular diseases.

Materials & Methods: This study performed cyclic voltammetry (CV) analysis using LIG sensors to identify EP, NE, and TY in complex environments. The tests were conducted with 1 mM epinephrine, norepinephrine, and tyrosine.

Results: The normal plasma concentration range of epinephrine (Fig. 1) has been established as 8-32 ng/L by laboratory guidelines, with deviations potentially indicating adrenal hyperactivity (YUI, 1980). Laser-induced graphene with moleculary imprinted polymers (LIG/MIP)-based sensors have demonstrated high sensitivity and selectivity for epinephrine, norepinephrine, and tyrosine, showing promise for clinical monitoring and rapid diagnostic applications.

Conclusions: The tests were conducted with 1 mM epinephrine, norepinephrine, and tyrosine, demonstrating the sensor's capability to simultaneously detect these hormones using a single sensor platform.

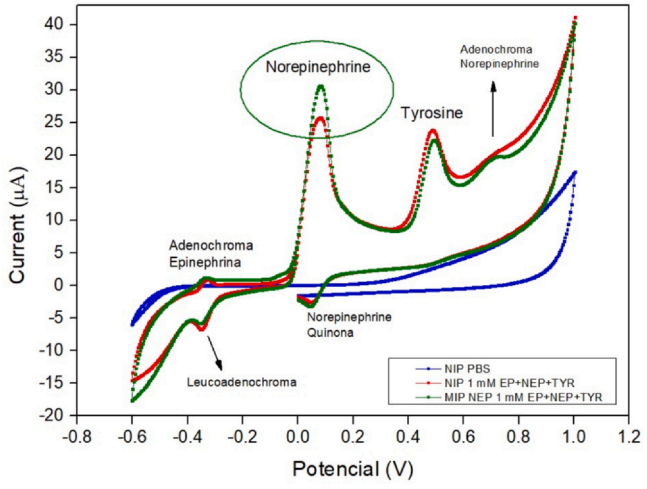

Figure 1

https://doi.org/10.1016/j.dental.2026.03.105

94

Cytotoxicity of high-concentration bleaching gel with calcium polyphosphate submicroparticles

DA Lima *[1], L de Jesus Gomes [1], RA de Oliveira Ribeiro [2], M Ortiz [1], JA da Silva [1], CA de Souza Costa [2], K Rischka [3]

[1] *Faculdade de Odontologia de Piracicaba, Universidade Estadual de Campinas (FOP-UNICAMP), Piracicaba, Brazil*
[2] *Faculdade de Odontologia de Araraquara, Universidade Estadual Paulista (UNESP), Araraquara, Brazil*
[3] *Fraunhofer Institute for Manufacturing Technology and Advanced Materials (IFAM), Bremen, Germany*

Purpose / Aim: To evaluate the bleaching efficacy and cytotoxicity of hydrogen peroxide (HP 35%) with sub-microparticles of calcium polyphosphate (CaPP) irradiated with or without a violet light-emitting diode (LED).

Materials & Methods: Bovine enamel-dentin discs (n = 48; 5.6 mm diameter, 2.3 mm thickness) were prepared and polished to simulate human lower incisors. The samples were divided into 8 groups (n = 6): Control Group (without treatment); LED; Commercial 35%HP (HP35%C); Commercial 35%HP + LED (HP35%CL); Manipulated 35%HP (HP35%M); Manipulated 35%HP + CaPP 1.5% w/t (HP35%MP); Manipulated 35%HP + LED (HP35%ML); Manipulated 35%HP + CaPP 1.5% w/t + LED (HP35%MPL). Specimens were mounted in artificial pulp chambers and exposed to odontoblast-like cells from the MDPC-23 cell line. Bleaching protocols involved the application of 35% hydrogen peroxide gels for 45 minutes, with or without violet LED irradiation. Experimental gels were prepared under darkroom conditions, incorporating calcium polyphosphate into the thickening agent for designated groups. Bleaching efficacy was assessed, and extracts were analyzed for cytotoxicity (viability, oxidative stress, and HP diffusion). Data were analyzed using generalized linear models and Kruskal–Wallis/Dunn tests were applied for WID ($\alpha = 5\%$).

Results: In the cell viability assay, all groups treated with HP showed significantly lower viability compared to the controls ($p < 0.0001$). Among the bleached groups, HP35%MPL exhibited the highest viability, followed by HP35%MP ($p < 0.0001$). Groups without CaPP showed the lowest viability, with no significant differences among them ($p < 0.0001$). Oxidative stress levels were significantly higher in all HP groups compared to the controls ($p < 0.0001$); however, the lowest oxidative stress was observed in the HP35%MPL and HP35%MP groups. HP diffusion was significantly lower in CaPP-containing groups (HP35%MP, HP35%MPL), whereas HP35%C, HP35%CL, HP35%M, and HP35%ML exhibited the highest diffusion rates ($p < 0.0001$). Color variation analysis (ΔE00) revealed no significant differences among groups ($p = 0.2334$). The WID analysis showed higher values for treated groups compared to the control and LED-only groups ($p = 0.0080$). SEM and fluorescence microscopy images confirmed better preservation of cell morphology and a greater proportion of viable cells when CaPP was incorporated. The addition of CaPP improved cell viability, reduced oxidative stress, and limited HP diffusion, with further enhancement when combined with LED. Moreover, CaPP did not impair bleaching efficacy.

Conclusions: The incorporation of calcium polyphosphate (CaPP) into hydrogen peroxide (HP) demonstrated effective whitening results, low cytotoxicity, increased cell viability, reduced oxidative stress, and decreased hydrogen peroxide diffusion into pulp cells. These effects were further enhanced when combined with violet LED.

https://doi.org/10.1016/j.dental.2026.03.106

95

OroSil-Q: Proof-of-Concept Antimicrobial Silk Bioplastic for Recyclable Oral Care Devices

U Mangal *[1], W Choi [2], J-S Kwon [1], J Hong [2], S-H Choi [1]

[1] *Yonsei University College of Dentistry, Seoul, Korea, Republic of*
[2] *College of Engineering, Yonsei University, Seoul, Korea, Republic of*

Purpose / Aim: To demonstrate the feasibility of OroSil-Q, a novel silk fibroin-based bioplastic incorporating quaternary ammonium groups, as a biofilm-resistant and recyclable material platform for dental applications such as orthodontic aligners.

Materials & Methods: OroSil-Q was developed using a template-guided molecular entanglement approach that integrates mechanical reinforcement (via dual ether linkers) with intrinsic antimicrobial functionality (via covalently attached quaternary ammonium moieties). This study assessed the material's mechanical integrity under simulated oral forces, in vitro resistance to pathogenic colonization, cellular biocompatibility and potential for recyclability through controlled molecular disentanglement.

Results: The proof-of-concept material demonstrated key functional benchmarks: (1) viscoelastic stress-relaxation suited for dynamic force transmission in orthodontic devices, (2) a marked reduction in colonization by S. mutans and S. aureus on material surfaces, and (3) favorable interactions with gingival fibroblasts and macrophages, indicating low inflammatory and cytotoxic risk. Importantly, OroSil-Q could be depolymerized and reprocessed without compromising antimicrobial or mechanical performance, validating its recyclability.

Conclusions: This work establishes OroSil-Q as a viable platform material for the future of oral care appliances. The combination of mechanical adaptability, biofilm resistance, and recyclability positions it as a candidate for sustainable, next-generation dental devices. Further in vivo and prototyping studies are warranted to optimize form factor integration and assess long-term performance in the oral environment.

https://doi.org/10.1016/j.dental.2026.03.107

96

Mesenchymal stem cell response on 3D-printed β-TCP scaffolds

JP Rangel-Coelho *, R Pes, MH Napimoga, EF Martinez, LN Teixeira

Faculdade São Leopoldo Mandic, Campinas, Brazil

Purpose / Aim: To evaluate the biological performance of β-tricalcium phosphate (β-TCP) scaffolds fabricated by additive manufacturing, focusing on mesenchymal stem cell (MSC) behavior in vitro.

Materials & Methods: Mesenchymal stem cells (MSCs) derived from the bone marrow of Wistar rat femurs were cultured on β-TCP scaffolds produced via additive manufacturing (12 mm in diameter and 3 mm in height). The following parameters were assessed: (1) cell morphology by epifluorescence microscopy at 30 min, 2 h, and 24 h; (2) cell viability by MTT assay at days 1, 2, and 3; (3) cell proliferation using a hemocytometer at days 1, 2, and 3; and (4) gene expression of RUNX2, COL1, and OPN by qPCR at days 7 and 10. MSCs cultured on polystyrene plates served as the control group. Data were statistically analyzed with a significance level set at 5% ($p < 0.05$).

Results: Epifluorescence analysis demonstrated that MSCs adhered to the β-TCP scaffolds, although they appeared less spread compared to the control group. MSC viability was significantly reduced on β-TCP scaffolds at all evaluated time points ($p < 0.05$). While overall cell proliferation was initially similar between groups, a significant reduction was observed on β-TCP at days 2 and 3 ($p < 0.05$). Gene expression analysis showed that RUNX2 and COL1 levels were significantly upregulated in MSCs cultured on β-TCP compared to controls at both 7 and 10 days ($p < 0.05$). Conversely, OPN expression was significantly downregulated on β-TCP scaffolds at the same time points ($p < 0.05$).

Conclusions: β-TCP scaffolds fabricated by additive manufacturing supported MSC adhesion and early proliferation and positively modulated the expression of key osteogenic genes. These findings suggest their potential application in bone tissue engineering and regenerative therapies.

https://doi.org/10.1016/j.dental.2026.03.108

97

Hydrolyzed PCL/nHA Scaffolds Enhance Regenerative Signaling for Pulp Therapy

IP Soares *[1,2], C Anselmi [2], L de Oliveira Fernandes [1], R de Oliveira Ribeiro [1], R Piazza [1], G Pinto [3], R Dal-Fabbro [2], CA de Souza Costa [1], MC Bottino [2], J Hebling [1]

[1] *São Paulo State University (UNESP), Araraquara, Brazil*
[2] *University of Michigan, Ann Arbor, USA*
[3] *University of Aveiro, Aveiro, Portugal*

Purpose / Aim: This study explored the effects of alkaline hydrolysis of poly(ε-caprolactone)/nano-hydroxyapatite (PCL/nHA) fibrous scaffolds on their physicochemical properties and the regenerative potential in human dental pulp cells (hDPCs) for vital pulp therapy.

Materials & Methods: Polymeric solutions containing 10% PCL and 2% nHA (m/v) were electrospun into fibers, which were subsequently treated with 5 M NaOH for 30 minutes (hydrolyzed group). Untreated fibers served as controls. Characterization was performed to assess changes in morphology, composition, contact angle, pH modulation, degradation behavior, and calcium release ($n = 8$). Biological assays involved hDPCs isolated from four human third molars, evaluating cell viability (alamarBlue), expression and synthesis of dentinogenic markers (RT-qPCR and immunofluorescence), and mineralization (alizarin red staining and soluble calcium quantification) ($n = 8$). Chemotaxis and fibronectin expression were also assessed using an indirect model with hDPCs ($n = 4$). Data were analyzed using t-tests and confidence intervals ($\alpha = 0.05$).

Results: Alkaline hydrolysis reduced fiber diameter ($p = 0.0053$) without compromising the structural integrity, preserving the interconnected fibrillar architecture. Although degradation rate and pH remained unchanged, hydrolyzed fibers reduced the water contact angle to 50º and increased calcium ion release by 25.8%, reaching 3.5 mM in 21 days. Hydrolyzed fibers enhanced hDPC viability at day 7 ($p = 0.0003$), upregulated ALPL and DSPP expression ($p \leq 0.01$), downregulated COL1A1 ($p = 0.088$), and increased DSPP protein synthesis ($p \leq 0.021$). DMP1 expression and synthesis were unaffected ($p \geq 0.1421$). Hydrolyzed scaffolds increased biomineralization by 40% ($p = 0.0034$) and reduced soluble calcium levels ($p = 0.0011$). Furthermore, hydrolysis increased both chemotactic potential and fibronectin expression ($p \leq 0.0024$).

Conclusions: Alkaline hydrolysis presents a simple and effective surface modification strategy for enhancing the regenerative properties of PCL/nHA fibrous scaffolds. This approach modulates dentinogenic and chemotactic signaling in hDPCs by increasing hydrophilicity and calcium release, highlighting its potential for clinical translation in vital pulp therapy.

https://doi.org/10.1016/j.dental.2026.03.109

98

S-PRG Bioactive Composites: Antibacterial and Virulence Modulation

M Dal Picolo *[1], JP Rangel-Coelho [1], L Teixeira [1], E Bridi [1], F do Amaral [1], K Kantovitz [2], R Basting [1]

[1] *Faculdade São Leopoldo Mandic, Campinas, Brazil*
[2] *University of Maryland, Baltimore, USA*

Purpose / Aim: To evaluate the effect of bioactive resin composites containing S-PRG fillers, with different viscosities, on the antibacterial activity and gene expression of Streptococcus mutans.

Materials & Methods: Discs (2 mm × 4 mm) of bioactive resin composites with low viscosity (Beautifil Flow Plus F00/BP0 and F03/BP3) and high viscosity (Beautifil II/BII, Beautifil LS/BLS, and Beautifil Bulk Restorative/BR) were compared to a conventional high-viscosity composite resin (Filtek Z350 XT/Z350) regarding colony-forming unit (CFU/mL) counts of S. mutans (n = 6) after 24 hours and 5 days of incubation. After each period, biofilms were collected, and the pellets were frozen in Trizol at –80 °C for RNA extraction. Total RNA was converted into cDNA for real-time qPCR analysis of gtfD, vicR, and covR gene expression. Reactions were normalized by 16S rRNA expression. Statistical analyses were performed with a significance level of 5%.

Results: After 24 hours, no significant differences were observed among groups, except between BII and BP3 ($p = 0.0112$), with higher CFU/mL in BII and lower in BP3. After 5 days, Z350, BP0, and BP3 showed the highest CFU/mL values, followed by BLS, BR, and BII ($p = 0.0001$). BLS showed no significant differences compared to BP3, BR, or BII, which were also statistically similar. Regarding gene expression, no significant differences were observed at 24 hours ($p > 0.05$). After 5 days, gtfD expression was significantly reduced in BII, BP0, and BP3 ($p < 0.05$), and vicR expression was lower in BP0 ($p < 0.05$). covR expression was higher in BR, BII, BP0, and BP3 compared to Z350 ($p < 0.05$), with lower levels in BII, BLS, and BP3 than in BR and BP0 ($p < 0.05$).

Conclusions: The antibacterial activity was influenced by the viscosity of the resin composites. After 24 hours, S-PRG-containing flowable resins showed reduced S. mutans adhesion, while after 5 days, high-viscosity resins were more effective. The modulation of gtfD, vicR, and covR expression supports the bioactive potential of these materials.

https://doi.org/10.1016/j.dental.2026.03.110

99

Enhanced Mineral Precipitation and Physicochemical Properties of Modified GIC System

K Tsuchiya *[1,2], S Sauro [2], J Matinlinna [3,4], M Yamauti [5], H Sano [1], A Tomokiyo [1]

[1] *Department of Restorative Dentistry, Hokkaido University, Sapporo, Japan*
[2] *Departamento de Odontología, Facultad de Ciencias de la Salud, Universidad CEU-Cardenal Herrera, Valencia, Spain*
[3] *Faculty of Dentistry, The University of Hong Kong, Hong Kong, Hong Kong*
[4] *Dentistry, School of Medical Sciences, The University of Manchester, Manchester, United Kingdom*
[5] *Indiana University School of Dentistry, Indianapolis, USA*

Purpose / Aim: This in vitro study evaluated the physicochemical characteristics and mineral precipitation potential of glass ionomer cements (GICs) incorporating either fluoride-doped calcium phosphates (FDCP) or zinc-polycarboxylate bioactive glass (BAG-Zn), in comparison with commercially available GIC formulations.

Materials & Methods: The independent variables in this study included the type of glass ionomer cement (two levels: Fuji™ IX GP [IX-GP] and Fuji™ II LC [II-LC]), the incorporated particle type (two levels: fluoride-doped calcium phosphate [FDCP] and zinc-polycarboxylate bioactive glass [BAG-Zn]), and the particle concentration (four levels: 0, 5, 10, and 20 wt.%). Each experimental formulation was mixed and molded into disc-shaped specimens, which were subsequently evaluated for pH, calcium (Ca^{2+}), and fluoride (F^-) ion release, as well as compressive strength, following immersion in deionized water for 1, 7, and 28 days at 37 °C. Mineral deposition after phosphate-buffered saline (PBS) storage was analyzed at baseline and after 28 days using Fourier-transform infrared spectroscopy (FTIR) and scanning electron microscopy with energy-dispersive X-ray analysis (SEM/EDX).

Results: The experimental IX-GP groups exhibited significantly lower compressive strength and lacked clear evidence of calcium phosphate (CaP)-based mineral deposition. In contrast, the II-LC formulations incorporating 10% or 20% FDCPs or 5% BAG-Zn demonstrated significantly enhanced compressive strength, along with evident CaP-based mineral formation on the material surfaces.

Conclusions: The incorporation of 5 wt.% BAG-Zn into the II-LC formulation may represent a promising approach for developing restorative materials with enhanced F^- release and mechanical performance. Conversely, the addition of 10 or 20 wt.% FDCPs produced GICs characterized by reduced acidity, increased F^- release, pronounced CaP-based mineral deposition, and improved compressive strength.

https://doi.org/10.1016/j.dental.2026.03.111

100

Rheology and Cytocompatibility of Thermoreversible Hydrogels for Regenerative Endodontics

L de Oliveira Fernandes [1], IP Soares *[1], V Peruchi [1], C Anselmi [2], F Mon [1], M Pires [1], J Oliveira [1], CA de Souza Costa [1], J Hebling [1]

[1] *São Paulo State University (UNESP), Araraquara, Brazil*
[2] *University of Michigan, Ann Arbor, USA*

Purpose / Aim: To evaluate rheological properties and the cytocompatibility of synthetic thermoreversible hydrogels based on Pluronic F-127, at different concentrations and storage times, using human apical papilla cells (hAPCs).

Materials & Methods: hAPCs were obtained from healthy human third molars (N = 4) and characterized using flow cytometry. For biological analysis, the following experimental groups were established: collagen hydrogel (control), and Pluronic F-127 hydrogels at concentrations (w/v) of 15% (P15%), 17.5% (P17.5%), 20% (P20%), 22.5% (P22.5%), 25% (P25%), and 30% (P30%) (n = 8). Cells were cultured on freshly prepared hydrogels for 24 hours or on hydrogels that had aged for 4 months. Cell viability and proliferation assays (alamarBlue; Live/Dead) were conducted on days 1, 3, and 7. All Pluronic F-127 hydrogels were subjected to rheological testing to

determine the sol-gel transition temperature, gelation time, and viscosity parameters related to stability and injectability. Data were analyzed using t-tests and ANOVA with appropriate post hoc tests ($\alpha = 5\%$).

Results: The established cell culture exhibited a high percentage of undifferentiated mesenchymal cells ($\geq 77.7\%$). After 1 and 3 days, cell viability was significantly higher for Pluronic F-127 hydrogels compared to the control, except for the two lowest concentrations (P15% and P17.5%). However, after 7 days, there were no statistically significant differences among groups. The cytocompatibility of hydrogels stored for 4 months remained comparable to that of freshly prepared formulations over 7 days, excluding P30%. P25% demonstrated the most favorable rheological profile for potential clinical use.

Conclusions: Thermoreversible Pluronic F-127-based hydrogels are cytocompatible with hAPCs and maintain their biological performance even after 4 months of storage. The 25% concentration (P25%) appears particularly promising for use in pulp regeneration procedures.

https://doi.org/10.1016/j.dental.2026.03.112

101

In situ study of EGCG-chitosan nanoparticles dentifrice on dentin permeability

K Pintado-Palomino *[1,2], L de Sousa Franco [1], R Scatolin [3], L Gusmão [4], A Tedesco [4], M Owasawara [5], S Coron [1]

[1] *School of Dentistry of Ribeirão Preto, University of São Paulo, Ribeirão Preto, Brazil*
[2] *Federal University of Minas Gerais, Belo Horizonte, Brazil*
[3] *Herminio Ometto University Center, School of Dentistry, Araras, Brazil*
[4] *Department of Chemistry, Center of Nanotechnology and Tissue Engineering- Photobiology and Photomedicine Research Group, University of Sao Paulo, Ribeirão Preto, Brazil*
[5] *Faculty of Pharmaceutical Sciences of Ribeirão Preto, University of Sao Paulo, Ribeirão Preto, Brazil*

Purpose / Aim: To evaluate the effect of experimental dentifrices containing epigallocatechin-3-gallate (EGCG)-loaded chitosan nanoparticles on dentin permeability

Materials & Methods: The study protocol was approved by the Ethics Committee of the School of Dentistry of Ribeirão Preto, University of São Paulo (Protocol number CAAE: 72718223.5.0000.5419). This in situ study included five phases (5 days each) and a washout period (7 days). The phases corresponded to use the following dentifrices: placebo (PL-negative control), chitosan nanoparticles (NCh), epigallocatechin 3-gallate (EGCG), EGCG-loaded chitosan nanoparticles (NCh + EGCG), and a commercial dentifrice (Elmex Sensitive - ES). Eighty dentin discs (Ø 4 mm × 1 mm) were obtained from bovine teeth and treated with 0.5 M EDTA to expose the dentin tubules. Eight participants meeting the eligibility criteria wore custom-made mandibular intraoral appliances containing two dentin discs that exposed in situ. The samples were eroded extraorally using 0.3% citric acid (pH = 2.6) four times daily and brushed intraorally with the assigned dentifrices (15 s, twice daily) for five days. Dentin permeability was assessed by a hydraulic conductance system (10 psi for 5 minutes) at two time points: T1 (after tubule exposure with EDTA) and T2 (after erosion and treatment with dentifrices). Data were analyzed by two-way ANOVA for repeated measures and Bonferroni post hoc test ($\alpha = 0.05$).

Results: Statistical analysis indicated significant effects of dentifrice ($p = 0.034$), dentin condition factors ($p < 0.001$), and their interaction (dentifrice × dentin conditions, $p = 0.028$). All groups (Table 1) showed a significant difference between T1 and T2 ($p < 0.05$). No significant differences in permeability among the dentifrice groups at T1 ($p > 0.05$). However, at T2, the PL group exhibited significantly higher permeability than all other groups ($p < 0.05$).

Conclusions: All tested dentifrices reduced dentin permeability under erosion conditions. Experimental dentifrices containing EGCG-chitosan nanoparticles were more efficient in reducing permeability than placebo and showed comparable effects to the commercial dentifrice.

Filing of patent application No. BR 10 2025 009040-6

Funding: CNPq- Research Productivity Grant (Process #308735/2023-4)

Table – Mean values (standard deviation) of dentin permeability (Lp) after exposure of dentinal tubules and after erosion and dentifrice treatment

Dentifrices	Dentin Condition			
	After tubule exposure (T1)		After erosion and treatment with dentifrices (T2)	
PL	0.123 (0.041)	aA	0.066 (0.039)	aB
Nchi	0.128 (0.048)	aA	0.025 (0.014)	bB
Nchi + EGCG	0.118 (0.046)	aA	0.021 (0.009)	bB
EGCG	0.139 (0.052)	aA	0.032 (0.017)	bB
ES	0.108 (0.041)	aA	0.025 (0.012)	bB

Different uppercase letters indicate significant differences between columns for intragroup analysis ($p<0.05$). Different lowercase letters indicate significant differences among rows for intergroup analysis ($p<0.05$).

https://doi.org/10.1016/j.dental.2026.03.113

102

A novel report for oral microbiota characterization

T Maravic *, C Mazzitelli, C D'Alessandro, G Palladino, D Scicchitano, S Rampelli, M Candela, U Josic, E Mancuso, A Mazzoni, L Breschi

University of Bologna, Bologna, Italy

Purpose / Aim: The oral microbiota represents a rich source of information for understanding the connections between oral health and systemic diseases. Its characterization is essential for the development of innovative therapies and the support of personalized care based on patient's conditions. However, due to its vast and complex composition, characterizing the oral microbiota in a straightforward manner that provides immediate clinical support remains challenging. Therefore, the aim of this study is to introduce a novel reporting method (Patent number 102024000020053 – Alma Mater Studiorum – University of Bologna) for the characterization of the oral microbiota, offering a more practical and effective tool for patient management.

Materials & Methods: Oral samples were collected from patients depending on their conditions. Total microbial DNA was extracted with standardized column-based protocols according to the sampled matrix (i.e. plaque, saliva or gingival swab). The V3-V4 hypervariable region of the 16S rRNA gene was PCR amplified using universal bacterial primers 341F and 785R. Amplified products were purified and indexed libraries were prepared by limited-cycle PCR using Nextera technology (Illumina) and purified again. Sequencing was performed using a 2x250bp paired-end protocol according to manufacturer's instructions (Illumina). The microbiome compositional profile was obtained for each sample, and the corresponding γ-distribution of bacterial abundances was calculated. This was then compared to a reference set of healthy γ-distributions for the oral

microbiome. This approach (protected by the aforementioned patent) enables the identification of different types of dysbiotic transitions based on specific shifts in the γ-distribution relative to the healthy reference.

Results: Based on the results of the microbiome characterization, we can detect and characterize any potential dysbiotic shift in patient's oral microbiome. We can also identify which of the characterized microbial taxa component deviates from the reference intervals. Based on the cooperative or competitive relationships between the various microbiota component, a series of bacteria associated with those identified outside the reference intervals are indicated, as possible targets to promote or contrast the observed dysbiosis.

Conclusions: The reporting method presented in this study proved to be a valuable tool for the characterization of the oral microbiota, offering simplicity, predictability, and cost-effectiveness. Further studies are required to validate its applicability across various dental settings.

https://doi.org/10.1016/j.dental.2026.03.114

103

Post-curing Methods Influence on 3D Printed Resin Properties

P Magao [1], G Mesquita [1], G Moura [1], G Mendonça [2], A Furuse [3], F Rizzante *[1]

[1] *MUSC, Charleston, USA*
[2] *VCU, Richmond, USA*
[3] *FOB-USP, Bauru, Brazil*

Purpose / Aim: This study aimed to assess the impact of different post-curing methods on the mechanical behavior of three 3D-printed dental resins after artificial aging through thermocycling, focusing on changes in flexural strength and Knoop microhardness over time.

Materials & Methods: Three 3D-printed dental resins—Crown and Bridge (Dentca), Ceramic Crown (SprintRay), and OnX (SprintRay)—were evaluated. Specimen bars (2x2x10mm) were fabricated according to manufacturers' guidelines using a Pro95 3D printer and subjected to seven distinct post-curing protocols. Flexural strength was assessed using a three-point bending test (n = 10) in a universal testing machine (OM150, Odeme), and Knoop microhardness was measured on the top surface using a microhardness tester (Micromet 5114, Buehler). All materials were tested at baseline (after 24 hours storage in water at 37ºC/ 0 cycles) and after 10,000, 30,000, and 50,000 thermocycles (5˚C–55˚C; 25 s dwell time). Three-way ANOVA was used to analyze both flexural strength and microhardness data, considering resin type, post-curing method, and thermocycling condition as factors. Tukey's post-hoc test was applied for multiple comparisons (α = 0.05).

Results: For flexural strength (Table 1), statistically significant differences were observed for all main factors: resin type, post-curing method, and number of thermocycles, as well as for all interaction effects (all $p<.001$). A general decreasing trend in flexural strength was observed with increasing thermocycling: 0 cycles > 10,000 cycles > 30,000 cycles = 50,000 cycles. Among the materials, OnX demonstrated the highest flexural strength values across conditions, while Crown and Bridge and Ceramic Crown exhibited lower and similar results. For Knoop microhardness, statistically significant differences were found for all main factors: type, post-curing method, and number of thermocycles (all $p<.001$), as well as for interaction effects between resin type and post-curing method ($p<.001$), resin type and number of thermocycles ($p<.001$), and resin type, post-curing method and number of thermocycles ($p<.001$). The general trend observed during artificial aging was an initial increase from 0 to 10,000 cycles, followed by another decrease to baseline: 0 cycles = 30,000 cycles = 50,000 < 10,000 cycles.

Conclusions: Post-curing protocols and thermocycling significantly influence the mechanical performance of 3D-printed dental resins. Flexural strength decreases progressively with age, while microhardness initially increases and then stabilizes. OnX consistently exhibits superior flexural strength compared to the other materials. These findings highlight the importance of selecting the appropriate materials and post-curing strategies to enhance the long-term stability of 3D-printed restorations under thermal aging conditions.

Resin	Curing Chamber	0 cycles	10000 cycles	30000 cycles	50000 cycles
Crown and bridge	Custom 60 minutes	138.94 (9.2)	110.9 (21.5)	109.47 (13.55)	119.02 (15.64)
Crown and bridge	Custom 120 minutes	145.6 (13.98)	118.54 (11.83)	136.29 (8.22)	129.29 (9.3)
Crown and bridge	Procure 2	116.87 (18.14)	103.45 (15.36)	115.63 (8.74)	114.32 (5.83)
Crown and bridge	Elegoo 120 minutes	151.06 (11.5)	113.47 (9.93)	99.96 (9.57)	103.93 (19.2)
Crown and bridge	Elegoo 240 minutes	143.44 (9.1)	98.01 (17.5)	129.22 (10.7)	121.39 (16.26)
Crown and bridge	Valo 120s	131.15 (14.49)	111.69 (11.16)	97.25 (25.22)	101.87 (20.23)
Crown and bridge	Valo 240s	140.76 (11.78)	114.6 (5.06)	115.69 (15.87)	111.2 (23.58)
Ceramic crown	Custom 60 minutes	175.24 (14.69)	132.76 (13.13)	110.55 (10.55)	105.89 (9.83)
Ceramic crown	Custom 120 minutes	182.64 (13.03)	138.67 (11.82)	105.63 (10.87)	107.22 (10.57)
Ceramic crown	Procure 2	167.55 (19.8)	113.94 (7.11)	100.32 (10.41)	89.25 (13.69)
Ceramic crown	Elegoo 120 minutes	173.16 (9.38)	125.81 (9.46)	109.5 (12.5)	107.86 (14.54)
Ceramic crown	Elegoo 240 minutes	192.89 (12.57)	135.51 (7.49)	107.64 (7.21)	110.17 (8.79)
Ceramic crown	Valo 120s	166.99 (20.49)	119.42 (16.41)	96.73 (14.06)	103.93 (8.75)
Ceramic crown	Valo 240s	182.23 (11.05)	133.04 (12.97)	104.27 (5.18)	100.92 (9.54)
OnX	Custom 60 minutes	182.05 (11.62)	160.48 (12.74)	143.3 (13.63)	154.25 (15.63)
OnX	Custom 120 minutes	182.3 (17.01)	146.27 (18.56)	144.27 (8.66)	155.98 (12.83)
OnX	Procure 2	183.58 (11.65)	124.98 (8.83)	125.03 (6.18)	125.12 (4.31)
OnX	Elegoo 120 minutes	176.48 (15.24)	154.38 (27.69)	144.46 (13.34)	143.47 (19.24)
OnX	Elegoo 240 minutes	199.54 (15.42)	153.76 (18.09)	139.47 (23.06)	147.45 (9.84)
OnX	Valo 120s	122.48 (7.55)	116.3 (13.14)	105.59 (17.77)	114.69 (11.47)
OnX	Valo 240s	110.75 (10.4)	124.7 (13.79)	110.29 (16.8)	102.88 (14.2)

Table 1

https://doi.org/10.1016/j.dental.2026.03.115

104

FDM with PLA: A Sustainable Dental Printing Solution

G Nima *[1], Y Gallardo [2,3], B Karayazgan [2], E Mukai [4], C Peña [3], C Sukotjo [2]

[1] *Universidad de los Andes, Santiago de Chile, Chile*
[2] *Pittsburgh university, Pittsburgh, USA*
[3] *Universidad Científica del Sur, Lima, Peru*
[4] *Universidade Sao Leopoldo Mandic, São Paulo, Brazil*

Purpose / Aim: This study aimed to assess the accuracy of fused deposition modeling (FDM) using biodegradable polylactic acid (PLA) and compare it with four resin-based additive manufacturing techniques.

Materials & Methods: A virtual model of a maxillary arch was digitally created using DentalCAD software (exocad). Ten models (n = 10) were printed for each manufacturing technologies: fused deposition modeling (FDM), stereolithography (SLA), digital light processing (DLP), liquid crystal display (LCD), and PolyJet (PJ) resulting in 50 printed cast. All printed models were digitized using an intraoral scanner (Primescan, Dentsply Sirona), and the resulting STL files were analyzed in comparison with the original digital design. This comparison was performed using Geomagic Control X (3D Systems), a specialized metrology software.

The accuracy of each model was evaluated through 3D analysis, which including both the full arch and specific regions: anterior, right posterior, and left posterior. Trueness was quantified by calculating the mean root mean square (RMS) error values between the scanned and reference models, while precision was determined by computing the standard deviation of those RMS values across the repeated prints. Additionally, color maps were produced to visually assess surface deviations.

Data for precision and trueness did not satisfy the assumptions of normality or homogeneity of variances. Therefore, a generalized linear model (GLM) was employed as an alternative to conventional parametric tests. Post hoc pairwise comparisons were conducted using the Bonferroni adjustment method to control for multiple comparisons ($P < 0.05$).

Results: FDM demonstrated overall trueness and precision comparable to SLA (Table 1), though both were lower than PJ, which showed the highest accuracy with statistically significant differences among the five methods. No significant differences were observed between FDM and SLA, or between DLP and LCD (Table 1). Regionally, PJ achieved the highest trueness and precision in all areas. While FDM showed reduced trueness in the anterior region, it performed better than DLP and LCD in posterior regions for both accuracy and precision.

Conclusions: FDM with biodegradable PLA demonstrated accuracy comparable to resin-based PJ and SLA, highlighting its potential as a sustainable alternative for dental cast fabrication.

Printing technology	Accuracy	
	Trueness	Precision
FDM	89.13 ± 7.02 B	87.17 ± 7.30 B
DLP	163.37 ± 56.06 C	143.02 ± 63.90 C
LCD	151.27 ± 52.36 C	145.02 ± 63.90 C
SLA	104.34 ± 30.92 B	103.54 ± 30.48 B
PJ	57.35 ± 17.73 A	54.92 ± 16.89 A

*Values meaning Mean ± SD in µm. ** Groups labeled with the same uppercase letter indicate no statistically significant differences (P<0.05), based on a one-way GLM followed by Bonferroni-corrected comparisons of estimated marginal means.

Table 1

https://doi.org/10.1016/j.dental.2026.03.116

105

Assessing Attachment Wear from Repeated Placement and Removal of Aligners

DL Ordaz, B Van Heel, Y Xing, Alex Fok *

Minnesota Dental Research Center for Biomaterials and Biomechanics, School of Dentistry, University of Minnesota, Minnesota, USA

Purpose / Aim: To estimate, in vitro, the material loss on attachments from repeated placement and removal of aligners over the course of an orthodontic treatment.

Materials & Methods: A 4-unit CAD model replicating the buccal half of a human molar was 3D-printed, with 4 rectangular attachments (4 mm × 2 mm × 1 mm) made of a dental resin composite (Tetric EvoCeram, Ivoclar Vivadent Inc., Schaan, Liechtenstein) later adhered to the model. The setup thus included two symmetric molars with two attachments each. Samples were tested using a reciprocating machine, custom-made to simulate the placement and removal of an aligner (Zendura FLX, Bay Materials LLC, Fremont, CA, USA) positioned opposite the model. The aligners underwent cyclic sinusoidal motion of amplitude 28 mm at a frequency of 1 Hz for a total of 5600 cycles, simulating a standard treatment duration of 1.5 years. A total of 40 aligners per set of attachments (n = 4) were used, assuming one aligner per 14-day period.The attachments were scanned before and after testing using a micro-CT (XT H 225, Nikon Metrology Inc., Brighton, MI, USA) with a resolution of 9.18 µm. Material loss was quantified by superimposing scans using Geomagic Control X (3d Systems Corporation, Rock Hill, SC, USA).

Results: Attachment loss averaged 0.041 ± 0.021 mm^3. The corners showed the greatest wear depth, ranging from 0.025 mm to 0.083 mm, with no systematic differences observed between the gingival and occlusal surfaces (Figure 1).

Conclusions: The combination of a custom-built reciprocating device to simulate aligner insertion and removal, along with high-resolution micro-CT scanning and 3D superimposition analysis, provides a reliable approach for evaluating wear in composite attachments.

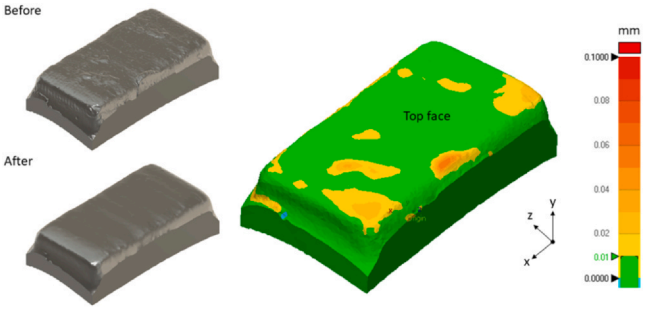

Figure 1

https://doi.org/10.1016/j.dental.2026.03.117

106

Predicting Deciduous Tooth Exfoliation Timing in Pediatric Patients Using AI

S Syed *, M Martin, J Gammichia, M Rocha, W Duncan, D Oliveira

University of Florida, Gainesville, USA

Purpose / Aim: The aim of this study was to employ proof-of-concept AI techniques to retrospectively analyze deidentified radiographs of pediatric patients aged 6-15 years to predict the timing of deciduous tooth exfoliation.

Materials & Methods: The study was approved by IRB (#202401087). A retrospective dataset of 174 deidentified periapical and bitewing dental radiographs from pediatric patients aged 6-15 years who had already undergone tooth exfoliation processing was annotated and manually segmented by two calibrated examiners and used to develop a machine learning model. We implemented a two-stage training and validation approach: first, a tooth segmentation model based on a U-Net architecture with a pre-trained ResNet18 backbone was developed to identify 52 distinct tooth classes. This segmentation model was specifically adapted for dental radiographs through several key modifications: the first convolutional layer was redesigned to process grayscale images by averaging RGB weights, skip connections were implemented to preserve spatial information critical for tooth boundary delineation, and strategic dropout was applied to prevent overfitting while maintaining fine detail capabilities. The model was trained with distributed processing across multiple GPUs using cross-validation to ensure robustness. Second, we built a specialized dental age predictor using a ResNet34 backbone for image encoding combined with a custom CNN for segmentation mask encoding, fusing these features through transformer-inspired attention layers. The model incorporated separate output heads for years and months prediction, and was trained with a composite loss function consisting of Huber loss for years (reducing outlier impact), a cyclic loss for months (handling circularity), and a total age difference penalty. We employed stratified 5-fold cross-validation with early stopping and trained for up to 200 epochs using AdamW optimization with mixed-precision arithmetic for both models.

Results: The segmentation model achieved a cross-validation Dice score of 0.73 across 5 folds, demonstrating promising accuracy in identifying and segmenting primary and permanent teeth. The age prediction model (Fig. 1) achieved a mean absolute error of 1.49

years for the year component and 2.15 months for the month component, resulting in a total age prediction error of approximately 18.51 months. Further optimization may improve clinical reliability.

Conclusions: This study demonstrates the potential of AI to enhance pediatric dental age assessment. While showing promising performance, refinement through larger datasets and model optimization could further improve accuracy. These tools may eventually support clinicians in timing interventions related to deciduous tooth exfoliation, improving orthodontic treatment planning and outcomes.

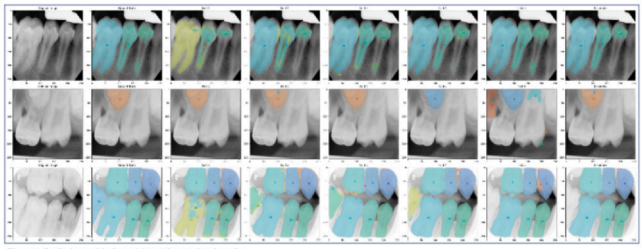

Figure 1: Predictive model after training with ground truth masks

https://doi.org/10.1016/j.dental.2026.03.118

107

Influence of glass infiltration on fatigue resistance of 5Y-PSZ zirconia

K Souza *[1], A Demachkia [1], T Campos [2], A Samran [3], MA Bottino [1], R Melo [1]

[1] *São Paulo State University, São José dos Campos, Brazil*
[2] *Universidade Federal de Pelotas, Pelotas, Brazil*
[3] *Dar Aluloom University, Riyadh, Saudi Arabia*

Purpose / Aim: To evaluate the effect of glass infiltration on 5Y-PSZ endocrowns in terms of fatigue performance and failure mode.

Materials & Methods: Forty maxillary premolars were endodontically treated and divided into four groups (n = 10) according to the glass infiltration surface of the 5Y-PSZ endocrown: no glass infiltration (Zr ctr), glass infiltration on the occlusal surface (Zr inf-occ), glass infiltration on the fitting surface (Zr inf-fit), and glass infiltration on the axial surfaces (Zr inf-axi). The samples were subjected to progressive fatigue loading (initial load of 200 N; 20 Hz). An incremental load of 100 N was applied every 10,000 cycles until failure. The fatigue failure load (FFL) and the number of failure cycles (CFF) were statistically analyzed using one-way ANOVA and the Kaplan-Meier test ($\alpha = 0.05$). Fractured samples were examined under a stereomicroscope at 25× magnification and failure modes were classified into three types: type I: Only ceramic fracture or ceramic and tooth fracture above the CEJ; type II: Ceramic and tooth fracture below the CEJ (non-repairable); type III, split fracture, ceramic and tooth split vertically (non-repairable).

Results: Fatigue failure load and number of failure cycles were significantly influenced by glass infiltration ($p < 0.05$). Zr inf-occ (1730 N) and Zr inf-axi (1750 N) exhibited significantly higher FFL values compared to Zr inf-fit (1210 N). However, no significant differences were found among Zr inf-occ (1730 N), Zr inf-axi (1750 N), and Zr ctr (1480 N). Regarding CFF, Zr inf-axi (146950 cycles) withstand significantly higher number of cycles compared to Zr inf-fit (94250 cycles), while no significant differences were observed among the other groups. Overall, 85% of the samples exhibited non-repairable fractures, regardless of the glass infiltration surface.

Conclusions: Glass infiltration on the fitting surface of zirconia endocrowns should be avoided, as it reduces fatigue resistance. In contrast, glass infiltration on the axial and occlusal surfaces can be used as a glaze without negatively affecting the zirconia.

https://doi.org/10.1016/j.dental.2026.03.119

108

Potential of silane-free and silane-containing universal adhesives on zirconia interaction

V de Witt *[1], T Scheidt [2], M Michel [2], G Schmidt [2], MF Gutierrez [1], AD Loguercio [2], JC Gomes [2]

[1] *Universidad de los Andes, Santiago, Chile*
[2] *State University of Ponta Grossa, Ponta Grossa, Brazil*

Purpose / Aim: To investigate the effect of silane-free and silane-containing universal adhesives containing 10-MDP on the micro-shear bond strength (μSBS) to zirconia ceramic, both immediately (IM) and after thermal ageing (TC), as well as to evaluate the chemical interaction with zirconia.

Materials & Methods: Yttria-stabilized tetragonal zirconia polycrystals were sectioned into blocks (n = 56), cut into segments, and sintered. The segments were randomly assigned into seven experimental groups (n = 8 per group) based on the following independent variables: Surface treatment: Alloy Primer (Control), Ambar (AMB), Ambar Universal APS (AMU), Ambar Universal APS Plus (AMU+), Adper Single Bond 2 (SB2), Scotchbond Universal (SBU), and Scotchbond Universal Plus (SBU+); Time: Immediate (24 h) or after 10,000 thermocycles. Additionally, sixteen zirconia sections (n = 2 per group) were subjected to micro-Raman spectroscopy to assess the chemical interaction after bonding procedures. After surface treatment, cylinder-shaped matrices were filled with resin cement and light-cured. All specimens were tested for μSBS at a crosshead speed of 1.0 mm/min. Data were analyzed using Kruskal-Wallis and Mann-Whitney tests ($\alpha = 0.05$).

Results: At the immediate time point, AMU+ and SBU+ exhibited the highest μSBS values, significantly higher than those of the control, AMB, and SB2 groups ($p < 0.05$). After thermocycling, all groups showed a significant decrease in μSBS. However, AMU, AMU+, SBU, and SBU+ maintained significantly higher values compared to the control, AMB, and SB2, which dropped to 0 MPa ($p < 0.05$). Raman analysis confirmed chemical interaction between the adhesives (AMU, AMU+, SBU, SBU+) and the zirconia surface.

Conclusions: Universal adhesives containing 10-MDP, with or without silane, demonstrated promising bonding efficacy and chemical interaction with zirconia, particularly in maintaining bond strength after artificial aging.

This project was funded by ANID through Initation Fondecyt grant number 11221070

https://doi.org/10.1016/j.dental.2026.03.120

109

Lithium-doped bioactive glass on biological-mechanical properties of universal adhesives

A Montebruno *[1], R Aliaga-Galvez [1], F Montiel [1], H Plaza [2], R Castro [2], MC Inostroza [1], R Ñaupari-Villasante [3], AD Loguercio [3], MF Gutierrez [1]

[1] *Universidad de los Andes, Santiago, Chile*
[2] *University of Chile, Santiago, Chile*

[3] *State University of Ponta Grossa, Ponta Grossa, Brazil*

Purpose / Aim: This study evaluated the effects of addition of lithium-doped bioactive glass microparticles (μBGLi) into a universal adhesive system on its biological properties such antimicrobial activity (AMA) and cytotoxicity (CTX), as well as mechanical properties such Knoop microhardness (KHN) and in vitro degree of conversion (v-DC),

Materials & Methods: μBGLi was added to a universal adhesive at different concentrations (0% [control, commercial adhesive]; 5, and 10 wt%). The AMA was evaluated against Streptococcus mutans, and CTX was assessed using the GMSC cell-line. For KHN and v-DC, specimens were tested after 24 hours (24h) and 28 days (28d) of storage in water. Data were analyzed statisticallly ($\alpha = 0.05$).

Results: The addition of 5% of μBGLi increase AMA ($p < 0.05$), while CTX remained unchanged in adhesives containing μBGLi ($p > 0.05$). KHN remained stable with the addition of 5% and 10% of μBGLi at both 24h and 28d, but showed significantly higher values compared to the control after 28d ($p < 0.05$). v-DC did not change with the incorporation of μBGLi.

Conclusions: The addition of μBGLi in concentrations up to 5 wt % into a universal adhesive can enhance antimicrobial activity without biological hazards, without compromising mechanical properties.

https://doi.org/10.1016/j.dental.2026.03.121

110

Sandblasting effect on roughness surface and adhesive properties to dentin

F Bustos *[1], R Ñaupari-Villasante [2], L Hilgert [3], F de Oliveira [4], R Falacho [5], JC Ramos [5], MF Gutierrez [1], AD Loguercio [2]

[1] *Universidad de los Andes, Santiago, Chile*
[2] *Universidade Estadual de Ponta Grossa, Ponta Grossa, Brazil*
[3] *Universidade de Brasília, Brasilia, Brazil*
[4] *Universidade de Aveiro, Aveiro, Portugal*
[5] *Universidade de Coimbra, Coimbra, Portugal*

Purpose / Aim: This study evaluated the effect of different sandblasting particles and techniques on dentin surface roughness and the longevity of the adhesive properties of a universal adhesive system.

Materials & Methods: Surface roughness analysis was performed using 3D optical profilometry on dentin discs obtained from 10 sound molars (n = 10), each divided into the following groups: Control (no sandblasting), dry sandblasting (25 μm and 50 μm aluminum oxide), and wet sandblasting (29 μm and 53 μm aluminum oxide, and bioglass). For bond strength (BS) and nanoleakage (NL) tests, 96 sound third molars were assigned to experimental groups followed by the application of Scotchbond Universal Plus using either the etch-and-rinse or self-etch strategy (n = 8), evaluated immediately and after thermocycling (2500 cycles).

Results: Surface roughness analysis was performed using 3D optical profilometry on dentin discs obtained from 10 sound molars (n = 10), each divided into the following groups: Control (no sandblasting), dry sandblasting (25 μm and 50 μm aluminum oxide), and wet sandblasting (29 μm and 53 μm aluminum oxide, and bioglass). For bond strength (BS) and nanoleakage (NL) tests, 96 sound third molars were assigned to experimental groups followed by the application of Scotchbond Universal Plus using either the etch-and-rinse or self-etch strategy (n = 8), evaluated immediately and after thermocycling (2500 cycles).

Conclusions: It was concluded that sandblasting increased dentin roughness, and its impact on adhesion significantly varied according to particle size/moisture and the adhesive strategy used, with no evident advantage in long-term performance.

Funding:
Conselho Nacional de Desenvolvimento Científico e Tecnológico (CNPq) - 304444/2025-1; Coordenação de Aperfeiçoamento de Pessoal de Nível Superior (CAPES) - Code 001.

https://doi.org/10.1016/j.dental.2026.03.122

111

Determining the concentration of TiO2 incorporation into Biosilicate-enriched bleaching gels

B Santos [1], V Hutema [2], M Queiroz [2], G Santos [1], M Trevelin [3], A Lima [2], R Dascanio [1], V Cavalli [1], M Kury *[2]

[1] *University of Campinas, Piracicaba, Brazil*
[2] *Paulista University, São Paulo, Brazil*
[3] *Federal University of São Carlos, São Carlos, Brazil*

Purpose / Aim: To determine the optimal concentration of titanium dioxide (TiO2) to be incorporated into experimental bleaching gels enriched with Biosilicate (BioS)

Materials & Methods: Experimental gels composed of carboxymethylcellulose, 10% BioS, and 1%, 2%, or 3% TiO2 were mixed with hydrogen peroxide (HP) and subjected or not to violet LED light. The gels were characterized through digital titration and photocatalytic activity analysis. Subsequently, bovine enamel-dentin discs were randomly assigned to groups (n = 10) based on bleaching protocols: 35% HP (commercial), 6%HP, 6%HP + BioS, 6%HP + BioS + 1%TiO2, 6%HP + BioS + 2%TiO2, and 6HP% + BioS + 3% TiO2, with or without LED irradiation. Three bleaching sessions of 30 minutes each were performed at 7-day intervals, with specimens stored in artificial saliva among sessions. The whiteness index change (ΔWID) was measured using a hand-held spectrophotometer 14 days elapsed from bleaching and submitted to two-way ANOVA and Tukey's test ($\alpha = 5\%$).

Results: Irradiation of 6%HP with LED significantly increased the ΔWID; however, it did not eliminate the significant difference compared to 35% HP with LED. Among the light-irradiated groups, the only gels that rendered ΔWID without significant differences to 35%HP were 6HP% + BioS + 1%TiO2 and 6HP% + BioS + 2%TiO2. Analysis of HP decomposition revealed that BioS enhanced HP consumption, and this effect was influenced by the presence of TiO_2. However, this outcome was not affected by time, light irradiation, or TiO_2 concentration. In contrast, photocatalytic activity was influenced by both light irradiation and TiO_2 concentration, with the 6% HP + BioS + 1%TiO_2 formulation exhibiting the highest photocatalytic performance among the tested groups.

Conclusions: BioS increased HP decomposition in the presence of TiO_2, independent of light or TiO_2 concentration. The incorporation of 1% TiO_2 into BioS-enriched bleaching gels enhanced both bleaching efficacy and photocatalytic activity.

https://doi.org/10.1016/j.dental.2026.03.123

112
Deep Margin Elevation on Upper Incisors: Mechanical Behavior and Microleakage

E Grassi *[1], G Andrade [2], R Machry [3], H Velho [4], L Valandro [5], C Casarini [1], A Borges [1], G Saavedra [1]

[1] *São Paulo State University (UNESP), São José dos Campos, Brazil*
[2] *Private Practice, Cascavel, Brazil*
[3] *Universidade Federal de Minas Gerais (UFMG), Belo Horizonte, Brazil*
[4] *Private Practice, Santa Maria, Brazil*
[5] *University of Santa Maria (UFSM), Santa Maria, Brazil*

Purpose / Aim: This study evaluated the stress distribution, fatigue behavior, and marginal quality of endodontically treated maxillary central incisors, restored with lithium disilicate glass-ceramic full crowns and fiberglass posts, in the absence of a ferrule, varying the presence and location of Deep Margin Elevation (DME).

Materials & Methods: A 2×3 factorial design was used: two levels for elevation (with [E], without [SE]) and three locations (mesial [P], buccal [V], lingual [L]). 120 bovine roots were used for the fatigue test (n=10) and for the marginal leakage test (n=10). The fatigue test was performed using the stepwise stress method (10,000 cycles/step; 50 N load/step; 20 Hz; 100 N initial load) until fracture. The failure mode was evaluated using stereomicroscopy and recorded with a Nikon Z7 camera (105mm F/2.8 macro lens). For the marginal quality test, thermal aging (6,000 cycles at 5–55ºC) and mechanical aging (100 N for 100,000 cycles) were performed. After cycling, the specimens were immersed in dye for 24 hours and sectioned vertically and horizontally for evaluation under stereomicroscopy. Stress distribution was evaluated using finite element analysis. For this purpose, the groups were reproduced in 3D models and analyzed using engineering simulation software. The models were considered isotropic, linear, and homogeneous, except for the fiberglass post, which was considered orthotropic. An axial load (100 N, 30°) was applied to the lingual fossa of the incisors. Stress concentration in the restoration, interfaces, and dental structure was analyzed using the Maximum Principal Stress criterion.

Results: SEV and EL showed the best fatigue performance (FFL ≥ 790 N; CFF > 140,000), while EV had the lowest values (FFL = 535 N; CFF = 87,233). EP, SEP, and SEL had intermediate results, with EP also comparable to EL. Marginal microleakage was highest in SEL (1.65 ± 0.54),but not significantly different from EL (1.47 ± 0.53). SEV (1.07 ± 0.46) and EV (0.77 ± 0.27) were similar, as were SEP (1.47 ± 0.63) and EP (1.41 ± 0.31). EV showed significantly lower infiltration than SEL, EL, and EP. At the cement–dentin interface, SEP had the highest stress (9.64 MPa), while EP showed the highest stress on the subgingival dentin surface (6.94 MPa).

Conclusions: The EV group showed low fatigue performance and high dentin stress but fewer catastrophic failures and minimal microleakage, likely due to shrinkage.

https://doi.org/10.1016/j.dental.2026.03.124

113
Introducing bioactivity to (PEEK) /bioactive glass for use as implant

B Alolayani *, A Agha, M Patel, N Karpukina

QMUL, London, United Kingdom

Purpose / Aim: To introduce bioactivity to polyether-ether-ketone (PEEK), an inert polymer, by coating it with bioactive glass, using a grit blasting technique. This will potentially improve the implant material's osseointegration with bone.

Materials & Methods: The preliminary study involved BioMinF glass abrading the length of rectangular PEEK samples (Goodfellow, UK, 20 x 10 x 2 mm3; n=6 per test) either twice or 12 times using the air abrasion instrument (Aquacare) - grit blast technique. Conditions included air abrasion handpiece at a distance of 3 mm, a velocity of 0.5 mm/sec, and either a high pressure of 4 bars or low pressure of 0.5 bars, The samples were then immersed in individual bottles containing tris-buffer solution (10 ml) or simulated body fluid (SBF, 10 ml) for seven days. The samples were characterized using FTIR, XRD and SEM-EDX, before and after abrasion, and after 7 days of immersion. These techniques were also used to analyze BioMinF alone.

Results: BioMinF showed an amorphous structure (XRD). The FTIR of PEEK samples following air abrasion at low pressure with BioMinF and following immersion in both solutions, showed evidence of surface alteration. Air abrading at high pressure showed no evidence of surface alteration. The results of SEM-EDX confirmed that there was glass embedded in the PEEK samples and possible apatite formation at low pressure. Interestingly at high pressure there appeared to be more glass embedded in PEEK's surface and apatite formation.

Conclusions: These interesting results confirmed that air abrading PEEK samples (12 times), at low and high pressure, with bioactive glass particles altered PEEK's surface. SEM-EDX confirmed that there was glass embedded in the PEEK samples and possible apatite formation.

https://doi.org/10.1016/j.dental.2026.03.125

114
Occlusal Correction influence on Crack Propagation in CAD/CAM Materials

A Baldi, L Giordano, A Comba, C Rolando, T Rossi, R Ahmed, L Yang, N Scotti *

University of Turin, Turin, Italy

Purpose / Aim: Occlusal correction techniques play a critical role in determining the mechanical behavior, wear resistance, and durability of metal-free CAD/CAM materials. This in vitro study aimed to analyze the effect of different occlusal corrections on crack initiation, crack propagation, wear, and surface roughness in lithium disilicate, cubic zirconia, and hybrid ceramic materials used for chairside restorations. The purpose was to determine the crack growth pattern and wear behavior of these ceramic materials under various occlusal corrections and cyclic fatigue.

The null hypothesis tested was that there is no difference between the CAD/CAM materials and different occlusal corrections on crack initiation, crack propagation, wear, and surface roughness during fatigue.

Materials & Methods: Four types of monolithic CAD/CAM materials (Initial LiSi Block, Cerasmart270, IPS e.max CAD, Katana Zirconia Block STML) were selected to mill identical flat-surface single crown restorations that were cemented on replicated acrylic preparations. The crowns were cleaned and polymerized using an LED light-curing device under 1 kg pressure for 60 seconds per side.

Specimens of each material were randomly divided into three groups:

1. No intervention (control specimens),
2. Occlusal correction using a fine football-shaped diamond bur,
3. Occlusal correction using a fine football-shaped diamond bur followed by polishing.

A chewing simulator (SD Mechatronik) performed fatigue cycling mechanical aging in wet conditions for 250,000 cycles with alternating temperatures. Fatigue damage as crack initiation and propagation was evaluated using optical coherence tomography at baseline and after each cycle and confirmed by SEM analysis. Wear and surface roughness were analyzed using 3D profilometry and SEM. Data were statistically analyzed using a three-way ANOVA test and post-hoc Tukey test ($p < 0.05$), conducted with STATA software.

Results: Cracks formed and propagated more in lithium disilicate (LiSi) compared to other materials. Occlusal corrections, particularly in group 3 (bur + polishing), significantly influenced crack development. Regarding wear, Cerasmart exhibited the highest wear, while zirconia showed the least ($p < 0.0001$). LiSi and IPS e.max CAD had intermediate wear, with IPS exhibiting higher rates ($p = 0.021$). Surface roughness did not differ significantly across materials or treatments ($p > 0.05$). Polishing did not significantly impact wear ($p = 0.89$), and the number of cycles did not affect wear or roughness significantly ($p = 0.111$).

Conclusions: The null hypothesis can be rejected. Both the type of CAD/CAM material and the occlusal correction technique significantly affect crack formation, propagation, and wear behavior.

https://doi.org/10.1016/j.dental.2026.03.126

115

Effect of Sintering Duration on the Color of Multi-Layered Zirconia

M Mutluay *[1,2], A Tezvergil-Mutluay [1,2]

[1] *Department of Oral and Maxillofacial Diseases, Faculty of Medicine, University of Helsinki, Helsinki, Finland*
[2] *Institute of Dentistry, University of Turku, Turku, Finland*

Purpose / Aim: Accelerated sintering protocols offer significant time savings in the fabrication of zirconia restorations. This pilot study investigated the effect of two sintering durations-90 minutes and 18 minutes-on the color parameters of three multilayer zirconia materials: Katana™ HTML Plus, STML, and UTML (Kuraray Noritake Dental Inc., Japan).

Materials & Methods: Anatomically shaped maxillary anterior crowns were fabricated from each zirconia type using a standardized STL design (n = 5 per group). Each crown was sintered using both a standard (90-minute) protocol in the Programat® CS4 (Ivoclar, Liechtenstein) and an accelerated (18-minute) protocol in the CEREC® SpeedFire (Dentsply Sirona, Germany) furnace. Color measurements (L, a, b) were obtained from the incisal, middle, and cervical layers using a VITA Easyshade® spectrophotometer (VITA Zahnfabrik, Germany). CIE ΔEab values were calculated to quantify color differences between sintering protocols. Descriptive statistics and multifactorial ANOVA were used to assess the influence of sintering time, material, and crown layer on the color parameters.

Results: ΔEab values between sintering protocols ranged from 2.20 to 7.06. The largest color difference was observed in the middle layer of Katana HTML Plus (ΔEab = 7.06), while the smallest was in the incisal layer of UTML (ΔEab = 2.20). ANOVA revealed statistically significant effects of material type and crown layer ($p < 0.05$) on all color parameters. Sintering duration also had a significant effect on L, a, and b values, with more pronounced differences observed in HTML Plus and STML.

Conclusions: Accelerated sintering alters the color outcomes of multilayer zirconia crowns, particularly in Katana HTML Plus and STML. These findings suggest that material-specific responses to fast sintering protocols should be considered in clinical shade matching, especially in esthetically demanding cases. Further studies are warranted to confirm these trends and evaluate their clinical relevance.

https://doi.org/10.1016/j.dental.2026.03.127

116

Reduced dentin etching time in cervical restorations: 18-month clinical trial

A Toutin *[1], A Beniscelli-Vásquez [1], N Amo-Nicolás [1], M Rodriguez [1], R Aliaga-Gálvez [1], S Cavagnaro [1], R Iriarte [1], AD Loguercio [2], MF Gutiérrez [1]

[1] *Universidad de los Andes, Santiago, Chile*
[2] *Universidade Estadual de Ponta Grossa, Ponta Grossa, Brazil*

Purpose / Aim: To evaluate the effect of reduced dentin etching time on the 18 months clinical performance of two universal adhesive systems used as etch-and-rinse application mode in non-carious cervical lesions (NCCLs).

Materials & Methods: The local scientific ethics committee reviewed and approved the study protocol and consent form (protocol CEC2024055). 144 restorations were randomly placed in 36 subjects (17 male and 19 female) according to the following groups (n = 36): SUP5 (Scotchbond Universal Plus adhesive on dentin etched for 5 seconds); SUP15 (Scotchbond Universal Plus adhesive on dentin etched for 15 seconds); GBU5 (Gluma Universal Bond adhesive on dentin etched for 5 seconds); GBU15 (Gluma Universal Bond adhesive on dentin etched for 15 seconds). For all groups, the enamel was etched for 15s. All groups were light-cured for 10s/1,000 mW/cm^2. A resin composite was placed by applying three increments and each one was light cured for 20s/1,000 mW/cm^2. The restorations were finished immediately with fine diamond burs and polishers. The restorations were evaluated at baseline and after 18 months by using the FDI criteria. The following outcomes were evaluated: retention, marginal staining, marginal adaptation, post-operative sensitivity and recurrence of caries. The differences among the groups were calculated using Friedman repeated measures analysis of variance rank ($\alpha = 0.05$).

Results: The recall rate was 100% at 6- and 18-months. Ten restorations were lost at six months (two for SUP5, two for SUP15, three for GBU5 and three for GBU15). After 18-month recall, additionally, five restorations were lost (one for SUP15, one for GBU5 and three for GBU15). According to FDI criteria, the 18-month retention rates (95% confidence interval) were 94.4% for SUP5, 91.7% for SUP15, 88.9% for GBU5 and 83.3% for GBU15. Ten restorations (one for SUP5, four for SUP15, two for GBU5 and three for GBU15) showed minor marginal staining, and 32 restorations (six for SUP5, six for SUP15, eleven for GBU5 and nine for GBU15) presented minimal marginal adaptation defects. No significant differences among the groups were observed in all clinical parameters evaluated ($p > 0.05$).

Conclusions: The reduced dentin etching time did not improve the clinical performance of resin restorations in NCCLs after 18 months. Therefore, a reduced dentin etching time could be used in adhesive clinical procedures, reducing chair time.

Funding: This project was funded by ANID through Initiation Fondecyt grant number 11221070.

https://doi.org/10.1016/j.dental.2026.03.128

117

Polishability of novel CAD/CAM fiber-reinforced resin composites

R Babaier *[1], E Sailynoja [2,3]

[1] *King Saud University, Riyadh, Saudi Arabia*
[2] *Department of Biomaterials Science and Turku Clinical Biomaterial Center -TCBC, Institute of Dentistry, University of Turku, Turku, Finland*
[3] *Research Development and Production Department, Stick Tech Ltd-a GC Europa AG Company, Turku, Finland*

Purpose / Aim: This study investigates the effectiveness of three polishing systems on the surface roughness and gloss of three reinforced CAD/CAM composites, one of which is an experimental short fiber-reinforced composite.

Materials & Methods: Ninety plate-shaped specimens were prepared from three resin composites: experimental short fiber-reinforced composite (SFRC), TRINIA (TR) and Lava Ultimate (LU). The surface roughness and gloss measurements for all the specimens were determined at baseline. Then, material specimens were divided into three polishing groups (n = 10): Sof-Lex diamond polishing system (SOF), OptraGloss polishing system (OPT), and silicon carbide papers (SIC). The surface roughness, gloss and SEM images were determined for each specimen at baseline and after polising. Two-way ANOVA and Games-Howell post hoc tests were performed to determine the effectiveness of polishing on roughness and gloss on each material ($p < 0.05$).

Results: Polishing significantly reduced surface roughness and increased gloss (Table 1) in CAD/CAM composites with overall Ra ranging between 0.121 and 3.635 μm and gloss ranging from 5.9 to 124.9 GU ($p = 0.00$). SFRC and LU showed smoother surfaces with SOF and SIC ($p = 0.00$), while LU exhibited higher gloss with OPT. TR had the roughest surfaces and lowest gloss, especially with OPT ($p = 0.00$).

Conclusions: Polishing the new short fiber reinforced composite (SFRC) showed comparable surface qualities to the well-established nano ceramic composite (LU), with slight differences depending on the polishing system applied. The study found that SFRC and LU composites achieved smoother surfaces with SOF and SIC polishing systems, while LU composites exhibited higher gloss with OPT. In contrast, TR composites had the roughest surfaces and lowest gloss, particularly with OPT. These findings highlight the importance of selecting appropriate polishing systems to optimize the surface properties of different composite materials.

Table 1. Surface roughness (μm) of study materials (SFRC, LU, TR) before and after three polishing systems (SOF, OPT and SIC).

	Ra (μm)											
Materials	SFRC				LU				TR			
Polishing system	**Pre-polishing**		**Post-polishing**		**Pre-polishing**		**Post-polishing**		**Pre-polishing**		**Post-polishing**	
	Mean	SD	Mean	SD	Mean	SD	Mean	SD	Mean	SD	Mean	SD
SOF	3.264^{aA}	0.32	0.121^{aB}	0.03	3.235^{aA}	0.68	0.792^{aC}	0.23	3.999^{aD}	1.07	0.548^{aE}	0.16
OPT	3.307^{aA}	0.34	0.395^{bB}	0.10	3.597^{aA}	0.46	0.122^{bC}	0.03	4.114^{aD}	0.85	3.635^{bE}	0.25
SIC	3.287^{aA}	0.46	0.124^{aB}	0.01	3.599^{aAC}	0.47	2.591^{cD}	0.28	4.071^{aEC}	0.83	0.359^{cF}	0.04

For each column, different *lowercase letters* indicate statistically significant differences between polishing groups within one material ($p < 0.05$). For each row, different *uppercase letters* indicate statistically significant differences between the study groups ($p < 0.05$). Pairwise comparisons showed statistically significant differences between all pre- and post-polishing for each pair (Bonferroni, $p = 0.000$).

https://doi.org/10.1016/j.dental.2026.03.129

118

Comparison of Endogenous MMPs on Deciduous Dentin vs Permanent Dentin

R Seseogullari-Dirihan *[1], A Tezvergil-Mutluay [2]

[1] *Marquette University, School of Dentistry, Milwaukee, USA*
[2] *University of Turku, Institute of Dentistry, Turku, Finland*

Purpose / Aim: Matrix Metalloproteinases (MMPs) are crucial enzymes for tissue remodeling, including dentin, dental pulp and periodontal tissues. While their distribution and roles in permanent teeth have been extensively studied, there's less information specifically comparing their distribution in deciduous (primary) and permanent teeth.

Materials & Methods: To determine the extractable MMPs, dentin. powder was prepared from permanent molars' coronal dentin (CD) & root dentin (RD) and deciduous molars' coronal dentin (DCD) after removing enamel and pulp tissue. Dentin fragments were dipped into liquid nitrogen for 5 min and then pulverized using a steel mortar. The powder was completely demineralized with 10 wt % H3PO4 for 10 minutes at 4°C and then neutralized with 70 μl 4 N NaOH. Demineralized dentin powder (100 mg/sample, n = 5) was incubated in 1.8 mL of extraction buffer for 24h at 4°C. Aliquots of specimens were concentrated with centrifugal concentrator tubes down to a volume of 100 μL. Aliquots of media were used for measuring the quantity of selected MMPs by means of a fluorescent microsphere immunoassay (Human MMP-MAP multiplex kit, R&D Systems, Inc., Minneapolis, MN, USA). The aliquots were taken from the wells in replicate with an MMP bead cocktail according to manufacturer's instructions. The total amount of MMP -1, -2, -3, -7, -8 and -9, -10, -12, -13 was measured by operating a multiplex analyst device and supported software and calculated with known concentration were fitted with a 5-point fitting curve. Data were analyzed with ANOVA at $\alpha = 0.05$

Results: The amount of extracted MMP-2 ranged from 2000 to 14000 pg/mg was significantly higher than other MMPs (-1, -3, -7, -8, -9, -10, -12, -13) for all experimental groups while MMP-7 level (8-20 pg/mg) was the lowest for all ($p < 0.05$). Among the groups, deciduous coronal dentin showed the highest quantity for each MMP compared to permanent coronal and root dentin($p < 0.05$). The level of extracted MMP-9 was not detectable as in the range of used detection kit (Table 1).

Conclusions: The result of our present study indicated that screened MMPs' concentration in deciduous coronal dentin is significantly higher than permanent dentin in both crown and root since deciduous teeth shows higher potential of remodeling.

Table – Surface morphology of the groups evaluated.

Groups	Surface morphology
3Y-TZP	Relatively smooth ceramic surface but exhibited fine linear patterns from the cutting process, reflecting the movement of the diamond disk.
3Y-TZP + APA	The ceramic surface appeared roughened with a uniformly textured, matte finish due to the APA. The APA created micro-pits and peaks, increasing surface area.
3Y-TZP + APA + benchmark primer	The ceramic surface retained the roughened texture from APA, with subtle changes in topography.
3Y-TZP + APA + novel binding promoter	The ceramic surface became more textured and exhibited enhanced micro-retention features.
3Y-TZP + APA + benchmark primer + resin cement	The surface looked highly polished, very smooth, free of irregularities.
3Y-TZP + APA + benchmark primer + resin cement	The surface looked highly polished, very smooth, free of irregularities.

https://doi.org/10.1016/j.dental.2026.03.130

119

Dopamine mechanism and potential in treating dentin hypersensitivity

J de Lima Marques [1], M Falcon *[2], W Vieira-Júnior [2], K Rischka [3], F Aguiar [2]

[1] *Universidade Federal de Rio Grande do Norte, Natal, Brazil*
[2] *Universidade Estadual de Campinas, Piracicaba, Brazil*
[3] *Fraunhofer Institute for Manufacturing Technology and Advanced Materials, Bremen, Germany*

Purpose / Aim: Inspired by mussel chemistry, catechol-containing molecules have demonstrated potential in dental applications by binding to demineralized dentin and promoting mineral formation. This study investigated the adhesion mechanism and dentin remineralization of dopamine, a catechol-containing molecule, as well as its effect on dentin morphology and permeability following an erosive/abrasive cycling protocol.

Materials & Methods: Initially, dentin samples were demineralized and immersed in phosphate-buffered saline (PBS) containing dopamine, dopamine + laccase, pyrocatechol + laccase, laccase alone, or PBS only, except for the untreated group (n = 5). Samples were then immersed in a calcium- and phosphate-rich remineralizing solution for 10 days with daily changes. The effects of the treatments were evaluated using scanning electron microscopy (SEM) and X-ray photoelectron spectroscopy (XPS).

Separately, dentin hypersensitivity was simulated structurally in human dentin discs by applying EDTA for 5 minutes. After assessing maximum dentin permeability (initial), specimens were randomly assigned to: distilled water (control), 0.05% NaF solution, a commercial solution (Colgate® Sensitive Pró-Alívio™), or an experimental solution containing dopamine + laccase (n = 15). An erosive/abrasive cycling protocol was applied, consisting of 0.3% citric acid immersion for 2 min four times/day, brushing for 5 s twice/day, and treatment application for 5 min twice/day. Dentin permeability was reassessed (final), and percentage permeability at each time was calculated relative to maximum permeability (%Lp) and analyzed using generalized linear mixed models ($\alpha = 0.05$). Surface effects were analyzed by SEM.

Results: SEM images, supported by XPS, revealed that samples treated with dopamine, dopamine + laccase, and pyrocatechol + laccase exhibited complete dentin surface coverage with mineral deposits and mineral formation in dentinal tubule walls. Conversely, the untreated group and those treated with laccase or PBS alone showed partial tubule occlusion and minimal surface mineral deposition. Following abrasive-erosive cycling, all groups showed a significant reduction in permeability ($p < 0.05$), but no statistically significant differences were detected between groups ($p = 0.6082$). However, smaller tubule diameters were observed in samples treated with Colgate® Sensitive Pró-Alívio™ and the experimental dopamine + laccase solution.

Conclusions: Overall, dopamine's adherence and mineralization capability are attributed to its catechol group, while laccase only accelerates and mediates dopamine polymerization reaction. However, under the abrasive-erosive conditions proposed, dopamine exhibited limited protective effects, not significantly reducing dentin permeability as well as the other treatment' solutions tested.

https://doi.org/10.1016/j.dental.2026.03.131

120

Characterization of MIH Using Raman Spectroscopy, SEM and OCT Imaging

A Comba *[1], A Baldi [1], C Rolando [1], C Orsello [1], C Mazzitelli [2], T Maravic [2], M Cadenaro [3], A Mazzoni [2], N Scotti [1]

[1] *University of Turin - Department of Surgical Sciences, Turin, Italy*
[2] *University of Bologna - Dibinem, Bologna, Italy*
[3] *University of Trieste, Trieste, Italy*

Purpose / Aim: Molar Incisor Hypomineralization (MIH) is a condition characterized by a qualitative enamel defect of systemic origin. It typically involves one to four permanent first molars and is often associated with morphological changes in the incisors. This study aimed to investigate, through Raman spectroscopy and scanning electron microscopy (SEM), the biochemical and structural characteristics of enamel affected by MIH compared to healthy enamel. Additionally, the study considers the role of Optical Coherence Tomography (OCT) as a non-invasive imaging tool for in vivo assessment and severity grading of MIH lesions to facilitate the treatment decision making process.

Materials & Methods: Samples of enamel affected by Grade II and III MIH, following the "Charting Criteria Lesion Extension" (Ghanim et al., 2017), were collected from patients referred to the department Pediatric Dentistry of the University of Turin. During restorative procedure, from each tooth, 2 × 2 mm enamel samples were collected from the affected area, including sound margins. Samples were stored at 4°C and analyzed with Raman spectroscopy using a monochromatic laser (λ: 1064 nm) and a BTC284N spectrometer (range: 100–2500 cm^{-1}, resolution: 10.56 cm^{-1}) coupled with a CCD sensor. Signal intensity was measured at the hydroxyapatite reference peak (960 cm^{-1}). The same samples underwent morphological evaluation with a Phenom™ XL G2 SEM. In addition, in vivo OCT images were acquired from patients selected for the study in order to correlate MIH severity with the internal appearance of the affected enamel tissues.

Results: A statistically significant difference ($p < 0.05$) in peak intensity at 960 cm^{-1} was observed between healthy and MIH-affected samples, with the latter showing lower intensities, indicating reduced mineral content. SEM images revealed that MIH enamel surfaces were non-homogeneous with circular fenestrations, contrasting with the intact, regular surfaces of healthy enamel. Finally, OCT imaging revealed differences in light scattering and hyperreflectivity patterns that reflected lesion severity and depth.

Conclusions: Raman spectroscopy and SEM are effective tools to qualitatively and quantitatively characterize changes in enamel affected by MIH. When combined with OCT imaging for in vivo assessment, these methods enhance diagnostic precision, severity grading, and clinical understanding. Together, they serve as a foundation for further investigation into targeted prevention and remineralization strategies for MIH-affected individuals.

https://doi.org/10.1016/j.dental.2026.03.132

121

Wear of Milled and 3D-Printed Resin-Based Materials in Acidic Environments

L Giordano *, A Baldi, L Yang, F Bellusci, A Comba, D Gaetano, T Rossi, N Scotti

University of Turin, Turin, Italy

Purpose / Aim: This in vitro study aimed to evaluate the three-body wear behavior of various milled and 3D-printed resin-based

dental materials when exposed to different acidic environments, utilizing the ACTA wear simulation machine. The null hypotheses tested were that all materials would exhibit comparable resistance to abrasive wear and that no significant differences would be observed between the acidic mediums.

Materials & Methods: Five different CAD/CAM restorative materials were selected: two milled composites (Grandio blocs, VOCO; CERASMART, GC), one milled polymer-infiltrated ceramic network (VITA Enamic, VITA), one 3D-printed composite (IRIX PLUS, DWS), and one 3D-printed resin-based ceramic (IRIX MAX, DWS). All specimens were fabricated in a standardized squared shape with 2 mm thickness. Milled specimens were sectioned from prefabricated blocks using a low-speed diamond saw under water cooling and subsequently polished with silicon carbide papers of increasing grit sizes. For the additive-manufactured materials, STL files of reference geometries were generated from scanned milled specimens and printed using a TSLA 3D printer, followed by appropriate post-processing protocols. Each material group was divided and immersed in one of three test mediums: distilled water (control), Red Bull, and synthetic gastric acid solution, representing different pH environments. Specimens underwent three-body wear testing in the ACTA machine for two intervals—100,000 and 200,000 cycles. Post-fatigue analysis involved volumetric wear measurement and surface roughness evaluation using a high-resolution laser scanning system. Microstructural surface changes were further characterized by scanning electron microscopy (SEM). Statistical analysis was performed using one-way ANOVA and Tukey's post-hoc test, with a significance level set at $p < 0.05$.

Results: The 3D-printed materials, IRIX MAX and IRIX PLUS, exhibited significantly lower volumetric wear compared to their milled counterparts. However, they demonstrated higher surface roughness following fatigue cycles. Statistically significant differences were found between the acidic environments and the neutral control group ($p < 0.05$), indicating that both Red Bull and gastric acid increased material degradation. No significant differences were observed between the two acidic mediums.

Conclusions: The results indicate that both material composition and environmental pH significantly influence wear performance. The null hypotheses were therefore rejected: different materials displayed varied resistance to wear, and the acidic mediums produced differential effects compared to water. Additively manufactured materials may offer enhanced volumetric wear resistance but with potential trade-offs in surface quality.

https://doi.org/10.1016/j.dental.2026.03.133

122

Impact absorption of conventional, reinforced-EVA and 3D-printed-mouthguards in veneered central-incisors

T Queiroz *[1], JP Tribst [2], LH e Borro [1], A Borges [1], T Paes-Junior [1]

[1] *Institute of Science and Technology of Sao Jose dos Campos, Sao Jose dos Campos, Brazil*
[2] *Academic Center for Dentistry Amsterdam (ACTA), Amsterdam, Netherlands*

Purpose / Aim: This in vitro study evaluated the impact-absorbing behavior of three mouthguards (MGs): conventional EVA (CV), EVA reinforced with a polyamide mesh (RF), and a 3D-printed MG (3D-P) on the dentoalveolar region of upper central incisors restored with ceramic veneers.

Materials & Methods: A skull model was printed in Spin Red resin (Quanton 3D) and the teeth were fabricated individually in Resilab Clear resin (Wilcos). Epoxy-G10 was used for central incisors and were prepared for IPS Empress CAD HT ceramic veneers (Ivoclar Vivadent), and the periodontal ligament was simulated with an elastomeric material. Strain gauges were bonded to the maxillary alveolar process and to the center of the veneers on teeth 11 and 21. MGs were fabricated from EVA (CV), mesh-reinforced EVA (RF), and KeyGuard photopolymer resin (Keystone Industries) printed by Asiga 3D printing (3D-P). Each group ($n = 10$) was subjected to a horizontal impact delivered by a custom device (FAPESP Process 2021/11159-7) using a 35 mm steel sphere. After confirming normality and homoscedasticity with the Shapiro–Wilk test, one-way ANOVA followed by Tukey post hoc was applied ($\alpha = 0.05$).

Results: MG type significantly affected alveolar bone strain ($p < 0.001$). The 3D-P group showed 283 ± 82 με, reductions of 52 % versus CV (590 ± 78 με) and 44 % versus RF (502 ± 79 με) (Tukey $p < 0.001$). The CV-to-RF difference was borderline ($p = 0.052$). For veneers, MG type was also significant ($p = 0.018$): 3D-P 24.0 ± 2.0 με; CV 28.7 ± 4.6 με; RF 27.0 ± 3.6 με, with a significant reduction only between 3D-P and CV ($p = 0.018$).

Conclusions: The 3D-printed KeyGuard mouthguard significantly lowered alveolar bone strain and less pronounced decrease in veneer strain. Digitally controlled manufacturing delivers uniform thickness, eliminating inconsistencies typical of conventional mouthguards, and positions this material as a promising option in the expanding field of digital dentistry.

https://doi.org/10.1016/j.dental.2026.03.134

123

Antimicrobial activity of 3D-resin with Biosilicate-functionalized with chlorhexidine or ZnO

V Cavalli *[1], R Dascanio [1], L Pavanello [1], L Souza [1], M Souza [2], ED Zanotto [2], M Giannini [1], M Özcan [3]

[1] *Piracicaba Dental School, Piracicaba, Brazil*
[2] *Federal University of São Carlos, São Carlos, Brazil*
[3] *University of Zurich, Zurich, Switzerland*

Purpose / Aim: Additive manufacturing has greatly advanced the development of resins for 3D printing in permanent restorations. However, these materials often lack essential bioactivity and antimicrobial properties, limiting their clinical effectiveness. Thus, this study evaluated the biological properties of a commercial 3D resin (3D) incorporated with Biosilicate (BioS), BioS functionalized with chlorhexidine (BioS_CHX), or zinc oxide (BioS_ZnO).

Materials & Methods: In Phase 1, to determine the ideal particle concentration, BioS was incorporated into 3D resin (0%, 5%, 10%, 15%, and 20% w/w) and colony-forming units (CFU) of S. mutans were assessed ($n = 6$). In Phase 2, BioS, BioS_CHX, and BioS_ZnO particles were evaluated for antimicrobial activity using minimum inhibitory concentration (MIC) and minimum bactericidal concentration (MBC) assays ($n = 10$). In Phase 3, 3D resins containing BioS, BioS_ZnO, BioS_CHX, ZnO, and CHX were evaluated for cell viability (MTT) and morphology (SEM, $n = 2$). In all phases, the experimental resins were compared to the control (3D). Data were submitted to one- or two-way ANOVA and Tukey test ($\alpha = 0.05$).

Results: In Phase 1, no differences were found among groups regarding CFU ($p > 0.05$). In Phase 2, BioS_CHX and BioS_ZnO exhibited lower MIC and MBC values ($p < 0.05$). In Phase 3, BioS_CHX exhibited reduced cell viability (MTT) compared to the control (3D) ($p < 0.05$).

Conclusions: The incorporation of BioS_CHX into the 3D resin promoted antimicrobial activity, indicating its potential to improve the biological performance of restorative materials produced through additive manufacturing.

https://doi.org/10.1016/j.dental.2026.03.135

124
Mechanical evaluation of 3D-resin with Biosilicate-functionalized with chlorhexidine or ZnO

R Dascanio *[1], L Pavanello [1], L Vasconcellos [1], M Trevelin [2], M Giannini [1], M Ozcan [3], V Cavalli [1]

[1] *Piracicaba Dental School, Piracicaba, Brazil*
[2] *Department of Materials Engineering, São Carlos, Brazil*
[3] *Center for Dental Medicine, Zurich, Switzerland*

Purpose / Aim: Additive manufacturing has enabled the development of resins for 3D printing in definitive restorations. However, the lack of bioactivity and antimicrobial properties limits their application. Therefore, this study evaluated the mechanical properties of a commercial 3D-resin (3D) incorporated with Biosilicate (BioS), BioS-functionalized with chlorhexidine (BioS_CHX), or zinc oxide (BioS_ZnO).

Materials & Methods: In Phase 1, the ideal particle concentration was determined: BioS was incorporated into the 3D resin (0%, 5%, 10%, 15%, and 20% w/w) and biaxial flexural strength (FB) ($n=10$) and the inhibition halo (IH) were evaluated. In Phase 2, 3D resins containing BioS, BioS_ZnO, BioS_CHX, ZnO, and CHX were tested for flexural strength (FB), microhardness (MH), and surface morphology via SEM ($n=2$). In both phases, experimental resins were compared to a control group (CT). Data were subjected to one- or two-way ANOVA and Tukey test ($\alpha=0.05$).

Results: In Phase 1, the CT group showed higher FB, followed by 5% and 10% BioS, and no significant differences were found among groups regarding IH ($p>0.05$). In Phase 2, no differences in MH were found between CT and 3D resins containing BioS (functionalized or not) ($p>0.05$). The resin with BioS did not differ from CT in terms of FB ($p>0.05$), while BioS_CHX and BioS_ZnO exhibited intermediate FB ($p<0.05$).

Conclusions: Although a reduction in flexural strength occurred, 3D resins containing BioS functionalized with CHX or ZnO presented microhardness similar to the commercial 3D resin, demonstrating a potential for developing enhanced materials for 3D dental restorations

https://doi.org/10.1016/j.dental.2026.03.136

125
Infrared Thermography of a Novel Binding Promoter Under Radiofrequency

SS Marocho *, A Kunapareddy, J Griggs, G Bishop, A Janorkar

University of Mississippi Medical Center, Jackson, USA

Purpose / Aim: To evaluate the thermo-response of the novel binding promoter through the resin cement, as well as the morphology and surface roughness resulting from its application on zirconia ceramic.

Materials & Methods: Fully sintered 3-mm thick 3Y-TZP slices (ZirCAD MO 0, Ivoclar) were subjected to customary air particle abrasion (APA) using 30 μm silica-coated aluminum oxide particles (Cojet, 3M). Following this treatment, either a benchmark MDP primer or the novel binding promoter was applied, with subgroups receiving the application of a thin layer of resin cement. The specimens were then subjected to radiofrequency (RF) for 90 s, and the average maximum temperature during RF application was recorded at 0.1-second intervals using an infrared thermal imaging camera. Surface roughness (Ra) and morphology following before and after the APA, as well as before and after the application of either primer, or cement were assessed ($n=3$/group). Surface roughness data were statistically analyzed using one-way ANOVA.

Results: The novel binding promoter applied to 3Y-TZP under RF was the only condition that exhibited a significant increase in temperature (~54 °C) surpassing the 44 °C damage threshold for pulp damage. However, when cement was applied over the primer, the transferred heat was lower (~40 °C). In contrast, all the other maintained temperatures comparable to the base temperature (26 °C). The highest Ra was promoted by the APA in combination with the novel binding promoter ($p = 0.005$). The morphology of 3Y-TZP after the customary surface treatment and primer application, with and without the subsequent application of cement, are presented in the Table.

Conclusions: The novel binding promoter demonstrated a significant thermos-response when applied to 3Y-TZP under RF. The presence of resin cement mitigated heat transfer, reducing the temperature increase of the binding promoter to acceptable levels. APA combined with the novel binding promoter resulted in enhanced surface roughness and a more favorable microretentive bonding surface of the 3Y-TZP ceramic.

https://doi.org/10.1016/j.dental.2026.03.137

126
Targeting Peptidoglycan Biosynthesis in E. faecalis with Repurposed Drugs

F Lucena *, M Logan, J Wong, G Rocha, S Lewis, C Pfeifer

Oregon Health & Science University, Portland, USA

Purpose / Aim: *Enterococcus faecalis* is a persistent endodontic pathogen, partly due to its ability to form resistant biofilms. UDP-N-acetylglucosamine enolpyruvyl transferase (MurA) is essential for bacterial cell wall biosynthesis and represents a promising drug target. This study aimed to repurpose FDA-approved drugs to inhibit MurA from *E. faecalis* and identify lead compounds for disrupting biofilm formation.

Materials & Methods: Molecular docking was performed using the crystal structure of *E. faecium* MurA (PDB ID: 7TB0), structurally homologous to *E. faecalis* MurA. The active site was centered at grid coordinates X: 24.31, Y: –23.85, Z: 33.58. Over 2,000 FDA-approved compounds were screened using PyMOL and ChimeraX. Docking scores and calculated lipophilicity (clogP) were used to rank candidates. Two top-scoring compounds, Zopolrestat and VS-5584, were selected for experimental validation. Compounds were initially dissolved in DMSO for full solubilization and subsequently diluted in sterile dH_2O to achieve ≤2% DMSO in final solutions, minimizing enzyme inhibition artifacts. *E. faecalis* V583 biofilms were grown in 96-well plates and treated with serial concentrations (0.001–100 μM) of each compound. Optical density of the planktonic bacteria, and biomass were quantified at 600 nm, or via crystal violet staining (λ = 562 nm), respectively.

Results: Blind docking confirmed that most top-scoring compounds localized to the active site, validating the defined grid box. Both Zopolrestat and VS-5584 showed strong binding to the MurA active site (–10.1 and –9.2 kcal/mol, respectively) and favorable physicochemical profiles (clogP < 3). Biofilm assays demonstrated a dose-dependent biomass reduction for both compounds, with significant inhibition observed at 100 μM ($p < 0.01$) for Zopolrestat,

and 1 and 100 μM ($p < 0.01$) for VS-5584 compared to the untreated control (Fig. 1). The exact same trend was observed for the planktonic bacteria. Currently, 13 additional lead compounds identified via in silico docking are undergoing microbiological experimental screening.

Conclusions: This study validated Zopolrestat and VS-5584 as MurA-targeting agents capable of reducing*E. faecalis* biofilm biomass. Notably, VS-5584 significantly inhibited biomass formation at 1 μM, demonstrating promising activity at a relatively low concentration. In contrast, Zopolrestat required higher doses to achieve similar effects. These findings support the potential of repurposed MurA inhibitors for targeting persistent biofilms and underscore the value of ongoing screening efforts to identify additional high-affinity, low-dose candidates.

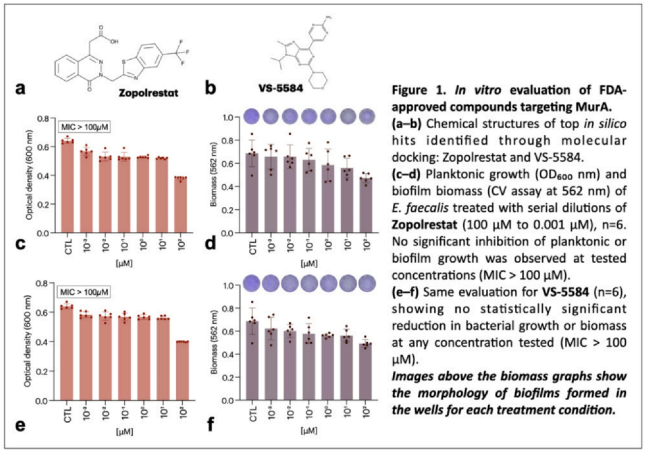

Figure 1. ***In vitro*** **evaluation of FDA-approved compounds targeting MurA.** **(a–b)** Chemical structures of top *in silico* hits identified through molecular docking: Zopolrestat and VS-5584. **(c–d)** Planktonic growth (OD_{600} nm) and biofilm biomass (CV assay at 562 nm) of *E. faecalis* treated with serial dilutions of **Zopolrestat** (100 μM to 0.001 μM), n=6. No significant inhibition of planktonic or biofilm growth was observed at tested concentrations (MIC > 100 μM). **(e–f)** Same evaluation for **VS-5584** (n=6), showing no statistically significant reduction in bacterial growth or biomass at any concentration tested (MIC > 100 μM). ***Images above the biomass graphs show the morphology of biofilms formed in the wells for each treatment condition.***

https://doi.org/10.1016/j.dental.2026.03.138

127

Development of Bioactive Universal Adhesives with Niobium Phosphate Nanoparticles

S Marcos *[1], R de Macedo [2], P Ferreira [2], F Silva [2], S Cardoso [2], L Silva [2], J Bauer [2]

[1] *UFRJ, Rio de Janeiro, Brazil*
[2] *UFMA, São Luiz, Brazil*

Purpose / Aim: The aim of this study was to develop and evaluate the physicochemical, mechanical, and biological properties of experimental universal adhesive systems incorporating different concentrations of niobium phosphate nanoparticles (Nb-HAP).

Materials & Methods: Nb-HAP nanoparticles were synthesized and characterized using Scanning Electron Microscopy (SEM), Energy Dispersive X-ray Spectroscopy (EDS), and X-ray Diffraction (XRD). Experimental adhesives containing 1%, 2.5%, and 5% (w/w) Nb-HAP were developed. A particle-free adhesive and a commercial adhesive (Optibond Universal) were used as controls. Specimens were prepared to evaluate pH, bioactivity, cytotoxicity, and antibacterial activity. Thirty-five human third molars were restored for microtensile bond strength (μTBS) and nanoleakage (NL) tests after 24 hours and 18 months. Bioactivity was assessed after 28 days of immersion in phosphate-buffered saline (PBS), with surfaces analyzed via SEM/EDS and XRD. Data were statistically analyzed using ANOVA and Holm-Sidak post hoc test ($\alpha = 0.05$), while pH and bioactivity were descriptively evaluated.

Results: SEM/EDS revealed rounded Nb-HAP particles containing niobium, calcium, and phosphorus. XRD confirmed the presence of hydroxyapatite. All adhesives exhibited an acidic pH (~1). Nb-HAP groups showed bioactivity through precipitation of hydroxyapatite, carbonate-hydroxyapatite, and calcium phosphate. Experimental adhesives showed mild cytotoxicity ($p > 0.05$), with no antibacterial activity ($p > 0.05$). After 24h, the 5% Nb-HAP group had higher μTBS than controls ($p = 0.01$), but results equalized after 18 months ($p > 0.05$). Only bioactive adhesives showed reduced μTBS over time ($p < 0.05$). NL values were lower in bioactive adhesives ($p < 0.05$).

Conclusions: Incorporation of Nb-HAP into universal adhesives promoted bioactivity via hydroxyapatite layer formation without compromising biocompatibility, bond strength, or nanoleakage resistance.

https://doi.org/10.1016/j.dental.2026.03.139

128

Resin containing copper-doped bioactive glass on adhesive and microbiological properties

MF Guitierrez *[1], MT Schneider [1], A Vender [1], R Aliaga-Galvez [1], S Geraldeli [2], G Abuna [2], M Contreras [1], C Inostroza [1], D Albers [1], AD Loguercio [3]

[1] *Universidad de los Andes, Santiago, Chile*
[2] *East Carolina University, North Carolina, USA*
[3] *State University of Ponta Grossa, Ponta Grossa, Brazil*

Purpose / Aim: To evaluate the effects of an experimental resin composite containing copper-doped bioactive glass nanoparticles (CuBG/Np) on the biological and adhesive properties of the resin-dentin interfaces, both after 24 hours and following an in situ cariogenic challenge (CC).

Materials & Methods: In this split-mouth design study, 96 extracted caries-free human third molars were restored with an experimental resin composite incorporating CuBG/Np at concentrations of 0%, 5%, 10% and 20%. Restorations were performed using two adhesive strategies: etch-and-rinse and self-etch. For each tooth, one restoration was tested immediately, while the other was inserted into an intraoral palatal device worn by twelve adult volunteers for 21 days. After this period, the teeth were removed and sectioned to obtain resin-dentin bonded sticks for microtensile bond strength (μTBS) and nanoleakage (NL) evaluations. Antibacterial properties and microbiota diversity were also evaluated. Data was analyzed by three-way ANOVA and Tukey's post hoc test ($\alpha = 0.05$).

Results: For μTBS, at the immediate time point, the addition of 10% CuBG/Np significantly improved μTBS for both adhesive strategies compared to the control group ($p < 0.05$). After the cariogenic challenge, the 5% and 10% CuBG/Np groups also demonstrated significantly higher μTBS than the control group ($p < 0.05$), regardless adhesive strategies. However, all groups experienced a significantly decrease in μTBS after the cariogenic challenge ($p < 0.05$). Regarding NL, at both time points, all CuBG/Np-containing groups exhibited significantly reduced NL compared to the control group ($p < 0.05$), regardless adhesive strategies. Nonetheless, NL significantly increased in all groups following the cariogenic challenge ($p < 0.05$). Microbiome analysis revealed that, regardless of the adhesive strategy used, the only bacteria genus significantly different between the control and the 10% CuBGNp was Prevotella, which showed greater abundance in the control group.

Conclusions: The incorporation of CuBG/Np into a resin composite—particularly at 10%—enhanced the biological and adhesive properties at resin-dentin interfaces, even in the presence of a cariogeniz challenge.

Funding: This project was funded by ANID through Initiation Fondecyt grant number 11221070.

https://doi.org/10.1016/j.dental.2026.03.140

129
Studies on Apatite-Forming Ability of Shaded Dental Flowable Composite

P Psuja *, Q Ma, B Suh

BISCO Inc, Schaumburg, USA

Purpose / Aim: For dental composites, shades commonly come from metal oxides. There are probably no studies about the influence of metal ions containing dyes, used in dental restoration materials, on the apatite formation process. In this work results of apatite-forming ability of Dental Flowable Composite (DFC) will be tested on A3 and Bleach shade version. Those shades were selected considering the highest volume (wt. %) of dyes in the composition. The purpose of this work was to examinate the influence of Fe^{3+}, Fe^{2+}, Al^{3+} and Ti^{4+} ions contained dyes on apatite formation ability. The tests were performed following ISO 23317:2014 standard, using simulated body fluid (SBF).

Materials & Methods: The DFC A3 and Bleach shade versions with fluorapatite and hydroxyapatite, as well as other inorganic fillers were formulated and tested for apatite-formation ability. The titanium dioxide, aluminum lake and iron oxides powders were used as dyes. The Bleach shade contains the largest (wt. %) volume of dyes (mainly TiO2). On the other hand, A3 shade contains the highest amounts of Al^{3+}, Fe^{3+} and Fe^{2+} ions. The tests were performed following ISO 23317:2014 standard. The SBF was used as a test medium. The reference samples were stored in DI water at 37 °C for the whole duration of the test. The Scanning Electron Microscopy (SEM, JEOL JSM-6010PLUS/LA) with Energy Dispersive X-ray Spectroscopy (EDS, JEOL JSM-6010PLUS/LA), Fourier Transform Infrared Spectroscopy (FTIR, Nicolet iS50) and X-Ray Diffraction Analysis (XRD, Bruker-Nano Discover 8 X-Ray Diffraction System) were used for determination of morphology, and composition of structures obtained during the test.

Results: The combined SEM, EDS, XRD and FTIR examinations confirm the presence of apatite-like structures on A3 and Bleach shaded DFC samples stored in SBF. The SEM & XRD analysis suggests that also other calcium phosphate's structures are present among obtained formations. The results of the whole survey on the appetite-forming ability of A3 and Bleach shades DFC, including the influence of dyes will be the subject of this conference presentation.

Conclusions: The apatite-forming ability, following the ISO 23317:2014 standard, was confirmed at A3 and Bleach shades of Dental Flowable Composite. The applied (wt. %) volume of dyes does not influence negatively on apatite forming ability of DFC. The admixture of trace amount (<0.04 wt.%) of: Ti^{4+}, Al^{3+}, Fe^{3+} and Fe^{2+}, metal ions, as well as (<0.1 wt. %) of Ti^{4+}, do not severely affected apatite formation in this case.

https://doi.org/10.1016/j.dental.2026.03.141

130
Anti-biofilm efficacy and Staining Evaluation of CPP-ACP/SnF2 Dentifrice

K Shiraki *[1], N Kimura [1], T Sato [2]

[1] *GC Laboratory America Inc., Alsip, USA*
[2] *GC R&D Corporation, Tokyo, Japan*

Purpose / Aim: Stannous fluoride (SnF2) is well-known and may help prevent plaque accumulation and gingivitis. However, there have been concerns that SnF2 can cause staining. This study was designed to evaluate the anti-biofilm activity and staining inhibitory effect of a novel dentifrice using casein phosphopeptide-amorphous calcium phosphate (CPP-ACP) and SnF2 combination technology.

Materials & Methods: Five dentifrices were selected for evaluation: MI Paste ONE Perio (MPP), Colgate Total (COL), Crest Gum Detoxify (CRE), Sensodyne Complete Protection (SEN), and Enamelon Fluoride Toothpaste (ENA). All products contained 0.454% W/W SnF2 (1,100 ppm F). Other components for each product are as follows: MPP (CPP-ACP), COL (pentasodium triphosphate), SEN (tetrasodium pyrophosphate), ENA (ACP). Ten-fold water-diluted slurry was centrifuged (10,000G, 10 min) and the supernatant was sterilized by filtration. To evaluate anti-biofilm efficacy, saliva-based biofilms were cultured for 24 hours in microtiter plates and exposed to supernatants for 5 min. Fluorometric resazurin assay was conducted to investigate bacterial metabolic activity immediately after exposure (0 hours) and after 4, 8, and 12 hours (N = 3). Metabolic activities of five dentifrices were compared to that of deionized water. To conduct staining evaluation, five-fold water-diluted slurry was prepared. 1% W/W l-Cysteine hydrochloride solution was prepared and neutralized to pH 7 with 2.5 mol/L Sodium hydroxide. By mixing 0.5 mL of each solution, the staining solutions were prepared. Restorative resin composite specimens (13 mm diameters x 1.5 mm thickness) were polished with P1000 SiC paper and immersed with 1.0 mL of the staining solution for 3 weeks. The staining solution was replaced with a new one every day except for holidays. CR specimens were measured with colorimeter before immersion and 1, 2, and 3 weeks after immersion (N = 3). Color difference (ΔE) was calculated between before/after immersion. All the results were statistically analyzed (ANOVA, Tukey's test, $p < 0.05$).

Results: Mean (SD) values of metabolic activities are presented in table. MPP exhibited lower metabolic activity level than other dentifrices at 4-, 8-and 12-hour intervals as well as maintaining higher anti-biofilm activity for 12 hours compared to other dentifrices. During 3 weeks immersion, ΔE of all the samples were less than 2, which showed that all of them had no staining effect (Table 1).

Conclusions: MPP can be considered as an effective clinical material for helping prolonged prevention of biofilm-induced caries and gingivitis. No staining effect was observed in all samples tested in this study.

Table. Time-dependent changes in metabolic activities of dentifrices, and color difference of CR after 3 weeks immersion.

Dentifrices	Calcium/phosphate source	Metabolic activities (%) Evaluation point (hours) 0	4	8	12	Color difference(Δ E) after 3 weeks immersion
MPP	CPP-ACP	21.2 (2.3) [a]	11.2 (1.4) [a]	19.4 (5.9) [a]	51.4 (11.5) [a]	1.28 (0.15)
COL	pentasodium triphosphate	26.9 (4.2) [a]	37.4 (15.5) [ab]	69.7 (1.8) [b]	70.5 (5.5) [bc]	1.46 (0.07)
CRE	-	20.4 (1.1) [a]	14.1 (3.6) [a]	29.1 (17.3) [a]	67.2 (3.6) [ac]	1.65 (0.06)
SEN	tetrasodium pyrophosphate	54.3 (1.8) [b]	24.0 (6.7) [a]	64.4 (11.8) [b]	65.5 (3.9) [ac]	1.06 (0.37)
ENA	ACP	69.9 (4.4) [c]	56.5 (20.0) [b]	75.6 (15.1) [b]	86.6 (5.4) [b]	1.42 (0.06)

Bacterial metabolic activities (percent compared to water-treated biofilm).
Different letters indicate significantly different values within each time period.

https://doi.org/10.1016/j.dental.2026.03.142

131
Niobium-containing bioactive glass prepared by sol-gel methods: a promising enhancement

J Mitchell *, M Lozoya, A Cade, T Porto

Midwestern University College of Dental Medicine - AZ, Glendale, USA

Purpose / Aim: Bioactive glasses have many common uses in dentistry. They are used as bone grafting materials and also used as fillers for dental composites and adhesives. Trace amounts of Nb ions

have been demonstrated to promote osteogenic differentiation and calcification. Additionally, since niobium functions as a glass network-former it may improve a bioactive glasses chemical durability by allowing greater control of the glass dissolution rate. Unfortunately, altering the chemical composition of the bioactive glasses often results in a negative impact on their bioactivity. This project synthesized a novel sol-gel-derived bioactive glass, containing 80 mol% SiO2; 4 mol% P2O5; 11 mol% CaO; and 5 mol% Nb2O5 using all alkoxide precursors. Following successful synthesis, we assessed the chemical homogeneity, ion release profile, and bioactivity of this new glass.

Materials & Methods: Alkoxide precursors for Si, Ca, P, and Nb were homogeneously mixed, and a sol-gel reaction was initiated via water hydrolysis under controlled conditions. The resulting sols were gelled, aged, and heated through a series of temperatures to form a stable final glass product. The glass was ground and micronized to a particle size of ~ 5-17 μm. Particles were examined by scanning electron microscopy (SEM) and energy dispersive X-ray analysis (EDX) to ensure chemical homogeneity. Glass samples were immersed into Simulated Body Fluid (SBF) and Milli-Q purified water, and the reaction fluid was analyzed by inductively coupled plasma-optical emission spectroscopy (ICP-OES) to determine ion-release profiles. Glass samples soaked in SBF were subsequently inspected via FT-IR to observe apatite formation on the surface.

Results: EDX spectra showed the niobium-containing glass to have a high degree of chemical homogeneity. ICP ion release profiles showed detectable Si, P, Ca, and Nb in the solutions, with longer immersion times resulting in higher ion release concentrations. Ion release concentrations into Milli-Q water were higher than the release into SBF. Apatite peaks were found on the FT-IR spectra after 15 days of soaking in SBF, and well-crystallized apatite was evident as a newly formed frosty layer on the particle surfaces.

Conclusions: The addition of niobium ions to Si-Ca-P bioactive glass formed by the sol-gel synthesis method resulted in a well-formed homogeneous, clear, white glass. The glass was able to readily release ions into solution and exhibited outstanding bioactivity. Further physiochemical testing and biological testing of this glass is currently underway.

https://doi.org/10.1016/j.dental.2026.03.143

132

Injectable naringenin/hydroxyproline-laden hydrogels for bone regeneration

LM Cardoso *, T Pansani, CA de Souza-Costa, FG Basso

Sao Paulo State University, Araraquara, Brazil

Purpose / Aim: Injectable hydrogels have been widely explored in bone tissue engineering and regenerative medicine due to their high-water content, tissue-mimicking mechanical properties, and minimally invasive delivery, making them excellent scaffolds and drug carriers. Gelatin methacryloyl (GelMA), a semi-synthetic polymer known for its biocompatibility, biodegradability, and tunable properties, is commonly used in hydrogel fabrication. Its combination with bioactive molecules can enhance osteogenesis, such as with the citrus flavonoid naringenin (NA), which has shown therapeutic potential for bone regeneration, and hydroxyproline (Hyp), an amino acid essential for collagen structure and function, and a major degradation product of collagen, the primary protein of the bone matrix. Therefore, this study aimed to synthesize and characterize GelMA hydrogels incorporated with NA and/or Hyp for applications in bone tissue engineering.

Materials & Methods: GelMA (15% w/v) was dissolved in phosphate-buffered saline containing 0% (control) or 0.5% (w/w) of NA and/or Hyp. An enzyme was used as a photoinitiator to promote hydrogel crosslinking by photopolymerization using a light-emitting diode device. The hydrogels were prepared in silicone molds, photocrosslinked, and characterized for their chemical composition, swelling/degradation profile, and NA/Hyp release. Osteoblasts (Saos-2; HTB-85) were cultured on the hydrogels, and cell viability, alkaline phosphatase (ALP) activity, and total protein (TP) production were evaluated at different time points. Data showed normal distribution and homoscedasticity and were analyzed using one- or two-way ANOVA followed by post-hoc tests ($\alpha = 5\%$).

Results: Chemical composition analysis confirmed the functional groups of GelMA. Incorporation of NA and/or Hyp reduced water absorption by approximately 6% compared to the GelMA control ($p < 0.05$). Groups containing Hyp or NA/Hyp exhibited similar degradation profiles to the control over 21 days ($p > 0.05$), while the NA-laden group showed faster degradation ($p < 0.05$). Hyp showed a rapid and stabilized release, whereas NA exhibited a slower, sustained release with a significantly lower overall amount. Incorporation of NA or Hyp significantly increased cell viability at 3 and 7 days ($p < 0.05$), while the NA/Hyp group, maintained levels similar to the control ($p > 0.05$). ALP activity was significantly enhanced in the NA group ($p < 0.05$), and TP production was higher in the NA/Hyp group ($p < 0.05$).

Conclusions: Hydrogels incorporated with NA and/or Hyp demonstrated controlled compound release, stability, hydrophilicity, and the ability to stimulate cellular functions related to bone regeneration, indicating their potential for bone tissue engineering applications.

https://doi.org/10.1016/j.dental.2026.03.149

133

Optimization of the geometric accuracy of 3D printed ceramic restoration

T Rossi *[1,2], E Zanetti [3], B Coppola [2], M Calì [4], A Audenino [2], G Serino [2], N Scotti [1]

[1] *University of Turin, Turin, Italy*
[2] *Politecnico of Turin, Turin, Italy*
[3] *University of Perugia, Perugia, Italy*
[4] *University of Catania, Catania, Italy*

Purpose / Aim: The integration of additive manufacturing, specifically 3D printing, into restorative dentistry has revolutionized the fabrication of dental restorations, offering the potential for enhanced precision, customization, and efficiency. This paradigm shift is particularly evident in the realm of ceramic restorations, where materials like zirconia and silica-based ceramics are increasingly employed due to their superior mechanical properties, biocompatibility, and aesthetic qualities. However, the geometric accuracy of these 3D printed restorations remains a critical factor influencing their clinical performance and longevity. Geometric accuracy, defined as the degree to which the fabricated restoration conforms to the intended design, directly impacts marginal fit, occlusal contacts, and overall restoration integration with the surrounding dentition.

Materials & Methods: This study investigates the geometric accuracy of 3D printed dental restorations fabricated from zirconia (5Y and 8Y) and silica-based ceramics, comparing them against the original.stl CAD file, which serves as the gold standard for the intended restoration geometry. To achieve this, restorations are 3D

printed using validated printing parameters for each material: Zirconia 5Y, Zirconia 8Y, and a silica-based ceramic (Bego, Iris Max). Then the restoration is scanned with 3Shape Trios 5 scanner and the comparison with the original.stl file will be performed utilizing specialized software such as CloudCompare. As regards zirconia, due to its volumetric contraction during sintering, the original CAD file was enlarged by various factors on the x, y and z axes to investigate the correct magnification scale. The comparison is carried out on both the occlusal and intaglio surfaces.

Results: As regards zirconia 5Y restorations, the group which performed significantly better is 1.27xy/1.36z. Regarding 8Y zirconia the best magnification is 1.28xy/1.36z. Iris Max performed better than Bego and Zirconia, both 5Y and 8Y.

Conclusions: The study's findings highlight the importance of optimizing printing parameters and compensating for material-specific behaviors to achieve high geometric accuracy in 3D printed ceramic restorations. Furthermore, the observed volumetric contraction in zirconia-based restorations during sintering emphasizes the importance of incorporating appropriate scaling factors into the CAD design to account for this phenomenon. The results emphasize the critical need for meticulous optimization of printing parameters and material-specific compensation strategies to attain superior geometric accuracy in 3D-printed ceramic restorations, thereby ensuring optimal clinical performance and durability.

https://doi.org/10.1016/j.dental.2026.03.150

ACADEMY OF DENTAL MATERIALS

www.academydentalmaterials.org

General information:

The Academy of Dental Materials is a body composed of individuals interested in the science of dental materials. The Academy of Dental Materials exists solely for the purpose of advancing the science and technology of dental biomaterials. This is accomplished by sponsoring annual scientific meetings, conferences, an international journal, transactions of scientific proceedings, awards for students, awards for outstanding scientists, and the confirmation of Fellowship for special members.

Membership information and instructions:

Membership dues are kept at a minimal level to encourage membership (US$ 149 Regular and Fellow, US$ 40 Student, US$ 55 Post-Doctoral, and US$ 2000 Corporate). These rates include an online subscription to the *Dental Materials* journal. Regular and ADM Fellow members can choose to additionally receive a hard copy of the journal for an additional US $26 (or UD$ 175 total). Academy members receive a discounted registration fee for the annual ADM meeting. ADM meetings are conducted using a style that promotes interaction among participants. The opportunity for student and faculty presentations is afforded through poster presentations during meeting days. For membership application forms, meeting information, and general instructions, please contact: Dr.Ricardo M. Carvalho, DDS, PhD, FADM, Email: rickmc@dentistry.ubc.ca

Corporate membership information:

As a Corporate Member, the company will be recognized in the *Dental Materials* journal (circulation approximately 1,800). The corporation name and logo will appear on a special page (in each issue of the journal) acknowledging the Corporate Members. In addition, a complimentary online and hard-copy subscription to *Dental Materials* will be sent to the corporate contact during the year of membership. Meeting sponsorship is independent of corporate membership. The Corporate Member fee is US$ 2000 per year. For corporate membership information, please contact: Lynn Reeves, Executive Manager, E-mail: admin@academydentalmaterials.org, Phone: (858) 272-1018 FAX: (858) 272-7687

Fellowship and Student Award information:

Academy members in good standing may apply for Fellowship in the Academy. Applications must include a current c.v. and two letters of recommendation from current Fellows of the Academy. The criteria to apply for Fellowship are (1) achievement of advanced degrees: at least a master's degree and preferably a Ph.D., Odont Dr., or equivalent degree; (2) publication of at least ten peer-reviewed, scientific articles in refereed journals of which the candidate should be first author on one-half of the articles; (3) at least five years of leadership through research, training, service, and/or education beyond formal education; and (4) normally at least five years membership in the Academy.

University Student Award

Each year, the members of the Academy of Dental Materials affiliated with various Dental Schools around the world, present awards to their most outstanding students or student researchers in the field of dental materials.

For information regarding Fellowship in the Academy and annual dental student awards, please contact: Prof. Ricardo Carvalho E-mail: rickmc@dentistry.ubc.ca.

Student Travel Award

The ADM offers Student Travel Awards to facilitate attendance and participation in the ADM annual meeting by outstanding students currently enrolled in an education program in areas relevant to the mission of the ADM.

Paffenbarger Award

Students pursuing graduate studies in dental materials or biomaterials sciences and dental students who have conducted research in dental materials or biomaterials sciences are encouraged to compete in the **Paffenbarger Award** competition at the annual meeting of the Academy. The winner of the award competition receives a prize of US$ 1,750, the second- place winner receives US$ 1,250, and the third-place winner receives US$ 1,000. All 3 students also receive free registration for the next ADM Meeting. In addition to the Paffenbarger Award, the Academy presents an annual award at each dental school to the student who has demonstrated outstanding academic achievement in dental materials science. For information regarding the Paffenbarger Award competition, please contact: Dr. Arzu Tezvergil-Mutluay E-mail: arztez@utu.fi

Marshall Postdoctoral Award

The ADM offers the **Marshall Postdoctoral Award** to recognize and encourage excellence in dental biomaterials research performed by individuals in the transitional post-doctoral stage of their careers. The winner of this award competition receives US$ * and free registration to the following year's ADM annual meeting.

Founder's Award information:

The ADM has initiated an award to honor Dr. Evan Greener in recognition of his contributions to the Academy. The **Founder's Award** will be given to an ADM Member who is nominated by one or more fellow ADM members as exhibiting excellence in dental materials research and in service to the Academy. Nominations should document the contributions of the individual and should be sent to the President of the Academy: Prof. Dr. Ulrich Lohbauer E-mail: ulrich.lohbauer@fau.de. The nominations will be reviewed by the Board of Directors for acceptance. This is an honorary award, not a cash award, but up to US$ 1000 will be provided to the awardee for expenses in attending the annual Academy meeting to receive the award in person.

MEMBERSHIP APPLICATION

Complete all blank lines Please print or type

— — — — — — — — — — — — — — — — **PROFESSIONAL INFORMATION** — — — — — — — — — — — — —

LAST NAME:_____ FIRST NAME: _____

INSTITUTION/COMPANY/UNIVERSITY: _____

DEPARTMENT: _____

STREET ADDRESS: _____
(please note that journal will be sent to this address)

CITY: _____ STATE:_____

COUNTRY: _____ ZIP: _____

PHONE#:_____ FAX #: _____

E-MAIL: _____

IMPORTANT NOTE: STUDENTS AND POSTDOCTORAL APPLICANTS MUST SEND A CONFIRMATION LETTER OF STUDENT/POSTDOCTORAL STATUS FROM EITHER A SPONSORING MEMBER OR THEIR LEARNING INSTITUTE.

— — — — — — — — — — — — — — — — **FILING INFORMATION** — — — — — — — — — — — — —

MEMBERSHIP: Please check one of the following categories and see reverse side for information:

☐ MEMBER - option 1 US$175/year (includes **printed** and online journal) (US$100 for first year only).
☐ MEMBER - option 2 US$149/year (includes only the **online** journal) (US$74 for first year only).
☐ STUDENT MEMBER* US$40/year (includes only the online version journal).
☐ *STUDENT MEMBER – I do **not** have a PhD title
☐ *STUDENT MEMBER – I **am** enrolled in a Masters, PhD or dental degree program

☐ POSTDOCTORAL MEMBER* US$55/year (includes only the online version journal).
*Confirmation Letter of Student/Postdoctoral Status required to accompany application
☐ *POSTDOCTORAL MEMBER*I have **not** been a PhD member in the ADM for longer than 4 years

PAYMENT: Please check one of the following:

☐ Check ☐ Money Order ☐ Visa ☐ MasterCard ☐ Discover TOTAL: US$_____

Account or Card No.: _____ 3-digit security code: _____

Expiration date: _____ Cardholder's Name: _____

Signature: _____

SIGNATURE OF THE APPLICANT: _____DATE: _____

SEND FORM AND PAYMENT TO:

Academy of Dental Materials
Attn: Lynn Reeves
4425 Cass Street, Suite A
San Diego CA 92109 USA
Email: Lynn@RES-Inc.com
Phone: +01-858-272-1018
FAX: +01-858-272-7687